FORMATION OF POLYATOMIC CATIONS OF TELLURIUM, SULFUR AND ANTIMONY IN HSO_3F

By

Om Chand Vaidya Ph.D.

A Thesis

Submitted to the Faculty of Graduate Studies

in Partial Fulfillment of the Requirements

for the Degree

Doctor of Philosophy

McMaster University

December 1971

ACKNOWLEDGEMENT

My sincere thanks are due to Professor R. J. Gillespie for his advice and encouragement throughout this work. I would also like to thank the members of the Department of Chemistry for lively discussions, advice and criticism. The association with our Inorganic Research Group has been an enjoyable one. My thanks are due to Dr. T. Timusk of the Physics Department for the help in obtaining the i.r. spectra and Dr. C. Davies for X-ray diffraction studies.

Special thanks are due to my wife Kiran and son Rahul for their patience and support.

Financial assistance and travel grant by McMaster University is gratefully acknowledged. Finally, I would like to thank Mrs. Susan Hawley for typing this thesis.

DOCTOR OF PHILOSOPHY
(Chemistry)

McMaster University
Hamilton, Ontario

TITLE: Formation of Polyatomic Cations of Tellurium, Sulfur and Antimony in Fluorosulfuric Acid

AUTHOR: Om Chand Vaidya, Ph.D. (Panjab University)

SUPERVISOR: Dr. R. J. Gillespie

NUMBER OF PAGES: viii, 110

SCOPE AND CONTENTS:

Polyatomic cations of tellurium, sulfur and antimony have been studied in HSO_3F. Tellurium metal can be oxidised with $S_2O_6F_2$ in HSO_3F to the (+1) oxidation state. The cryoscopic measurements in HSO_3F suggest that the cation is not Te_2^{2+} but a higher polymer. Sulfur can be oxidised to the (+1/8), (+1/4) and (+1/2) oxidation states in acidic solvents. The cations S_{16}^{2+} and S_8^{2+} have been identified in the solutions from cryoscopic conductivity measurements and UV-visible absorption spectroscopy.

UV-visible absorption spectra, cryoscopy and conductivity measurements show that antimony metal is oxidised by HSO_3F to the (+1) and (+3) oxidation states. The compounds of antimony in the (+1) oxidation states have been prepared. Sb(I) reduces HSO_3F to sulfur cations and elemental sulfur. No evidence has been obtained for an oxidation state of antimony lower than (+1).

TABLE OF CONTENTS

LIST OF TABLES

LIST OF FIGURES

CHAPTER I

INTRODUCTION

1. Polyatomic Cations

It has recently been shown that the Group VI and VII B elements can be oxidised in acidic solvents to new low positive oxidation states that are unstable in aqueous solutions. The solutions of these elements in these new oxidation states are generally coloured. The coloured solutions of sulfur, selenium and tellurium in sulfuric acid and oleum have been known for a long time but the exact nature of these solutions has only been understood recently after the chemistry of solutions in these solvents had been fully investigated.

(a) Cations of Iodine

In the brown solutions of iodine and iodosyl sulphate in concentrated sulfuric acid evidence for the cations I_3^+ and I_5^+ was first obtained by Masson in 1938 (1). Symons and coworkers (2) have reported the cations I_3^+, I_5^+ and $H_2IO_3^+$ in the solutions of iodine and iodic acid in sulfuric acid and oleum from U V visible absorption spectra and conductivity measurements. Gillespie and coworkers (3) have carried out a detailed study of solutions of iodine in sulfuric acid in the presence of iodic acid. Cryoscopic and conductivity measurements on these solutions show the formation of I_3^+ and I_5^+ cations. Iodine can be oxidised with peroxydisulfuryldifluoride in fluorosulfuric acid. U V -visible absorption spectra of these solutions show that iodine reacts with peroxydisulfuryldifluoride in the $I_2/S_2O_6F_2$ mole ratios of 5:1, 3:1 and 2:1 to give I_5^+, I_3^+ and I_2^+ cations respectively.

1. $5I_2 + S_2O_6F_2 \longrightarrow 2I_5^+ + 2SO_3F^-$

2. $3I_2 + S_2O_6F_2 \longrightarrow 2I_3^+ + 2SO_3F^-$

3. $2I_2 + S_2O_6F_2 \longrightarrow 2I_2^+ + 2SO_3F^-$

Cryoscopic and conductivity measurements have confirmed the formation of the cations I_5^+ and I_3^+ at the $I_2/S_2O_6F_2$ mole ratios of 5:1 and 3:1 respectively. Conductivity measurements on the $I_2/S_2O_6F_2$ = 2:1 solution at 25°C were consistent with the formation of the cation I_2^+ but cryoscopic results show that I_2^+ dimerises at low temperatures to I_4^{2+}. The formation of I_4^{2+} was further confirmed by studies of the UV-visible absorption spectrum (4,5).

(b) Cations of Bromine

Attempts by Symons et al to obtain bromine cations in solution in sulfuric acid were not successful. However, these workers postulated that bromine is oxidised in oleum to a tervalent derivative via Br_3^+ (6). McRae (7) obtained some evidence for the Br_3^+ cation in a study of the vapour pressure diagram of the bromine-antimony pentafluoride system. Gillespie and coworkers (8,9) have shown that bromine can be oxidised with $S_2O_6F_2$ in fluorosulfuric acid to give Br_3^+ which is oxidised to $BrSO_3F$ in the presence of excess $S_2O_6F_2$. In super acid ($SbF_5/3SO_3/HSO_3F$) absorption spectral measurements show that the reaction of bromine with $S_2O_6F_2$ leads to the formation of Br_3^+ at the mole ratio $Br_2/S_2O_6F_2$ = 3:1 and the formation of Br_2^+ at the mole ratio $Br_2/S_2O_6F_2$ = 2:1. These cations have been further characterised by conductivity measurements and Raman spectroscopy. Edwards et al (10) have prepared the scarlet compound $Br_2^+(Sb_3F_{16})^-$ by the reaction of Br_2, BrF_5 and SbF_5 and have reported its structure from X-ray crystallographic studies.

(c) Cations of Chlorine

Olah and coworkers (11) have studied the e.s.r. spectra of the solutions of $C\ell F$, $C\ell F_3$ and $C\ell F_5$ in SbF_5/HSO_3F mixtures and interpreted the spectra on the basis of the formation of $C\ell_2^+$ radical cation in solution. This work has been refuted recently by a number of workers (12-14). Gillespie and coworkers (12) have obtained the solid $C\ell_3^+AsF_6^-$ compound by the reaction of $C\ell_2$ and $C\ell F$ with AsF_5 at -80°C. The $C\ell_3^+$ ion was clearly identified and shown to have an angular structure by its Raman spectrum. Attempts to prepare the $C\ell_3^+$ cation in solution even in super acid were not successful. There is at present no evidence for the existence of the $C\ell_2^+$ cation as a stable species in solution.

(d) Cations of Tellurium

The red colour of the solution of tellurium in sulfuric acid was one of the first properties reported for this element (15). Gillespie and coworkers (16) have shown that these red solutions of tellurium metal in sulfuric acid contain the cation Te_4^{2+}. The same species can be obtained by the oxidation of tellurium metal with $S_2O_6F_2$ in fluorosulfuric acid. The results of cryoscopic and conductivity measurements on the solution were consistent with the formation of the cation Te_4^{2+}. Compounds of the Te_4^{2+} cation have also been prepared by the reaction of Te metal with dilute solutions of $TeC\ell_4$ in molten $A\ell C\ell_3/NaC\ell$ eutectic (17). X-ray crystallographic studies of Te_4^{2+} have shown that it has a square planar structure (18).

Tellurium metal can also be oxidised to the (+1/3) oxidation state with arsenic and antimony pentafluorides (19) and the compounds $Te_6(AsF_6)_2$ and $Te_6(SbF_6)_2$ have been isolated. These compounds are not stable in solution

in fluorosulfuric acid or hydrogen fluoride.

Gillespie and coworkers have shown that a red solution of tellurium containing Te_4^{2+} in HSO_3F can be further oxidised to give a yellow solution. One of the objects of the work described in this thesis was to obtain further evidence on the nature of this yellow species.

(e) Cations of Selenium

Selenium dissolves in sulfuric acid or oleum to give green or yellow solutions (20,21). Gillespie and coworkers have studied solutions of selenium in sulfuric, disulfuric and fluorosulfuric acids (22). In fluorosulfuric acid selenium can be oxidised with $S_2O_6F_2$. At $Se/S_2O_6F_2$ mole ratios of 8:1 and 4:1, green and yellow solutions respectively are obtained. The cations Se_8^{2+} and Se_4^{2+} have been characterised in the 8:1 and 4:1 solutions respectively from absorption spectra, cryoscopic and conductivity measurements.

Infrared and Raman spectra and X-ray crystallographic studies show that Se_4^{2+} has a square planar structure (23,24). Corbett and coworkers (25,26) have shown by X-ray crystallography that the cation Se_8^{2+} has a structure consisting of two fused five-membered rings. This structure is intermediate between the structures Se_8 (27,28) and S_4N_4 (29,30).

2. The Fluorosulfuric Acid Solvent System

Polyatomic cations are very strong Lewis acids and are easily decomposed even by a very weak base. Strong acidic solvents provide a good medium for the study of these cations. Fluorosulfuric acid is one of the strongest protonic acids known and the strongest base in this solvent is the very weakly basic SO_3F^- ion.

The solvent properties of fluorosulfuric acid were first studied by

Woolf (31). He studied acid-base neutralization reactions in this solvent by the conductometric method.

Gillespie and coworkers have made a very extensive study of the solvent properties of fluorosulfuric acid (30-34) and this work has recently been summarised in a review (35). Some of the physical constants of this solvent are given in Table 1.

Because it has a low viscosity and relatively low boiling point fluorosulfuric acid has some advantages as a solvent when compared with sulfuric acid and oleum. The low freezing point of fluorosulfuric acid makes cryoscopic measurements more difficult than for sulfuric and disulfuric acids.

(a) Cryoscopic Measurements

Gillespie and coworkers (32) have described the apparatus and method for carrying out cryoscopic measurements in fluorosulfuric acid. These workers have studied the freezing point depression produced by a number of electrolytes and non-electrolytes and have determined a value for the cryoscopic constant of fluorosulfuric acid of 3.93±0.05 deg. $mole^{-1}$ kg. The freezing point depression produced by a solute in fluorosulfuric acid is given by the expression

$$\theta = k\nu m$$

where k = cryoscopic constant of fluorosulfuric acid;

m = conc. of the solute g mole kg^{-1};

ν = total number of moles of particles produced in solution per mole of the solute.

The ν value of the solute in solution can be determined from the slope of the freezing point depression curve.

(b) Conductivity Measurements

Conductivity and transport number measurement on solutions of acids

TABLE 1

Properties of Fluorosulfuric Acid (35)

Boiling point °C	162.7
Freezing point °C	-88.98
Density at 25°C g. cc^{-1}	1.726
Viscosity at 25°C cp	1.56
Cryoscopic constant ° °C $mole^{-1}$ kg.	3.93
Specific conductivity 25°C ohm^{-1} cm^{-1}	1.085×10^{-4}

TABLE 1

Properties of Fluorosulfuric Acid (35)

Boiling point °C	162.7
Freezing point °C	-88.98
Density at 25°C g. cc^{-1}	1.726
Viscosity at 25°C cp	1.56
Cryoscopic constant ° °C $mole^{-1}$ kg.	3.93
Specific conductivity 25°C ohm^{-1} cm^{-1}	1.085×10^{-4}

and bases in fluorosulfuric acid show that the $H_2SO_3F^+$ and SO_3F^- ions have abnormally high mobilities. The specific conductances of solutions of alkali metal fluorosulfates are very similar indicating that SO_3F^- carries the major portion of the current. On this basis Gillespie and coworkers (30) have defined the γ-value in fluorosulfuric acid. The γ-value is defined as the number of moles of SO_3F^- ions produced by the ionization of one mole of the solute. The γ-value of any solute can be obtained from the ratios of the concentrations of the solute and a standard fully-ionised mono fluorosulfate at which both the solute and standard electrolyte have the same specific conductance

$$\gamma = C_s/C$$

KSO_3F is a convenient and useful standard electrolyte (γ = 1).

(c) Peroxydisulfuryldifluoride as an Oxidising Agent

Peroxydisulfuryldifluoride as an oxidising agent has a particular advantage in fluorosulfuric acid as it is simply reduced to SO_3F^-

4. $S_2O_6F_2 + 2e \longrightarrow 2SO_3F^-$

The number of moles of SO_3F^- produced in solution can be determined very easily from conductivity measurements.

3. Purpose of this Work

It was observed during previous investigations in this laboratory that tellurium forms a cationic species in a higher oxidation state than (+1/2) and like tellurium and selenium sulfur, can also be oxidised to new positive low oxidation states. The purpose of the work reported in this thesis was to extend previous studies made in this laboratory on the formation of tellurium and sulfur cations in acid solvents and also to attempt to obtain

polyatomic cations of antimony in these solvents.

CHAPTER II

EXPERIMENTAL

1. Preparation and Purification of Materials

Dry Air

Compressed air was passed through a drying train consisting of a Dreschel bottle containing sulfuric acid, two 12 inch drying towers containing granular silica gel and molecular sieves, and a three-foot tube packed with phosphor us pentoxide supported on glass wool.

Fluorosulfuric Acid

Technical fluorosulfuric acid (Baker and Adamson) was purified by double distillation in a two-stage glass still, as described by Barr (36). The still was rigorously dried by flaming out, and by passing a slow stream of dry air through it overnight. Passage of dry air through the receiver was continued during distillation.

Occasionally the initial fluorosulfuric acid contained a large excess of sulfur trioxide, which was not effectively separated by distillation. In these cases the crude acid, contained in the first stage of the still, was cooled in the dry ice bucket and pellets of sodium bifluoride were added. The bulk of acid then distilled over in the required range of 162 to 164°C. The purity of a portion of the final product was checked cryoscopically and any excess of sulfur trioxide was titrated with hydrogen fluoride until the freezing point rose to -89.00°C. Additions of a 10% w/w solution of hydrogen fluoride in fluorosulfuric acid were made using an all teflon syringe fitted with platinum needle (Hamilton Syringe Co. Inc.) and

closed with a cap made from 1 mm Kel-F tubing. A calculated quantity of the hydrogen fluoride solution was then added to the bulk stock of the solvent.

Disulfuric Acid

Disulfuric acid was prepared by distilling sulfur trioxide into a weighed amount of 100% sulfuric acid. The acid so obtained was checked cryoscopically and titrated with SO_3 or H_2SO_4 until the freezing point rose to 35.11°C.

Peroxydisulfuryl Difluoride

Peroxydisulfuryl difluoride was prepared by the method of Dudley and Cady (37) by the reaction of fluorine and sulfur trioxide at 130°C over a silver catalyst. The catalyst was supported on copper mesh which had been coated with silver in a silver cyanide complex bath. The flow rates of each reactant, diluted with nitrogen, were monitored with flurolube oil bubblers. A small excess of fluorine was achieved by adjusting flow rates until solid sulfur trioxide ceased to form at the top of the collection trap, which was cooled in dry ice.

The product was shaken with 100% sulfuric acid to remove sulfur trioxide, and distilled at -76°C into storage traps fitted with teflon-glass valves (Fisher and Porter). Prior to use the compound was doubly distilled from dry ice on a pyrex vacuum line fitted with teflon taps.

Hydrogen Fluoride

Anhydrous hydrogen fluoride (Harshaw Chemical Co.) was used directly.

Sulfur Trioxide

Sulfur trioxide was distilled from Baker and Adamson 'Sulfan' in a still which was protected from moisture by a magnesium perchlorate drying

tube.

Sulfur Dioxide

Sulfur dioxide (Matheson Co.) was stored over P_2O_5 for 24 hours before use.

Antimony Pentafluoride

Antimony pentafluoride (Ozark Mahoning Co.) was doubly distilled in a pyrex glass still in an atmosphere of dry nitrogen. The fraction boiling between 142°C and 143°C was collected.

Arsenic Pentafluoride

Arsenic pentafluoride (Ozark Mahoning Co.) was condensed on a glass vacuum line which had been rigorously dried by flaming with a Bunsen burner.

2. Manipulation of Materials

Rigorous precautions were taken to exclude moisture in this work. Glassware was flamed under vacuum and all manual operations were performed in a dry box.

The dry box had an external circulating system and any moisture or acid vapour was removed in liquid nitrogen traps. It was equipped with a port which was flushed with extra-dry nitrogen for fifteen minutes before entry.

Solutions of fluorosulfuric acid were handled using smooth glass syringes fitted with teflon plungers, and platinum needles with Kel-F hubs (Hamilton Syringe Co.). The ends of the needles could be closed off with Kel-F tubing and the syringes could be weighed before and after addition.

Vacuum line operations were performed with a pyrex vacuum line fitted with 4 mm Fischer and Porter teflon glass valves. Attachments were made

either with 1/4" teflon Swagelok connectors or with B10 joints using Kel-F grease (3M.s.). Before use the line was flamed out under vacuum.

3. Cryoscopy in Fluorosulfuric Acid

The apparatus and technique for making cryoscopic measurements in fluorosulfuric acid has been described in detail by Gillespie, Milne and Thompson (32). The cryoscope, containing approximately 150 g solution, was cooled in a liquid nitrogen bath, and the pressure within its vacuum jacket was adjusted to give a cooling rate of between 0.3 and 0.4°C per minute; a tap to a mercury diffusion pump was opened for a few seconds at a time while the solution was still some twenty degrees above the freezing point, and a cooling rate was measured a minute later with a stop watch. The temperature was measured to 0.001°C with a Leeds Northrup platinum resistance thermometer used in conjunction with a Mueller resistance bridge. The thermometer calibration was checked periodically by determining its resistance at the triple point of water using a Trans-Sonics Inc. 'Equiphase cell'. A computer programme was written to calculate and print out the resistance at a temperature interval of 0.01°C.

Resistance readings were recorded at thirty second intervals starting when the solution had reached the estimated freezing point. When the solution had supercooled by approximately 2°C freezing was initiated by dropping in a small piece of platinum cooled in liquid nitrogen. The temperature rose rapidly, after which a cooling curve was plotted with readings at one minute intervals for fifteen minutes, with occasional reversal of the 1 m amp thermometer current. The cooling curve was extrapolated back to the freezing point, which was estimated to be accurate to ±0.005°C.

Additions were made using teflon-glass syringes through a B14 joint at the top of the cryoscope. At all other times this joint was capped with an 'anhydrone' guard tube which served as an exit for the slow stream of dry air continually sweeping the top of the cryoscope.

4. Cryoscopy in Disulfuric Acid

Freezing point measurements of the solutions in disulfuric acid were made in the cryoscope described by Gillespie and coworkers (39). The cryoscope was placed in an air jacket immersed in a thermostat which was kept at 0.5° above the freezing point of the solution in the cryoscope. The freezing points were measured with a Hewlett Packard quartz thermometer probe (Model 280 A) which could be set to read small temperature differences to ±0.001° which had been calibrated with a platinum resistance thermometer. In order to measure a freezing point the solution was melted and then allowed to cool by standing at room temperature until it had supercooled by approximately 1.5°. It was then placed in the air jacket in the thermostat and crystallisation was induced by dropping into the cryoscope a very small piece of platinum foil which had been cooled in liquid air. The temperature then rose rather slowly taking about 20 min. to reach a maximum value.

The observed freezing points were corrected for supercooling by adding the correction 0.014 S θ where S is the amount of supercooling and θ is the freezing point depression (38).

5. Conductivity Measurements in Fluorosulfuric Acid

Conductivity measurements at 25°C were made as described by Milne (39). The cell used had a capacity of 100 ml. and three platinum electrodes gave a choice of cell constant of approximately 3 or 30 cm^{-1}.

The cells were cleaned with aqua regia and the electrodes were plated with platinum black by electrolysing a 0.3% solution of chloroplatinic acid in dilute hydrochloric acid containing lead acetate (40). A current of ten m. amp was automatically reversed every ten seconds, and was passed for ten minutes.

The cell constants were found by measuring the conductance of a standard 0.01 D solution of potassium chloride (41) made up in distilled water from an ion exchange column. This solution has a specific conductance of 0.0014088 ohm^{-1} cm^{-1} at 25°C.

Conductivity measurements were made after the cell had been in an oil bath at 25°C for fifteen minutes. The temperature was measured with a calibrated mercury thermometer and was reproducible to ±0.05°C. All additions of concentrated solutions and solids were made in the dry box using weighed syringes.

The conductance of the solutions was measured with a Wayne-Kerr Universal Bridge operating at 1 KHz. The reading was repeated after agitation of the cell in the constant temperature bath, to ensure that a steady value had been reached.

6. U V and Visible Absorption Spectra

Absorption spectra were recorded from 220 to 700 nm. on either a Bausch and Lomb Spectronic 505, or on a Cary model 14 spectrometer. One centimeter path length silica cuvettes, with quartz inserts to vary the path length down to 0.02 mm, facilitated the study of concentrated solutions. Path lengths were calibrated with alkaline solutions of potassium chromate (42). Custom-made quartz cells (Hellma Ltd.) in which all four sides were optically

clear were also used. These cells had the obvious advantage of giving two different path lengths when used with the quartz inserts. The cells and inserts were rigorously dried, and stored in a vacuum desicator over phosphorus pentoxide. The cells were filled in a dry box, and teflon covers were clamped on, and bound with teflon tape.

7. Magnetic Susceptibility Measurements

Magnetic susceptibilities were determined by the Gouy method using an Alpha Scientific Laboratory Model AL 7500 electromagnet, and a Sartorius Vacuum Electronic microbalance. The sample consisted of ten cm of solid or solution sealed in a fifteen cm long 5 mm o.d. quartz tube. The sample was suspended in an atmosphere of dry nitrogen. The microbalance could be read to 1 μg. The quartz tube constant was calibrated with standard nickel (II) chloride solution (43).

8. Electron Spin Resonance Spectroscopy

Electron spin resonance spectra of the solutions were obtained on a JOELCO Model JES 3BS-X spectrometer. The g values were obtained by comparison with manganous ion (the 4th line from the lowest field has g = 1.981).

9. Nuclear Magnetic Resonance Spectroscopy

Fluorine nmr spectra were measured using either a Varian DP-60 Spectrometer operating at 56.4 MHz, or a Varian HA-100 spectrometer, operating at 94.1 MHz. Low temperature spectra were obtained using a Varian 4540 temperature controller with the variable temperature probe.

10. Raman Spectroscopy

Raman spectra were recorded using a Spex Industrial Model 1400 spectro-

meter employing a double monochromator and a phototube detector with an electrometer amplifier and recorder. The exciting radiation was the green 5165 Å line of a spectra-Physics Model 140 Ar ion laser, or the 6328 Å line of a spectra-Physics Model 125 He-Ne laser. Standard samples were sealed in 2 mm o.d. glass capillary tubes, and mounted horizontally in a brass holder. For low temperature spectra the sample tubes were mounted in a quartz tube with an evacuated jacket, silvered except for a 1-cm band around the centre. Nitrogen was boiled off at a variable rate from a Dewar, and passed through the tube, and the temperature was recorded with a thermocouple.

11. Infrared Spectroscopy

Infrared samples were prepared by mixing the sample with polyethylene powder in 1:20 w/w ratio. The mixture was subjected to a pressure of 25000 lbs. The pallates so obtained were covered with a Para film "M" (Marathon Division of American Can Company). This film was transparent below 400 cm^{-1} in the i.r. The spectrum was recorded on Backman IR-12 Infrared Spectrophotometer and Fourier Spectrophotometer FS 720, Module Research and Industrial Instrument Co.,London (Serial No. 0178).

CHAPTER III

FORMATION OF Te_n^{n+} CATION IN FLUOROSULFURIC ACID

1. Introduction

It has been shown by UV-visible absorption spectroscopy, cryoscopy and conductivity measurements that the red solutions of tellurium metal in the acidic solvents sulfuric acid, oleum and fluorosulfuric acid contain the cation Te_4^{2+} (44) which has a square planar structure (19). It has also been shown by Gillespie and coworkers that Te_4^{2+} can be oxidised to a species that gives a yellow solution in acids. The U V— visible absorption spectrum of this solution shows a strong absorption band at 250 nm and weak absorptions at 350 and 420 nm. In the present work the nature of this yellow species was further investigated.

Tellurium metal reacts with HSO_3F at room temperature to give a red solution. However, at temperatures below -20°C the reaction of the acid on the metal can be prevented and it can then be quantitatively oxidised by $S_2O_6F_2$ to give red or yellow solutions. The reaction of the metal was followed at -23°C. The tellurium metal reacts with $S_2O_6F_2$ in the mole ratio of 2:1 to give a yellow solution. This solution shows a strong absorption band at 250 nm and weak absorptions at 360 and 420 nm. A similar spectrum was reported earlier (16). The reaction of the metal with $S_2O_6F_2$ in a 2:1 mole ratio can be represented by the equation

$$n\ Te + \frac{n}{2} S_2O_6F_2 \longrightarrow Te_n^{n+} + n\ SO_3F^-$$

where n = 1, 2, 3, ... The magnetic behaviour of the solution was studied

by Dr. Ummat and it was concluded that the solution was essentially diamagnetic; hence it may be assumed that n can not be odd (44).

The solutions of tellurium in this oxidation state in HSO_3F are stable only below -20°C. Above this temperature the compound disproportionates to give Te_4^{2+} as one of the products. This causes a great difficulty in the handling of this solution. Every care was taken to keep the temperature of the solution below -20°C at all times.

2. Cryoscopic Measurements

To find the value of n in Te_n^{n+} freezing point measurements were made on solutions in HSO_3F having the composition $Te/S_2O_6F_2 = 2:1$. The freezing point depression results are given in Table II. Comparison of the experimental freezing point curve with theoretical curves for the reactions:

A. $2Te + S_2O_6F_2 \longrightarrow Te_2^{2+} + 2SO_3F^-$ $\quad \nu = 1.5$

B. $4Te + 2S_2O_6F_2 \longrightarrow Te_4^{4+} + 4SO_3F^-$ $\quad \nu = 1.25$

C. $6Te + 3S_2O_6F_2 \longrightarrow Te_6^{6+} + 6SO_3F^-$ $\quad \nu = 1.17$

D. $8Te + 4S_2O_6F_2 \longrightarrow Te_8^{8+} + 8SO_3F^-$ $\quad \nu = 1.12$

E. $\infty Te + \infty S_2O_6F_2 \longrightarrow Te_\infty^{\infty+} + \infty SO_3F^-$ $\quad \nu = 1.0$

A, B, C, D and E have been made in Fig. 1. The theoretical slopes required for these reactions are given in Table III. The slope required for reaction A differs very much from the experimental slope indicating that the cation Te_2^{2+} is not formed in the solution. The experimental slope is closer to the theoretical slopes required for reactions C or D suggesting the formation of the cation Te_6^{6+} or Te_8^{8+}. However the difference between the curves B, C and D are small and in view of possible

TABLE II

Freezing Point Depressions of $Te/S_2O_6F_2$ = 2:1 Solutions in HSO_3F

Concentration [mole (Te) kg^{-1}]	θ °C
0.0398	0.16
0.0757	0.31
0.0993	0.41
0.1336	0.55
0.1698	0.71

θ = freezing point depression.

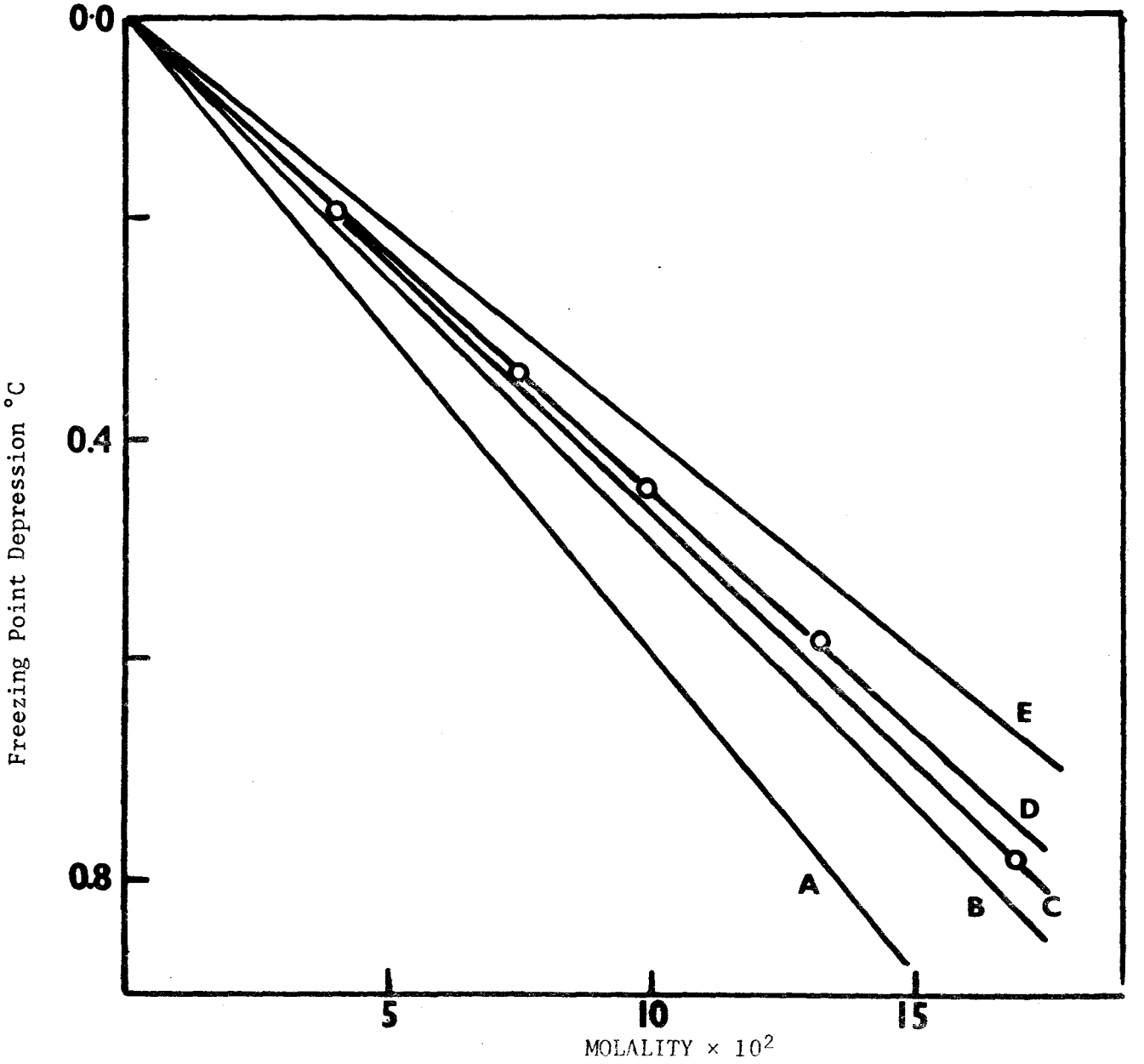

Fig. 1. Freezing point depression of $Te/S_2O_6F_2$ = 2:1 solutions in HSO_3F. The straight lines are calculated freezing point curves for A, Te_2^{2+}; B, Te_4^{4+}; C, Te_6^{6+}; D, Te_8^{8+}; E, $Te_\infty^{\infty+}$.

TABLE III

Calculated Slopes for Various Reactions of Tellurium with $S_2O_6F_2$

Reaction	ν	Theoretical Slope
A	1.50	5.89
B	1.25	4.91
C	1.17	4.60
D	1.12	4.40
E	1.00	3.93

experimental error no very definite conclusion concerning the degree of polymerisation of the cation can be drawn from this experiment except that it is unlikely that the cation is the simple dimer Te_2^{2+}.

3. Cryoscopy in Disulfuric Acid

As the value of n for the cation Te_n^{n+} could not be obtained with any certainty an attempt was made to study the behaviour of tellurium metal in disulfuric acid. Gillespie and coworkers (38,45) have studied the solvent properties of disulfuric acid. They have shown that the reaction of any solute with the solvent may be represented by the following general reaction:

$$\text{solute} + n\ H_2S_2O_7 \longrightarrow a\ X^+ + a\ HS_3O_{10}^- + b\ Y + c\ H_2SO_4$$

where all X are not necessarily identical and Y represents all the uncharged species. The H_2SO_4 produced in the reaction does not contribute very much towards the freezing point depression because of the very extensive solvent self-dissociation.

$$H_2S_2O_7 \rightleftharpoons H_2SO_4 + H_2S_3O_{10}$$

The ν value to a good approximation is given by the relation

$$\nu = 2a + b$$

where a = number of moles of $HS_3O_{10}^-$ produced per mole of the solute; and

b = total number of moles of uncharged particles produced per mole of the solute.

In the present investigations the ν values have been obtained by comparing the experimental curves already reported by Gillespie and coworkers for the formation of Se_4^{2+} and Se_8^{2+} from selenium in disulfuric acid (22).

Tellurium metal dissolves in disulfuric acid to give a red solution. The absorption spectrum of this solution shows absorption bands at 250, 280, 360, 420 and 510 nm (Fig. 2A). The U V - visible absorption spectra of tellurium solutions in HSO_3F and oleum have shown that the bands at 250, 360 and 420 nm are due to Te_n^{n+} and that the 510 nm band is due to Te_4^{2+} cation (44). The 280 nm band is due to SO_2 which is one of the reaction products. In a 2.3×10^{-3} m solution the 510 nm band disappeared after 36 hrs. and the bands at 250, 360 and 420 nm increased in intensity (Fig. 2B) indicating that Te_4^{2+} is gradually being oxidised to Te_n^{n+}. Te_4^{2+} appears to be the first reaction product and is presumably formed by the reaction

$$4Te + 6H_2S_2O_7 \longrightarrow Te_4^{2+} + 2HS_3O_{10}^- + SO_2 + 5H_2SO_4$$

The reaction of tellurium metal with disulfuric acid was followed cryoscopically. The results of freezing point depression measurements are given in Table IV. After a concentration of 0.6 m is reached a white solid starts separating out of the solution. The freezing point measurements were stopped at this point. Comparison of the freezing point curve with the theoretical curves required for the reactions (Fig. 3):

A. $8Te + 6H_2S_2O_7 \longrightarrow Te_8^{2+} + 2HS_3O_{10}^- + SO_2 + 5H_2SO_4$

B. $6Te + 6H_2S_2O_7 \longrightarrow Te_6^{2+} + 2HS_3O_{10}^- + SO_2 + 5H_2SO_4$

C. $4Te + 6H_2S_2O_7 \longrightarrow Te_4^{2+} + 2HS_3O_{10}^- + SO_2 + 5H_2SO_4$

shows that the number of particles formed in the solution are less than required for the reaction C to give Te_4^{2+} as indicated by the absorption spectrum. The freezing point curve suggests that tellurium is oxidised initially to a lower oxidation state than (+1/2) and tellurium in this oxidation state does not show any absorption spectrum. Sulfur and selenium

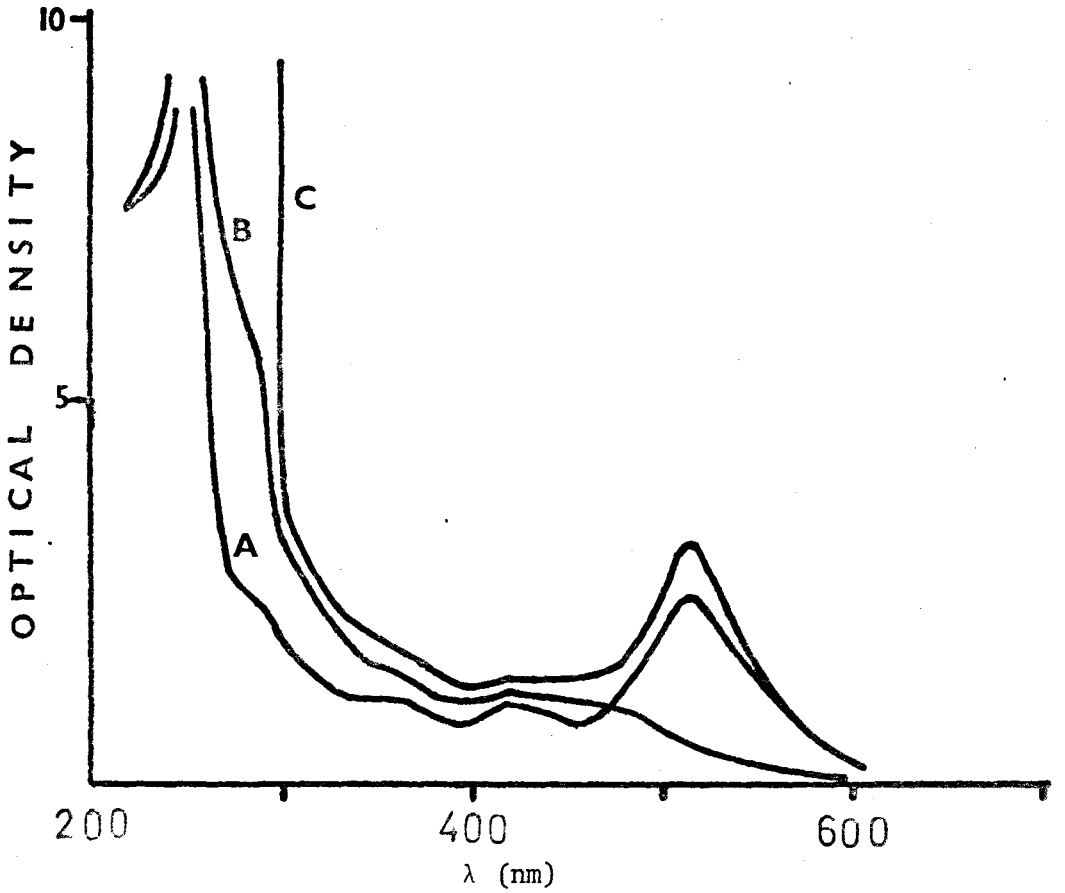

Fig. 2. U.V. and visible absorption spectra of tellurium solutions in $H_2S_2O_7$ (A) 2.3×10^3 M (Te) solution ; (B) Solution A after 36 hrs.; (C) 0.2076 M (Te) solution after 14 days from cryoscope.

TABLE IV

Freezing Points of Solutions of Tellurium in $H_2S_2O_7$

Concentration mole (Te) kg^{-1}	Freezing Point (°C)
0.0649	35.013
0.1689	34.670
0.2076	34.559
0.2917	34.104
0.5119	32.707

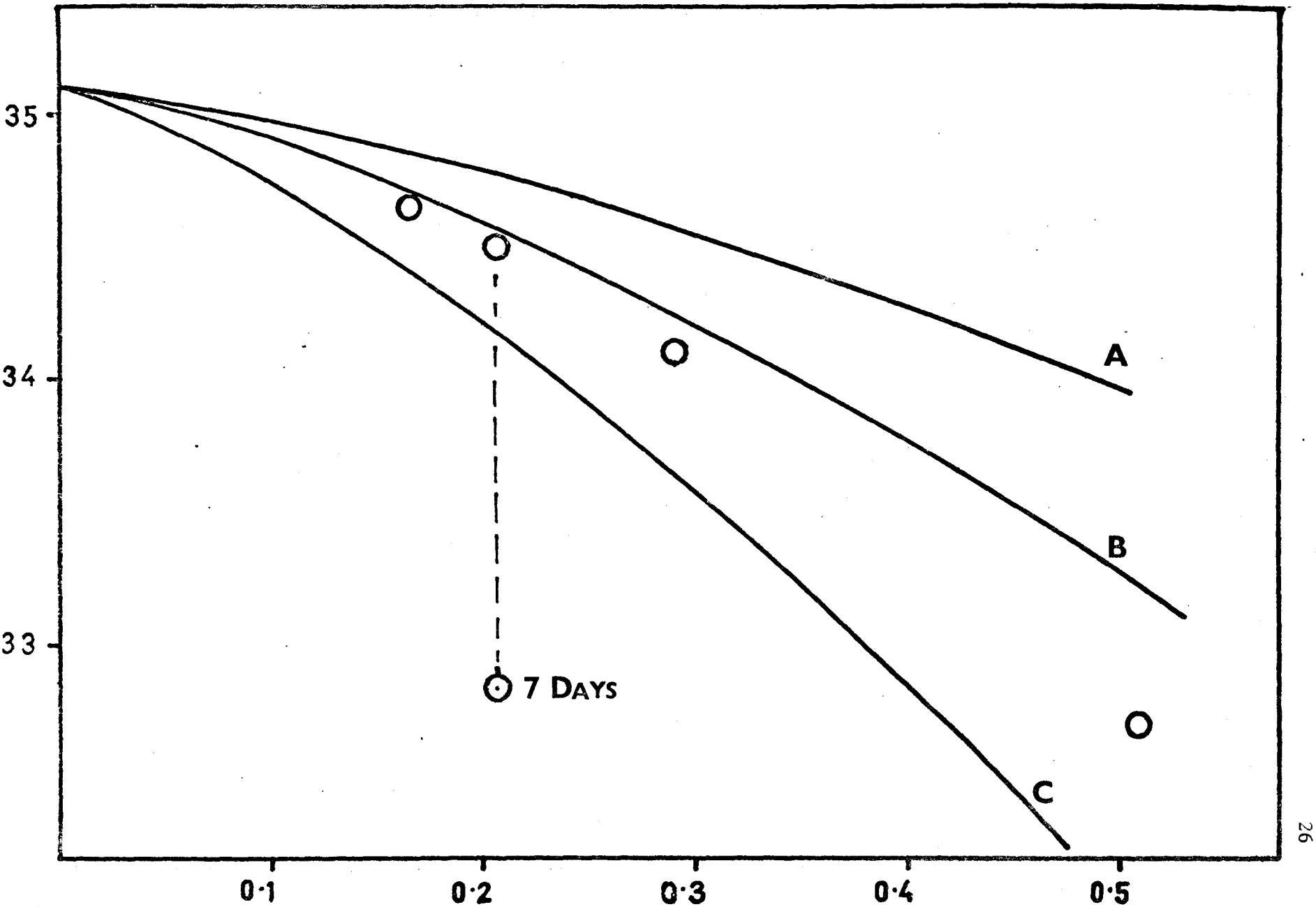

Fig. 3. Freezing points of tellurium solution in $H_2S_2O_7$. The lines are calculated curves for (A) Te_8^{2+}, (B) Te_6^{2+}, (C) Te_4^{2+}.

are known to dissolve in the (+1/4) oxidation states in disulfuric acid and the elements in these oxidation states are further oxidised to (+1/2) oxidation states. Gillespie and coworkers have shown that tellurium can be oxidised to the (+1/3) oxidation state. It appears that tellurium dissolves in disulfuric acid to give a mixture of +1/2 and lower oxidation states.

The solution of tellurium metal in disulfuric acid is not stable. The absorption spectrum shows that the metal is gradually being oxidised to higher oxidation state. This oxidation reaction has been followed cryoscopically. The freezing point measurements were made on a 0.2076 m solution. The variation of the freezing point depression with time is given in Table V and shown in Fig. 3. The decrease in freezing point of the solution with time shows that the metal is gradually being oxidised to a higher oxidation state. The colour of the solution changed from red to orange in two weeks. The absorption spectrum of this orange solution shows a strong absorption below 300 and at 360, 420 and 510 nm (Fig. 2C). Te_n^{n+} shows a strong band at 250 and weak bands at 360 and 420 nm and Te_4^{2+} at 510 nm. The spectrum thus shows that both these cations are present in the solution. Because of high extinction coefficient and high concentration of Te_n^{n+} the peak height of 250 nm could not be obtained and the ratio of concentrations of tellurium in the two oxidation states could not be obtained. Dilution of this solution in disulfuric acid resulted in an immediate change in the colour of the solution to yellow and no absorption at 510 nm of Te_4^{2+} cation is observed.

On leaving this solution for one month it became colourless. This can be best explained by assuming that the tellurium is gradually being oxidised

TABLE V

Change in Freezing Points of 0.2076 m(Te) Solution in $H_2S_2O_7$ with time

Time (hrs)	Freezing Point (°C)
0.42	34.559
2.42	34.449
4.25	34.413
9.50	34.395
21.50	34.357
32.50	34.342
54.00	34.058
76.00	33.770
101.00	33.507
119.00	33.410
167.00	32.846
221.00	32.068
310.00	31.448

to some oxidation state greater than (+1) probably Te (IV).

Thus no definite information could be obtained from this freezing point experiment.

4. Structures for Te_n^{n+}

It appears that the Te (+1) is probably one of the polyatomic cations Te_4^{4+}, Te_6^{6+} or Te_8^{8+}. Te_4^{4+} is isoelectronic with P_4 and would be expected to have a tetrahedral structure. Te_6^{6+} might have the benzene type or trigonal prism type and Te_8^{8+} could have a cubic structure.

Te_4^{4+}

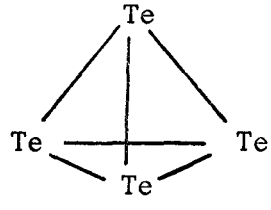

Te_6^{6+}

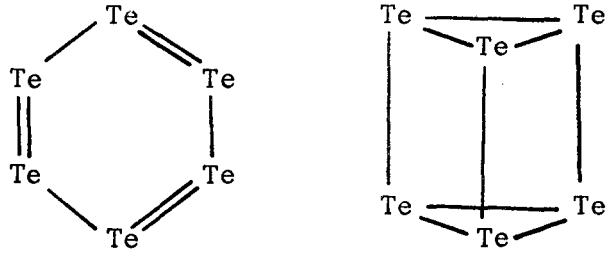

Te_8^{8+}

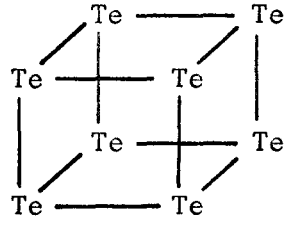

It would appear that it will only be possible to obtain the molecular weight and structure of this cation from X-ray crystallography. Unfortunately no suitable single crystal has yet been prepared.

5. Conclusion

The present work provided the confirmation of the existence of tellurium in the (+1) oxidation state. Cryoscopic measurements show that the tellurium is almost certainly present in the form of a polyatomic cation and that this is not Te_2^{2+}. Unfortunately the cryoscopic results were not accurate enough to distinguish, with certainty, between other possible formulae such as Te_4^{4+}, Te_6^{6+} and Te_8^{8+}.

CHAPTER IV

FORMATION OF SULFUR CATIONS IN FLUOROSULFURIC ACID

1. Introduction

Coloured solutions of sulfur in oleum and sulfuric acid have been known for a long time (20). In the previous chapter on the oxidation of tellurium, the evidence for the formation of cations Te_4^{2+} and Te_n^{n+} in solution in HSO_3F and $H_2S_2O_7$ has been discussed. It has also been shown that selenium can be oxidised in these acid solvents to the cations Se_4^{2+} and Se_8^{2+} (22).

Blue solutions of sulfur in strong acids have been the subject of considerable investigations. Weber (46), and Partington and coworkers (47), attributed the blue colour to the compound S_2O_3. Auerbach (48) made cryoscopic measurements on the solution of sulfur in oleum and concluded that sulfur dissolved as S_2 molecules. Brayford and Wyatt (49) made cryoscopic measurements on solutions of sulfur in oleum but found that the solutions were not very stable so that no definite conclusions could be drawn from these results. Symons et al (50-52) have made a series of experiments on the blue solutions of sulfur in oleum. They observed that during electrolysis the blue colour of the solution moved towards the cathode indicating that the blue colour is due to a cationic species. These workers have also reported that the solution shows an e.s.r. spectrum and must therefore contain radicals. Lux and Bohm (53) have suggested that the blue colour of the sulfur in oleum is due to a species S_x but they could not obtain the value of x. The reaction of sulfur with $S_2O_6F_2$ has been studied by Cady and

Shreeve. They reported that the colour of the mixture changes from yellow to orange, yellow blue and green and explained this colour change as being due to surface effects (54). Gillespie and Passmore (55) prepared blue and red compounds of sulfur by oxidising sulfur with AsF_5 in HF. The elemental analyses of these compounds were consistent with the empirical formulae $S_4(AsF_6)$ for the blue compound and $S_8(AsF_6)$ for the red compound. In the present work the oxidation of sulfur with $S_2O_6F_2$ in solutions in fluorosulfuric acid has been studied.

2. U V and Visible Absorption Spectra

Sulfur does not dissolve in pure fluorosulfuric acid. However in the presence of the oxidising agent $S_2O_6F_2$ it gives successively orange, green, blue and light yellow solutions. For a mole ratio $S/S_2O_6F_2$ 16:1 complete dissolution of sulfur was observed to give an orange solution. The U V visible absorption spectrum of this solution shows a maximum absorption at 235 nm (Fig. 4A). As the concentration of $S_2O_6F_2$ is increased the colour of the solution changes to green. The spectrum of the green solution ($S/S_2O_6F_2$ = 12:1) shows two absorption bands at 235 and 590 nm (Fig. 4B). The optical density is observed to increase at 590 nm and to decrease at 235 nm with the increasing concentration of $S_2O_6F_2$ in the solution. The 590 nm band has a maximum intensity at a $S/S_2O_6F_2$ mole ratio of 8:1. At this composition there is also an absorption at 330 nm and the 235 nm absorption has disappeared. Further addition of $S_2O_6F_2$ to the solution results in a decrease of the intensity of the absorption at 590 nm and an increase in that at 330 nm. At the $S/S_2O_6F_2$ mole ratio of 6:1 the spectrum shows two bands at 330 and 590 nm (Fig. 4D). The 330 nm band has a maximum

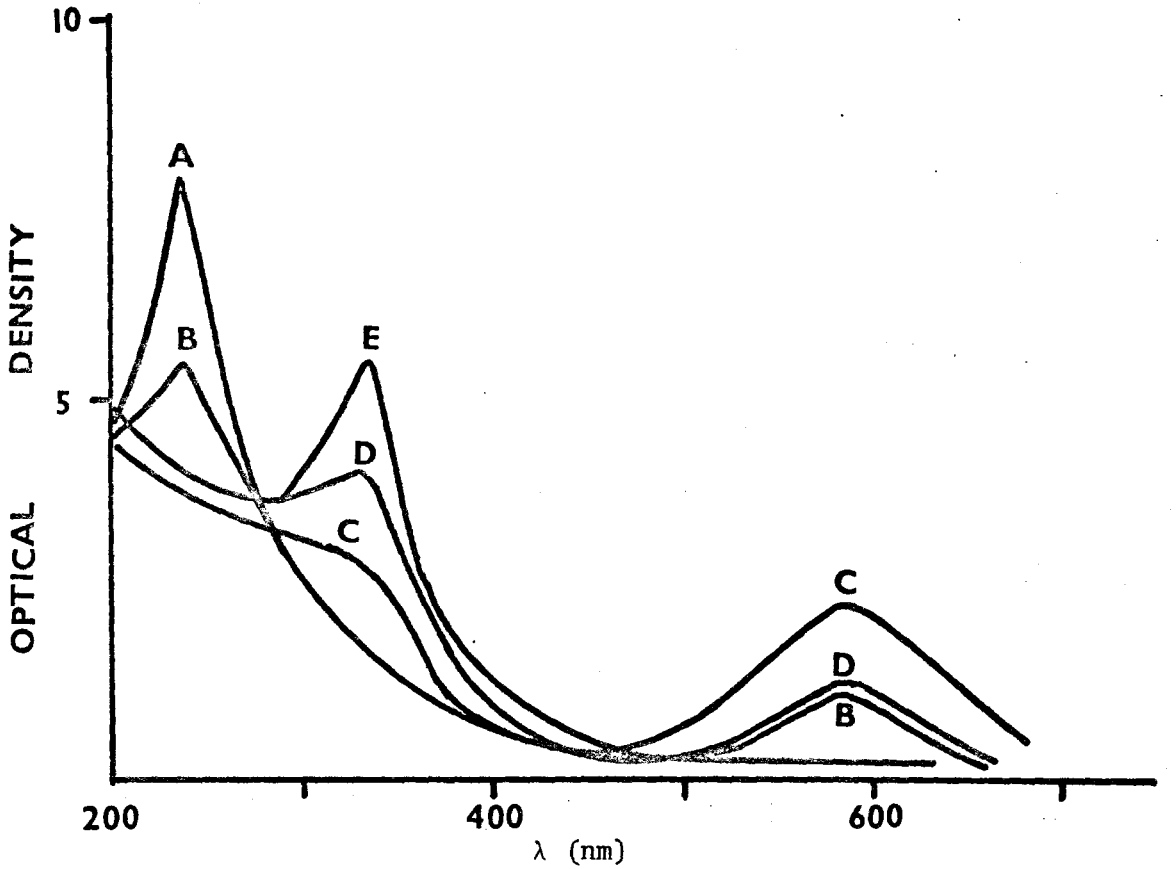

Fig. 4. U V and visible absorption spectra of $S/S_2O_6F_2$ mixtures in HSO_3F.
$S/S_2O_6F_2$ = (A) 16:1; (B) 12:1; (C) 8:1; (D) 6:1; (E) 4:1.

intensity at a $S/S_2O_6F_2$ mole ratio of 4:1 (Fig. 4E). At this mole ratio the solution does not show any absorption at 590 nm. Further addition of $S_2O_6F_2$ does not affect the 330 nm peak nor is any other absorption observed in the spectrum.

The absorption spectra measurements thus show the formation of three compounds in solution. Since $S_2O_6F_2$ acts as an oxidising agent according to the reaction

$$S_2O_6F_2 + 2e \longrightarrow 2SO_3F^-$$

It seems reasonable to conclude that the oxidation of sulfur with $S_2O_6F_2$ gives rise to one or more of the following cationic species corresponding to each of the oxidation states S(1/8), S(1/4) and S(1/2).

$S/S_2O_6F_2$	Possible Oxidation States
16:1	S_8^+ S_{16}^{2+} S_{24}^{3+} .....
8:1	S_4^+ S_8^{2+} S_{12}^{3+} .....
4:1	S_2^+ S_4^{2+} S_6^{3+} .....

Of these three solutions the orange solution (16:1) was found to be the most stable. No change was observed on storing this solution for 15 to 20 days. No pure solid compound could however be isolated from this solution as on evaporating the solvent some elemental sulfur was always formed. The blue solution was the most unstable and disproportionated rapidly to give a light yellow solution and elemental sulfur.

3. Cryoscopic Measurements

Cryoscopic measurements were made on the solutions having the composition $S/S_2O_6F_2$ = 16:1. The results of the freezing point depression

measurements are given in Table VI.

From the slope of the freezing point (Fig. 5) curve an average ν value of 1.54 per mole S_8 was obtained. This ν value is consistent with the reaction

$$2S_8 + S_2O_6F_2 \longrightarrow S_{16}^{2+} + 2SO_3F^-$$

which requires $\nu = 1.5$.

4. Conductivity Measurements

The cryoscopic experiment shows the formation of three particles per mole of S_8 and the solution is expected to be highly conducting. The results of specific conductivity measurements on solutions having the composition $S/S_2O_6F_2 = 16:1$ at 25°C are given in Table VII. From the comparison of the specific conductivity plot with that for barium fluorosulfate solution (30) in HSO_3F (Fig. 6), it may be seen that $\gamma = 1$ per mole S_8 or $\gamma = 2$ per mole S_{16}. The γ value is again consistent with the reaction

$$2S_8 + S_2O_6F_2 \longrightarrow S_{16}^{2+} + 2SO_3F^-$$

It is concluded that the orange solution of sulfur which shows a strong absorption at 235 nm contains the cation S_{16}^{2+}. As the red compounds $S_{8n}(AsF_6)_n$ and $S_{8n}(SbF_6)_n$ also have an absorption at 235 nm they may reasonably be formulated as containing the cation S_{16}^{2+}.

At the $S/S_2O_6F_2$ mole ratio of 8:1 the solution in HSO_3F has a deep blue colour. No freezing points could however be obtained on these solutions as they are not very stable and decompose to elemental sulfur and a light yellow solution. Attempts to measure the freezing points of solutions of the compound $S_{4n}(AsF_6)_n$ were also not successful as again

TABLE VI

Freezing Points of $S/S_2O_6F_2$ 16:1 Solution in HSO_3F

Concentration mol S_8 kg^{-1}	θ °C
0.1798	0.14
0.2764	0.19
0.5021	0.36
0.5035	0.39
0.7253	0.54
0.8763	0.62
0.9298	0.74
0.9542	0.76

θ = Freezing point depression.

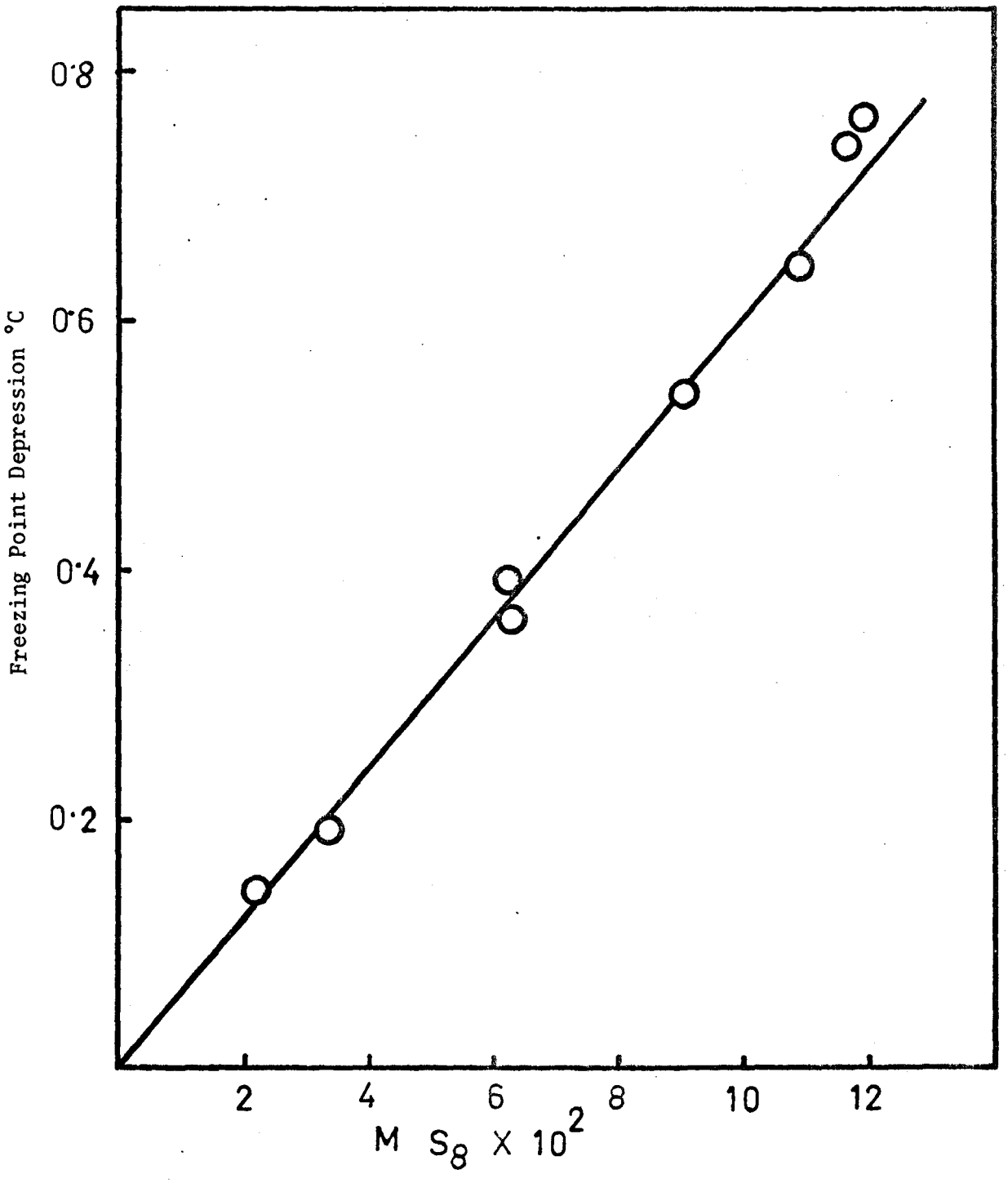

Fig. 5. Freezing point depressions $S/S_2O_6F_2$ 16:1 solutions in HSO_3F.

TABLE VII

Conductivity of $S/S_2O_6F_2$ 16:1 Solution in HSO_3F at 25°C

Concentration mol (S_8) kg^{-1}	Sp. Conductivity $\times 10^4$, $ohm^{-1}cm^{-1}$
0.0064	16.7533
0.0280	53.6710
0.0534	94.5562
0.0830	139.1607
0.1034	167.6795
0.1110	178.1289

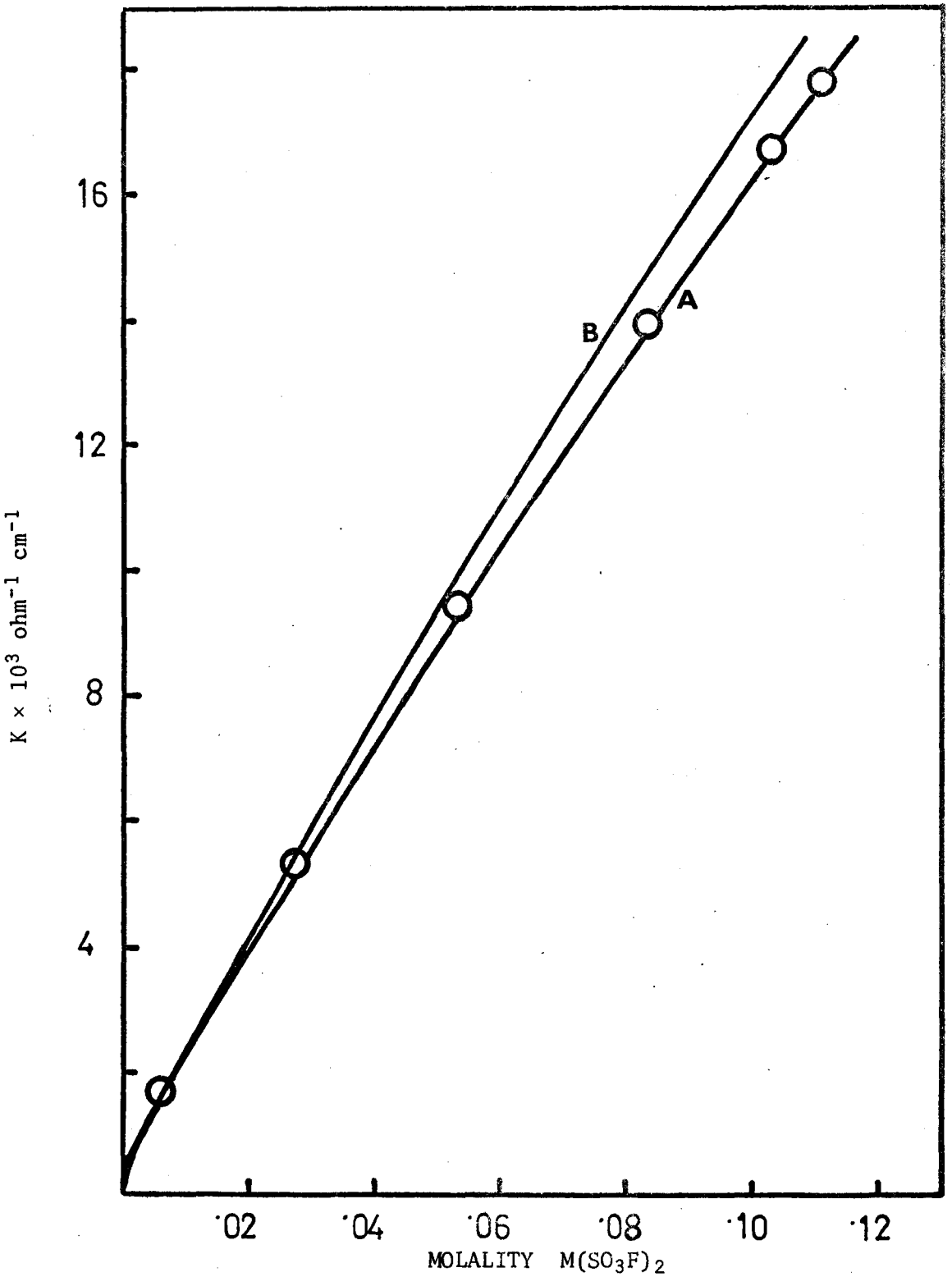

Fig. 6. Conductivities in HSO_3F at 25°C. (A) $S/S_2O_6F_2$ 16:1; (B) $Ba(SO_3F)_2$.

there was disproportionation in HSO_3F.

5. Solutions of sulfur in Disulfuric Acid

Sulfur dissolves in disulfuric acid to give a blue solution. The reaction of sulfur with the solvent can be represented by the following general equation

$$nS + 3H_2S_2O_7 \longrightarrow S_n^+ + HS_3O_{10}^- + 2.5H_2SO_4 + 0.5SO_2$$

U V - visible absorption spectrum of a 2.1×10^{-3} M solution shows three absorption bands at 280, 330, and 590 nm (Fig. 7A). The band at 280 nm is due to SO_2 which is one of the reaction products. The variation with time of the absorption spectrum and of the freezing points of solutions of sulfur in disulfuric acid show that they are not stable. In the absorption spectrum the intensity of the band at 590 nm decreases and that at 330 nm increases with time indicating that the compound which absorbs at 590 nm is formed first and is then gradually oxidised to a higher oxidation state.

6. Cryoscopy of Sulfur Solutions in Disulfuric Acid

The freezing point depressions of the solution of sulfur in disulfuric acid was studied with time. The results of measurements on solutions having the composition 0.3341 and 0.5470 mol(S)kg^{-1} are given in Table VIII. The freezing points of the solution at zero time was then obtained by extrapolation (Fig. 8). The freezing points thus obtained compare well with those expected for the reaction (Fig. 9)

$$8S + 6H_2S_2O_7 \longrightarrow S_8^{2+} + 2HS_3O_{10}^- + 5H_2SO_4 + SO_2$$

Hence it is reasonable to suppose that the absorption band at 590 nm of the solution of sulfur in disulfuric acid is due to the cation S_8^{2+}. The

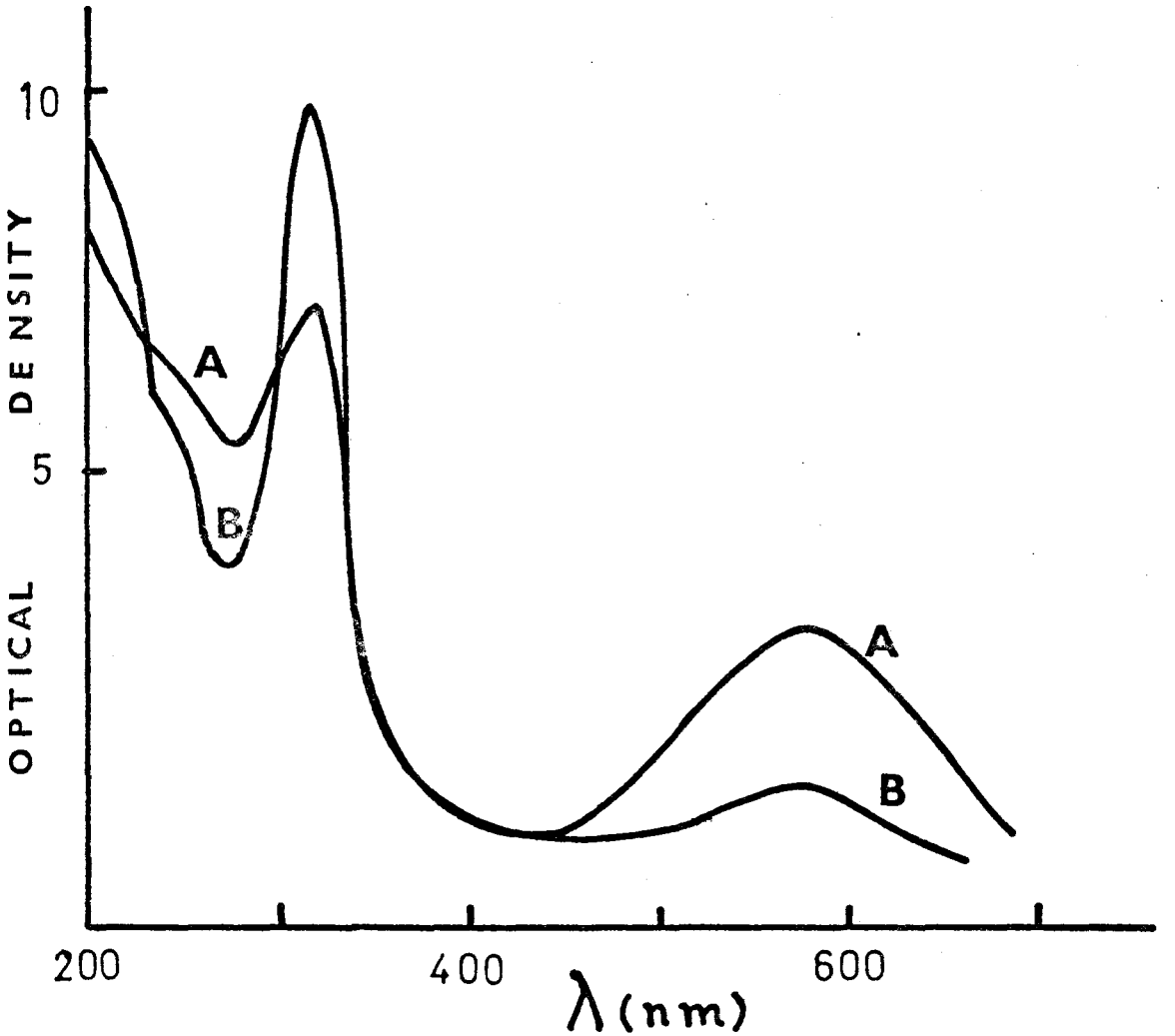

Fig. 7. U V and visible absorption spectra of sulfur solutions in $H_2S_2O_7$. (A) 2.1×10^{-3} M solution; (B) solution A after 24 hrs.

TABLE VIII

Freezing Points of Sulfur Solutions in $H_2S_2O_7$ with Time

0.3341 mol (S) kg^{-1}		0.5470 mol (S) kg^{-1}	
Time (hrs)	Freezing Point (°C)	Time (hrs)	Freezing Point (°C)
0.75	34.024	0.58	32.735
1.30	33.926	1.33	32.087
1.86	33.833	2.00	31.428
2.46	33.738	4.92	29.724
4.00	33.602	8.25	28.418
5.75	33.401	11.75	27.837
8.50	33.077	23.75	26.239
13.50	32.647		
24.75	31.491		
32.25	31.412		

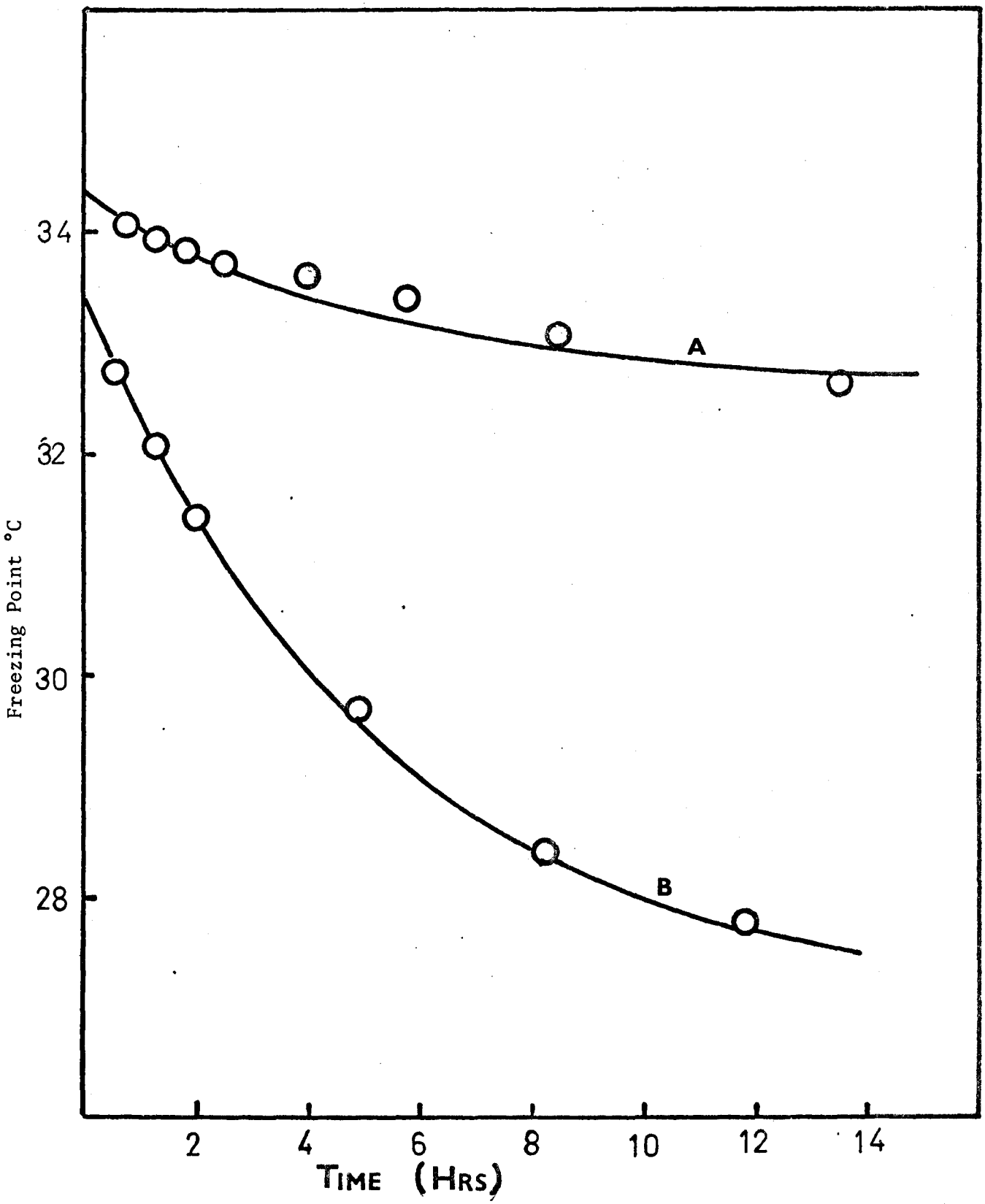

Fig. 8. Freezing points of sulfur solution in $H_2S_2O_7$. (A) 0.3341 mol solution; (B) 0.5470 mol solution.

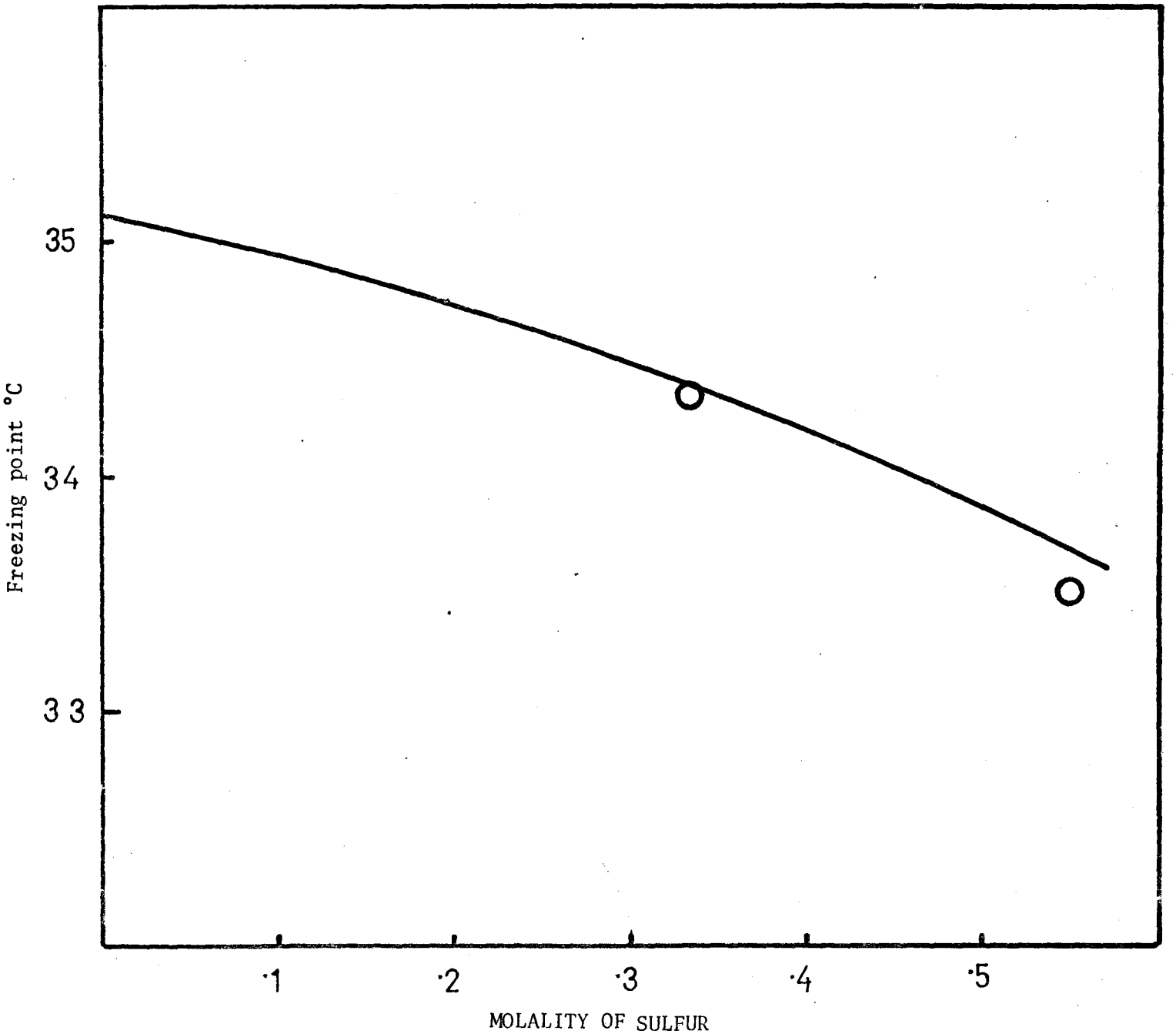

Fig. 9. Freezing point of fresh sulfur solutions in $H_2S_2O_7$.

blue solution of $S/S_2O_6F_2$ = 8:1 and the compounds $S_{4n}(AsF_6)_n$ and $S_{4n}(SbF_6)_n$ in HSO_3F also show the strong absorption band at 590 nm and they also therefore contain the S_8^{2+} cation.

The absorption band at 330 nm has been assigned to the S_4^{2+} cation in oleum and superacid (56). The solution of $S/S_2O_6F_2$ = 4:1 also shows a similar absorption band at 330 nm. We conclude therefore that the cation S_4^{2+} is present in the solution. It has also been found that the solutions of S_4^{2+} in HSO_3F are not stable with time so no attempt at cryoscopic and conductivity measurements were made on these solutions.

7. E.s.r. Spectrum

Symons et al (52) have studied the e.s.r. spectrum of the blue solution of sulfur in oleum at room temperature and at 77°C. The frozen solution shows strong e.s.r. signals (g 2.018, 2.003 sh, and 2.025, 2.032 sh). They attributed these signals to the radicals present in small concentration in the solutions.

A solution obtained by oxidising sulfur with $S_2O_6F_2$ in HSO_3F shows three e.s.r. signals with g = 2.027, 2.014 and 2.010 respectively. The intensity of the signals at g = 2.027 and g = 2.014 depends on $S/S_2O_6F_2$ mole ratio in the solution whereas the very weak signal with g = 2.010 is unaffected. At a mole ratio of $S/S_2O_6F_2$ = 16:1 the signal with g = 2.027 has the maximum intensity (Fig. 10). As the concentration of $S_2O_6F_2$ increases in solution the intensity of the signal g = 2.027 decreases and that at g = 2.014 increases till $S/S_2O_6F_2$ mole ratio of 8:1 is reached. At this mole ratio the signal with g = 2.014 has the maximum intensity. The intensity of this signal starts decreasing with the further increase in concentration of $S_2O_6F_2$. The solution does not show any e.s.r. signal at

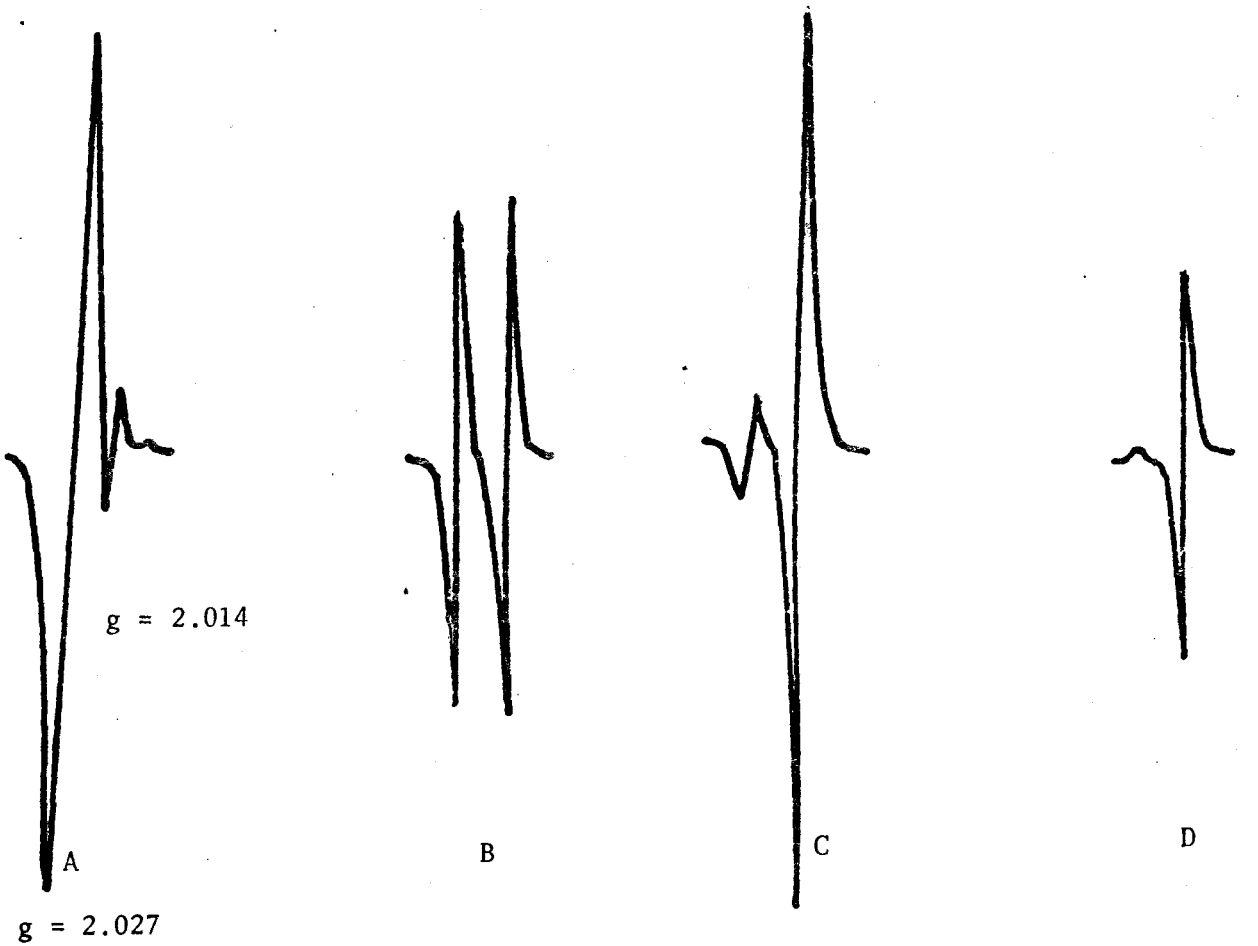

Fig. 10. E.s.r. spectra of $S/S_2O_6F_2$ mixtures in HSO_3F. $S/S_2O_6F_2$ = (A) 16:1; (B) 12:1; (C) 8:1; (D) 6:1.

the 4:1 mole ratio.

Cryoscopic and conductivity measurements have shown that at the $S/S_2O_6F_2$ mole ratios of 16:1 and 8:1, the cations S_{16}^{2+} and S_8^{2+} are present in HSO_3F respectively. Thus the e.s.r. signals with g = 2.027 and 2.014 are associated with the cations S_{16}^{2+} and S_8^{2+}. It seems most likely therefore that small amounts of the radicals S_8^+ and S_4^+ are present in equilibrium with S_{16}^{2+} and S_8^{2+} respectively.

$$S_{16}^{2+} \rightleftharpoons 2S_8^+ \qquad g = 2.027$$

$$S_8^{2+} \rightleftharpoons 2S_4^+ \qquad g = 2.014$$

The third signal with g = 2.010 could not be assigned. The oxidation of sulfur can be envisaged as taking place in stages. The first step is the loss of one electron giving the radical cation S_8^+ which dimerises to give S_{16}^{2+} having only a small equilibrium concentration of S_8^+. On further oxidation S_8^+ loses one more electron to become S_8^{2+} which presumably has a slight tendency to dissociate into the radical cation S_4^+ and this is further oxidised to S_4^{2+}.

Much interest has been shown in recent years about the radicals in the solutions of sulfur in oleum. In order to explain the observed e.s.r. spectra Gigenbach (57) has suggested that the blue solution contains the radicals S_4^+ (g = 2.0131) and an open chain S_n^+ (g = 2.026). He also claims that the radical S_4^+ dimerises to give diamagnetic S_8^{2+} cation which he considered to be the main species in the yellow solution. Symons and coworkers (58) have repeated their earlier e.s.r. studies of solutions of sulfur in 65% oleum using 21% ^{33}S enriched sulfur and reported that their spectra were consistent with the radical in this solution containing

S_8^+ (g = 2.013) and not S_4^+. Later work by Stephens (59) using 91% ^{33}S enriched sulfur has shown however that the spectra are in fact completely consistant with the radical S_4^+ (g = 2.0163). Gillespie and Ummat (60) have studied solutions of sulfur in oleum containing varying amounts of sulfur trioxide. From e.s.r. and U.V. visible absorption spectroscopy these workers have concluded that the cations S_{16}^{2+} and S_8^{2+} are formed in the solution in equilibrium with small concentrations of the radicals S_8^+ (g = 2.027) and S_4^+ (g = 2.014) respectively.

8. Structure of Sulfur Cations

S_4^{2+}

Stephens (61) has studied the m.c.d. of the solution of sulfur in 30% oleum. The m.c.d. of the 330 nm band due to S_4^{2+} is identical with that of Te_4^{2+} and Se_4^{2+} which have square planar structures and on this basis he proposed that S_4^{2+} also has a square planar structure. Gillespie and coworkers (62) have studied the Raman spectrum of S_4^{2+} and have confirmed the square planar structure of this cation.

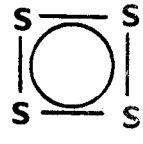

S_8^{2+}

The structure for S_8^{2+} has been recently reported from this laboratory from X-ray crystallographic studies (63). It has a bicyclic structure similar to that reported for Se_8^{2+}. The structure, bond lengths and bond angles for S_8^{2+} are:

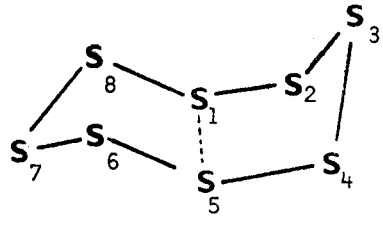

S_1S_5 = 2.86 Å

S_8S_6 = 3.00 Å

S_2S_4 = 2.94 Å

S_1S_7 = 3.07 Å

S_5S_7 = 3.09 Å

S_3S_1 = 3.14 Å

S_3S_5 = 3.17 Å

Average S-S bond length around the ring = 2.037 Å

$S_2S_3S_4 = S_6S_7S_8 = 93°$.

All other angles = 102°.

In the S_8^{2+} ring there is a number of S-S distances smaller than the van der Waal's non-bonding interactions of 3.3 Å, and presumably therefore there is some interaction between these sulfur atoms.

S_{16}^{2+}

No structural data is available so far for S_{16}^{2+}. It may have a structure in which two S_8 rings are joined together by a single sulfur-sulfur bond as

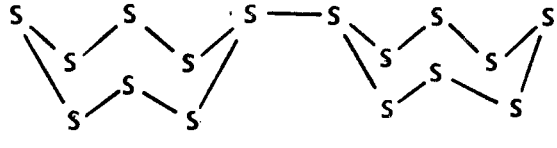

9. Conclusion

Photometric data of the oxidation reaction of sulfur with $S_2O_6F_2$ shows that sulfur is oxidised with $S_2O_6F_2$ in the $S/S_2O_6F_2$ mole ratios of 16:1, 8:1 and 4:1 respectively. Cryoscopic and conductivity measurements of $S/S_2O_6F_2$ = 16:1 solution in HSO_3F shows that the cation S_{16}^{2+} is formed in the solution. The solution $S/S_2O_6F_2$ = 8:1 in HSO_3F and the solutions of sulfur in disulfuric acid which have the same absorption spectrum are not stable. The cryoscopic measurements of the freshly prepared solutions of sulfur in disulfuric acid suggest the formation of the cation S_8^{2+} which however is

not stable and is further oxidised to S_4^{2+} and SO_2. The solutions of $S_8(AsF_6)_2$ and $S/S_2O_6F_2$ = 8:1 in HSO_3F and solution of sulfur in disulfuric acid are blue and show absorption bands at 590 nm. The solid $S_8(AsF_6)_2$ has been shown from X-ray crystallographic studies to contain the cation S_8^{2+} thus confirming that this cation is also present in $S/S_2O_6F_2$ = 8:1 in HSO_3F and solutions of sulfur in $H_2S_2O_7$. The cations S_{16}^{2+} and S_8^{2+} in HSO_3F are in equilibrium in small concentration with the radicals S_8^{+} and S_4^{+}. Similar e.s.r. evidence for these radicals have been obtained from solutions of sulfur in oleum.

CHAPTER V

FORMATION OF ANTIMONY CATIONS IN HSO_3F

1. Introduction

The purpose of the work described in this chapter was to attempt to prepare polyatomic cations of the Group V elements and in particular antimony. The cations and homopolyatomic cations of bismuth, Bi^+, Bi_5^{3+}, Bi_8^{2+} and Bi_9^{5+}, have been well characterised in molten salt media (64-67). The metal atom in these cations has a lower formal oxidation state than the most stable oxidation states known for this element in aqueous solutions. Woolf and coworkers (68) have reported that elemental arsenic and antimony dissolve in fluorosulfuric acid to give colourless solutions and white precipitates which they assumed to be fluorosulfates. Paul and coworkers (69) have claimed the formation of polyatomic cations Sb_8^{2+} and Sb_4^{2+} in fluorosulfuric acid by oxidising antimony metal with $S_2O_6F_2$. Gillespie and Dean (70) have studied the reaction of AsF_5 with antimony metal in liquid sulfur dioxide ; they obtained a white solid compound which on the basis of elemental analysis has been formulated as $Sb_n(AsF_6)_n$. In the present investigations the reactions of antimony metal with fluorosulfuric acid have been studied.

2a. Reaction of Antimony Metal with Fluorosulfuric Acid

When finely powdered antimony metal is added in small amounts to fluorosulfuric acid it dissolves gradually to give a colourless solution. The absorption spectrum of this solution shows strong bands at 225-250 and 280 nm (Fig. 11A). Sulfur dioxide absorbs strongly in the 280 nm region. After the solution had been kept under vacuum for 15-20 min. the absorption spectrum

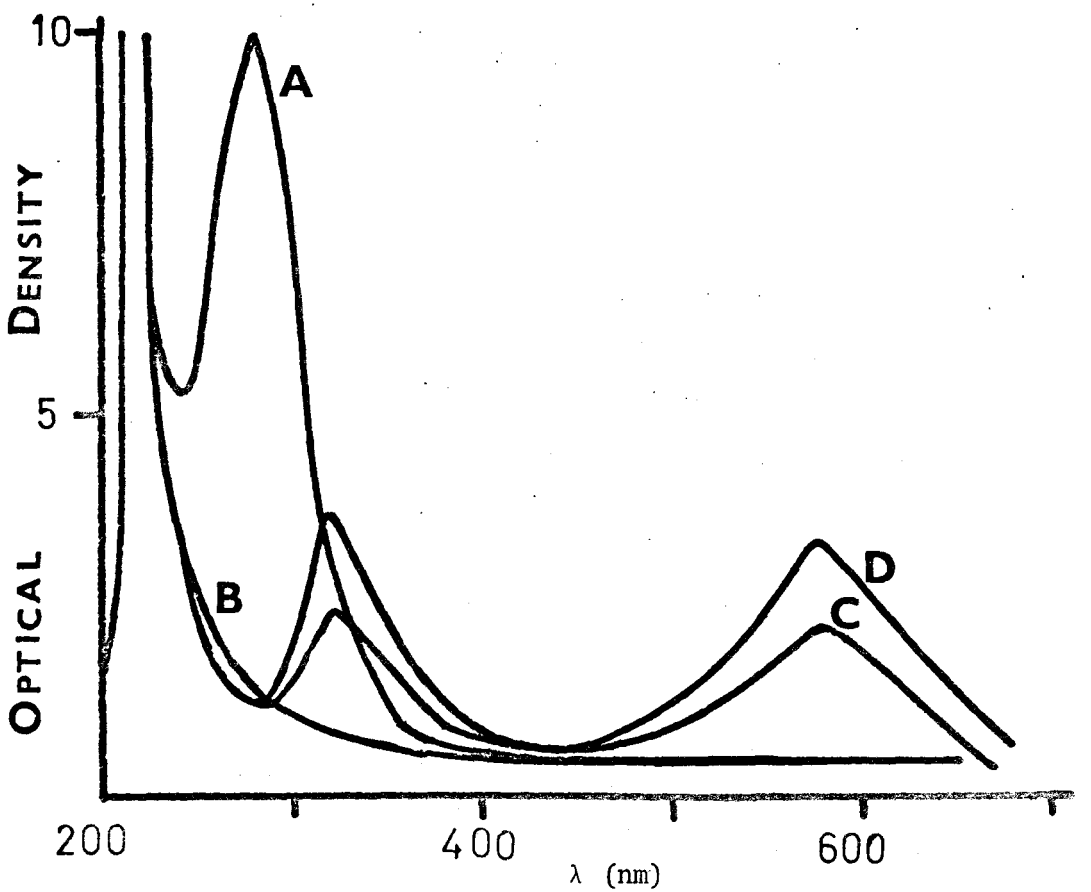

Fig. 11. U V and visible absorption spectra of antimony solutions in HSO_3F. (A) 0.0119 mol (Sb) solution; (B) solution A after kept in vacuum for 20 mins.; (C) solution B after 24 hrs. (D) solution B after 48 hrs.

showed the complete absence of the 280 nm peak (Fig. 11B). On storing this solution for 24-36 hrs a slight green colour developed in the solution. The spectrum of this solution showed absorptions at 225-250, 280, 330 and 590 nm (Fig. 11C and D). The amount of sulfur dioxide formed during the dissolution of antimony metal in fluorosulfuric acid was estimated from the absorption spectrum. A 0.0288 m solution of antimony gave a 0.0268 m solution in sulfur dioxide, indicating that in this experiment one mole of antimony reacts with fluorosulfuric acid to produce one mole of sulfur dioxide. The formation of sulfur dioxide clearly shows that antimony is oxidised when it dissolves in fluorosulfuric acid although Paul et al (69) concluded that it dissolved unchanged.

The metal dissolves up to a concentration of 0.08 molal but if one attempts to increase the concentration above this value a white precipitate separates out of the solution. This white solid was filtered off and washed with sulfur dioxide repeatedly to remove the last traces of the acid. The elemental analysis of this solid corresponded to the composition $Sb(SO_3F)$. Found: Sb, 52.54%; S, 14.30%; F, 8.33%. Required: Sb, 55.20%; S, 14.48%; F, 8.60%. The analytical results of this solid product indicate that antimony is in the (+1) oxidation state in this compound as was previously also observed for the compound $Sb(AsF_6)$.

Antimony metal reacts with fluorosulfuric acid at the boiling point to give a white solid having a very low solubility in fluorosulfuric acid. The elemental analysis of this compound was found to correspond to SbF_2SO_3F (found: Sb, 47.60%; S, 11.90%; required: Sb, 46.90%; S, 12.30%) showing that fluorosulfuric acid oxidises the antimony metal to the trivalent state at 162°C.

2b. Cryoscopic Measurements

The reaction of antimony metal with fluorosulfuric acid at room temperature has been followed cryoscopically. The freezing point data is given in Table IX. From the slope of the freezing point curve a ν-value of 4.3 per mol Sb was obtained (Fig. 12). The change in the absorption spectrum of a solution of antimony in fluorosulfuric acid with time shows that the solution is not stable; this is in agreement with the fact that the freezing point of a 0.0406 molsolution was found to decrease by -0.05°C in 48 hrs. After this time the solution had developed a yellowish-green colour and had the absorption spectrum as in Fig. 11D.

2c. Conductivity Measurements

The specific conductivity of solutions of antimony metal in HSO_3F was measured at various concentrations at 25°C (Table X). Comparison of the results with specific conductivity of KSO_3F solutions gave a γ-value of 0.56 (Fig. 13). The specific conductivity of a 0.0481 molsolution changed from 66.15×10^4 to 67.02×10^4 ohm^{-1} cm^{-1} in 30 hrs. The specific conductivity data was obtained by making up a fresh solution for each concentration (Table X).

Possible reactions of antimony metal with fluorosulfuric acid can be written as follows.

Ia $2Sb + 4HSO_3F \longrightarrow 2Sb^+ + 3SO_3F^- + H_3O^+ + SO_2 + HF$

$\nu = 4 \quad \gamma = 1.4$

Ib $\longrightarrow 2Sb(SO_3F) + SO_3F^- + H_3O^+ + SO_2 + HF$

$\nu = 3 \quad \gamma = 0.46$

TABLE IX

FREEZING POINT DATA OF ANTIMONY SOLUTIONS IN HSO_3F

Concentration $mol(Sb)kg^{-1}$	θ °C
0.0172	0.28
0.0285	0.46
0.0386	0.63
0.0406	0.64
0.0561	0.94
0.0640	1.03
0.0784	1.34

θ = freezing point depression.

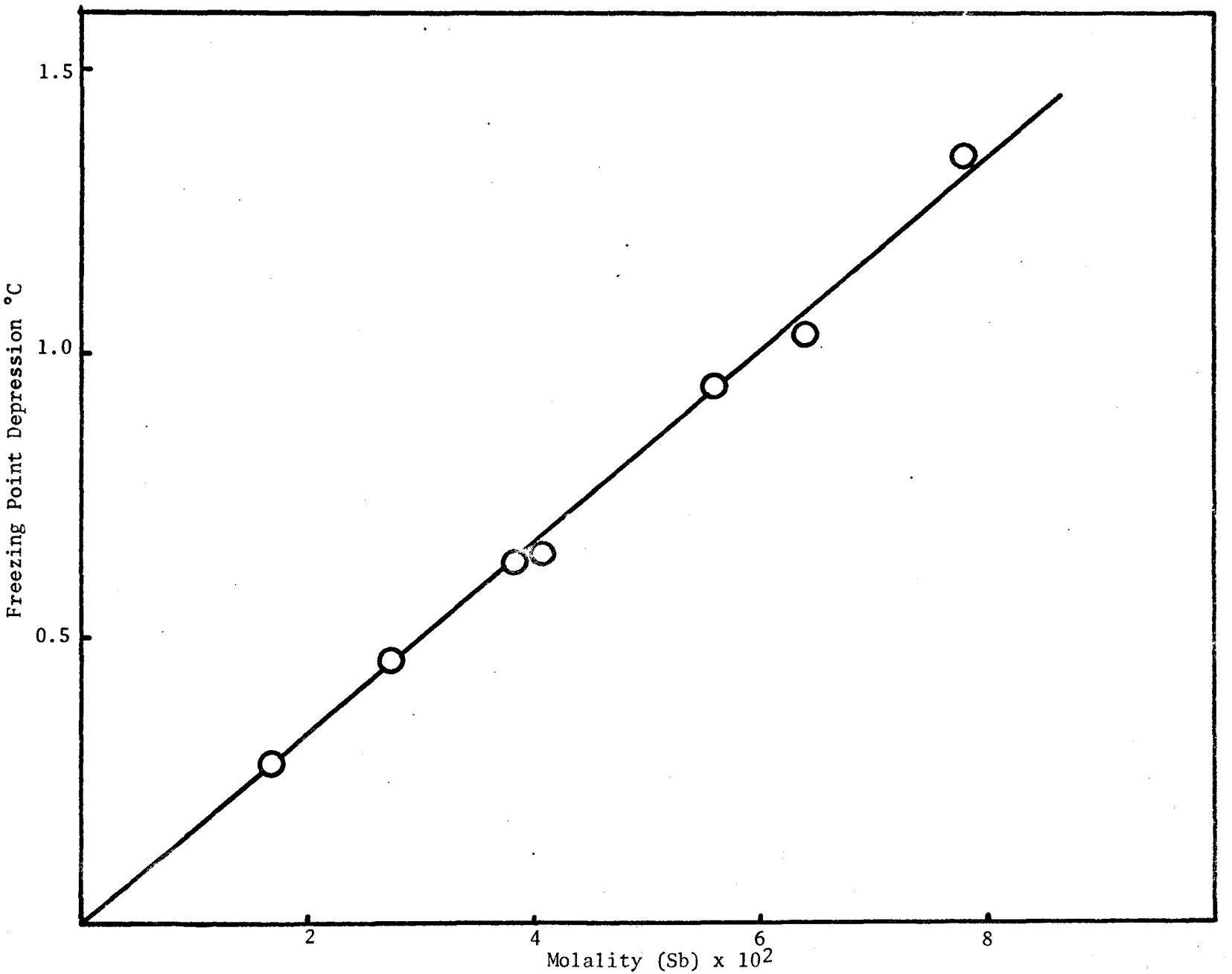

Fig. 12. Freezing point depression of antimony solutions in HSO_3F.

TABLE X

SPECIFIC CONDUCTIVITY OF ANTIMONY SOLUTIONS IN HSO_3F AT 25°C

Concentration $mol(Sb)Kg^{-1}$	Sp. Conductivity $\times 10^4$ ohm^{-1} cm^{-1}
0.0106	13.29
0.0154	23.32
0.0249	29.27
0.0481	66.15
0.0625	87.43

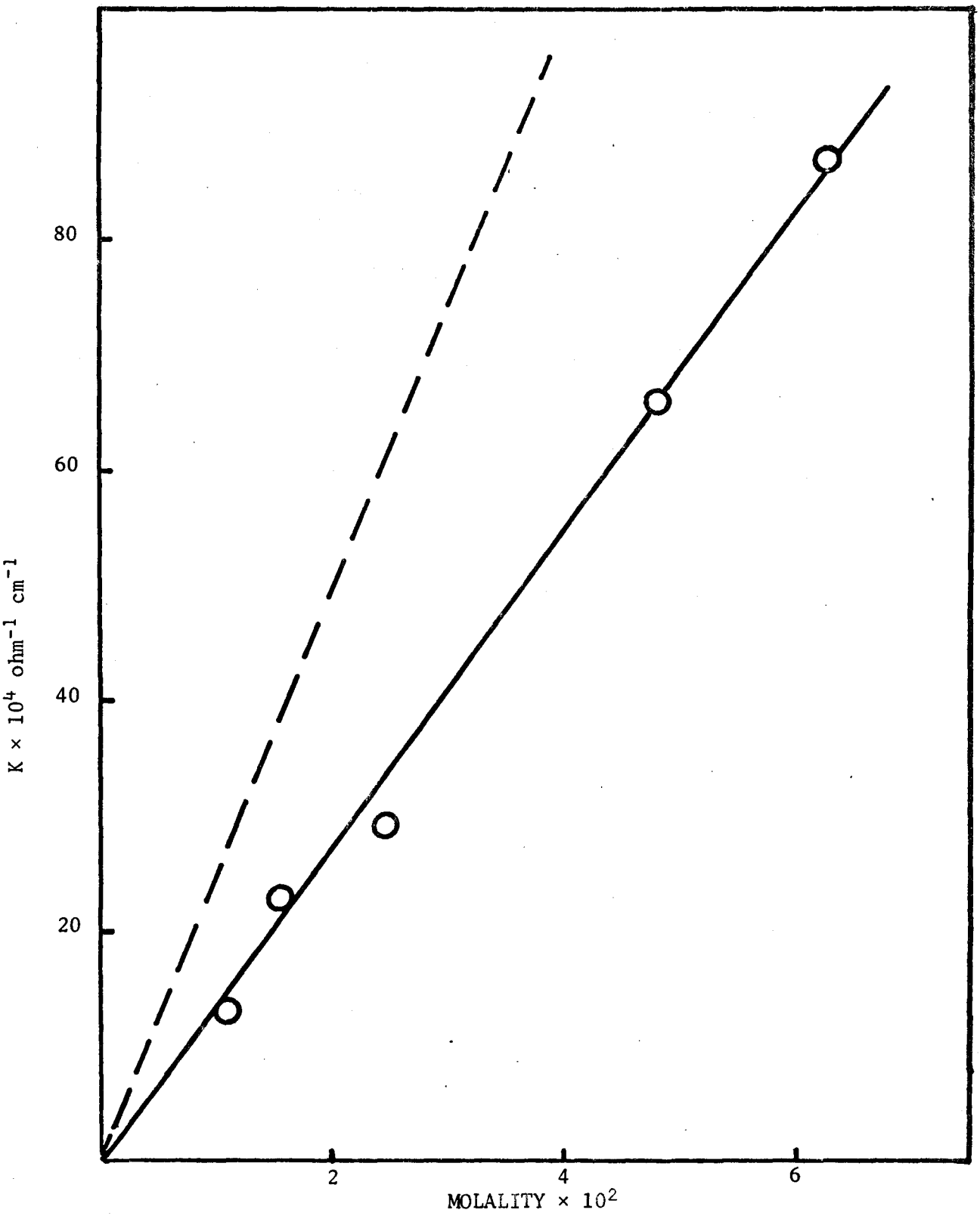

Fig. 13. Conductivities of antimony solutions in HSO_3F at 25°C (dotted line conductivities of KSO_3F solutions).

IIa $Sb + 4HSO_3F \longrightarrow Sb^{2+} + 3SO_3F^- + H_3O^+ + SO_2 + HF$

$\nu = 7 \qquad \gamma = 2.8$

IIb $\longrightarrow Sb(SO_3F)_2 + SO_3F^- + H_3O^+ + SO_2 + HF$

$\nu = 5 \qquad \gamma = 0.91$

III $2Sb + 12HSO_3F \longrightarrow 2Sb(SO_3F)_3 + 3H_3O^+ + 3SO_3F^- + 3SO_2 + 3HF$

$\nu = 7.0 \qquad \gamma = 1.45$

IV $2Sb + 8HSO_3F \longrightarrow 2SbF_2SO_3F + H_2SO_4 + 3SO_2 + 2H_3O^+ + 2SO_3F^-$

$\nu = 5 \qquad \gamma = 0.74$

In all these reactions water is liberated. Gillespie and coworkers have studied the reaction of water with fluorosulfuric acid (71) and they found that the following equilibrium is established:

$$H_3O^+ + SO_3F^- \rightleftharpoons H_2SO_4 + HF$$

As the number of particles on both sides of the reaction are the same, this equilibrium reaction does not affect the ν-value. However it does affect the concentration of the highly conducting anion SO_3F^-; hence it affects the γ-value. These workers found a value of 0.12 for the equilibrium constant K of the above reaction and have given a method for calculating the γ-value for such reactions. When a solute S ionizes according to the equation

$$S \longrightarrow aX^+ + bH_3O^+ + (a + b)SO_3F^-$$

$$K = \frac{x^2}{(b - x)(a + b - x)}$$

In the reaction

$$S \longrightarrow aX^+ + bH_3O^+ + bHF + (a + b)SO_3F^- + bSO_2$$

and HF is one of the reaction products, the equation for the equilibrium constant can be written as

$$K = \frac{x(x + b)}{(b - x)(a + b - x)}$$

and $\gamma = a + b - x$

where a = total number of moles of all cations other than H_3O^+; and

b = number of moles of H_3O^+ produced by 1 mole of the solute.

The reactions I, II, and III assume that antimony metal is oxidised to the (+1), (+2) and (+3) oxidation states, respectively. The suffixes a and b distinguish between the ionic and non-ionic formulations of the products.

Reactions Ia and b are not in agreement with the experimental ν and γ values with the theoretical values required for these reactions. Moreover, $SbSO_3F$, in which the metal atom is in the (+1) oxidation state, has a very low solubility in fluorosulfuric acid and a saturated solution of $Sb(SO_3F)$ gave no significant freezing point depression. We note also that formation of a polyatomic species, e.g., $Sb_n(SO_3F)_n$, would further reduce the ν value.

The high theoretical ν and γ values required for the reaction IIa are also not in agreement with the experimental values, but reaction IIb for which $\nu = 5$ and $\gamma = 0.91$ are in somewhat better agreement with the experimental values of $\nu = 4.3$ and $\gamma = 0.56$. Aggregation of the metal atoms to form polyatomic species would also reduce the ν value but it does not affect the γ value. For example aggregation to form a hexaatomic cluster will reduce the ν value from 5 to 4.1. Hexaatomic clusters of tantalum and niobium ($Ta_6Cl_{12}^{2+}$ and $Nb_6Cl_{12}^{2+}$) have been reported in the literature (72,73). The formal oxidation state of the metal in these compounds is (+2 1/3) and the formation of an analogous ion in HSO_3F would be represented by the equation

$$6Sb + 28HSO_3F \longrightarrow Sb_6(SO_3F)_{12}^{2+} + 9SO_3F^- + 7H_3O^+ + 7SO_2 + 7HF$$

which requires $\nu = 5.1$ and $\gamma = 1.46$. These values are also higher than the experimental values.

The experimental ν and γ values are also not in agreement with the theoretical values required for the reaction III. The possibility of this reaction is also not favoured by the low solubility of $Sb(SO_3F)_3$ in HSO_3F. The solution does not show any insoluble product in the concentration range studied in the cryoscopic measurements.

The theoretical values $\nu = 5$ and $\gamma = 0.74$ required for the reaction IV are reasonably close to the experimental values of $\nu = 4.3$ and $\gamma = 0.56$. Fluorine on Sb(III) has also been shown by the ^{19}F n.m.r. experiment.

The experimental ν value is close to that predicted for reaction IIB but the high γ-value is not consistent with this reaction. Also attempts to oxidise antimony to the (+2) oxidation state with $S_2O_6F_2$ and AsF_5 were not successful. The products obtained contained antimony and were in the (+1) or (+3) oxidation states. The reaction Ib requires smaller ν and γ values and reaction IV requires slightly higher values than those observed. It appears that a mixture of compounds in the (+1) and (+3) oxidation states are formed in the solution

2d. ^{19}F n.m.r.

The ^{19}F n.m.r. spectrum of the solution of antimony metal in HSO_3F at -80°C shows a single signal from the solvent when excess of antimony metal is added or the solution is left for 8-10 hrs. A signal at +83 ppm with respect to $CFCl_3$ appears in addition to the solvent signal (Fig. 14). This signal is in the region of fluorine on Sb(III). A solution of SbF_3 in HSO_3F shows a signal with a chemical shift of +82 ppm with respect to $CFCl_3$. When SbF_3 is added to a solution of antimony in HSO_3F containing excess of metal, the signal shifts slightly to the high field side +85 ppm and is

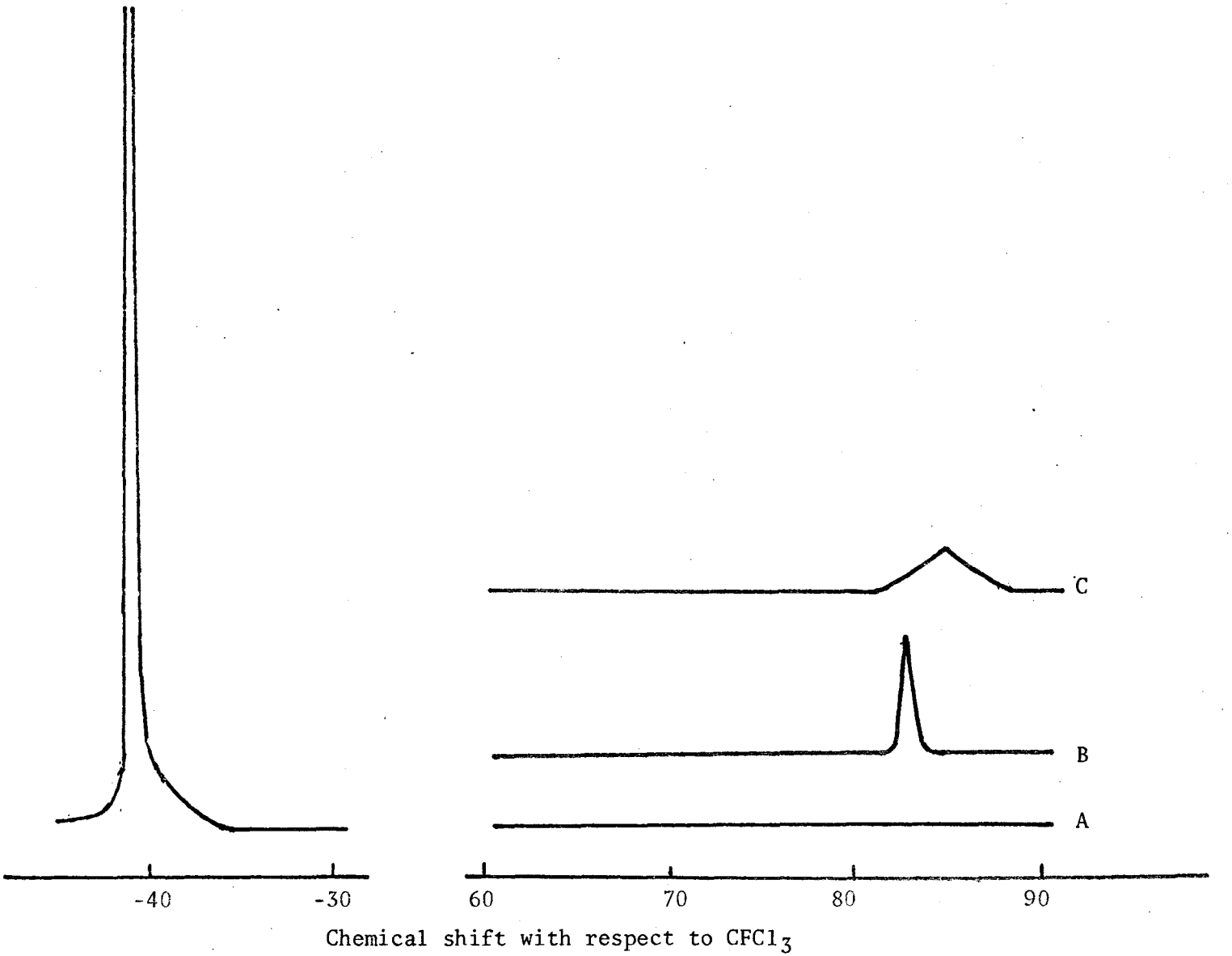

Fig. 14. ^{19}F n.m.r. spectrum of antimony solutions in HSO_3F at -80°C.
(A) 0.0119 mol(Sb) solution; (B) saturated Sb solution; (C) when SbF_3 is added to solution B.

broadened suggesting that the fluorine of SbF_3 exchanges with the fluorine present on antimony in the solution. This also indicates that the two fluorines are not present in exactly the same chemical environment.

No signal is observed in the region of HF in the spectrum although HF is one of the expected reaction products. The signal at +83 may arise from the compounds $SbF_n(SO_3F)_{3-n}$ formed in the solution by the reaction of HF with $Sb(SO_3F)_3$. On leaving this solution for 2-3 days no change was observed in the spectrum except a new signal with a chemical shift of +162 ppm with respect to $CFC\ell_3$ appears in the spectrum. This signal is in the region of fluorine on silicon indicating that the HF formed in the reaction also attacks glass.

The ^{19}F n.m.r. spectrum indicates the formation of compounds such as $SbF(SO_3F)_2$ or $SbF_2(SO_3F)$ in the solution of antimony metal in HSO_3F. The formation of the compound $SbF_2(SO_3F)$ has been explained by the reaction IV and a similar reaction for the formation of $SbF(SO_3F)_2$ would require the $\nu = 6$ and $\gamma = 1.21$ which are higher than the experimental values.

2e. E.s.r. spectrum

A freshly prepared solution of antimony in HSO_3F does not show any e.s.r. spectrum. Upon leaving this solution for 24-36 hrs, it develops a greenish yellow colour and shows two e.s.r. signals with g = 2.027 and 2.014 respectively (Fig. 15).

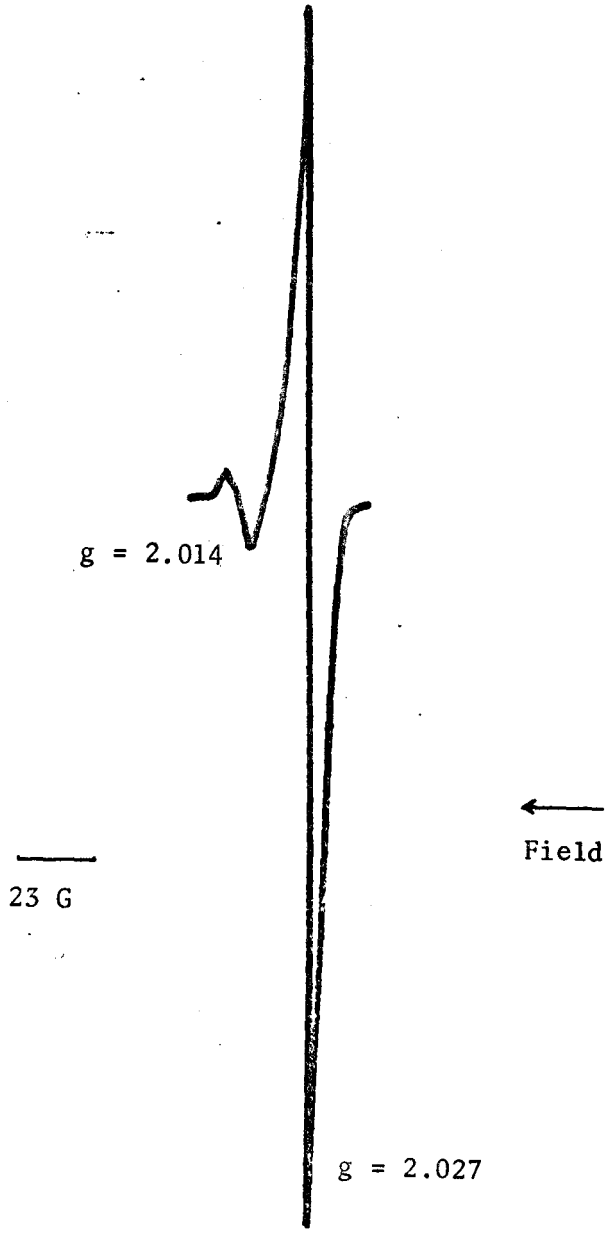

Fig. 15. E.s.r. spectrum of coloured solution of antimony in HSO_3F at 22°C.

3a. Solutions of $Sb_n(SO_3F)_n$

When an excess of antimony metal is added to the solution in HSO_3F a white solid compound separates out of the solution. The elemental analysis of this compound shows its empirical formula to be $Sb(SO_3F)$ in which the metal is apparently in the (+1) oxidation state.

Cryoscopic measurements on solutions of $Sb(SO_3F)$ could not be carried out as this compound has a very low solubility in HSO_3F at low temperatures.

The results of specific conductivity measurements at 25°C are given in Table XI. A γ-value of 0.2 is obtained on comparing the specific conductivity with the solutions of KSO_3F in HSO_3F (Fig. 16). The γ-value of 0.2 could possibly be explained in terms of an ionization such as one of the following:

$$Sb_4(SO_3F)_4 \rightleftharpoons Sb_4(SO_3F)_3^+ + SO_3F^-$$

$$Sb_5(SO_3F)_5 \rightleftharpoons Sb_5(SO_3F)_4^+ + SO_3F^-$$

which requires a theoretical γ-value of 0.25 and 0.2 respectively. As already pointed out the solution is not very stable; a greenish yellow colour appears in the solution with time. The conductivity measurements were not carried out after the solution had become coloured. However no appreciable change in conductivity is observed with time. The conductivity of a 2.74×10^{-2} m solution of $SbSO_3F$ changes from 16.3×10^{-4} to 16.7×10^{-4} ohm^{-1} cm^{-1} in 20 hrs. It has been shown that in solutions of antimony metal in HSO_3F the metal is gradually oxidised to Sb(III). The solution will not be expected to be very conducting if the $SbSO_3F$ is largely oxidised to Sb(III) in the dilute solution according to either or both of the reactions

V $$SbSO_3F + 2HSO_3F \longrightarrow SbF_2SO_3F + SO_2 + H_2SO_4$$

VI $$3SbSO_3F + 6HSO_3F \longrightarrow 2SbF_2SO_3F + Sb(SO_3F)_3 + 3H_2SO_4 + S$$

TABLE XI

SPECIFIC CONDUCTIVITY OF SOLUTIONS OF $Sb_n(SO_3F)_n$ IN HSO_3F AT 25°C

Concentration $m(SbSO_3F)Kg^{-1}$	Sp. Conductivity $\times 10^4$ ohm^{-1} cm^{-1}
0.0037	1.809
0.0101	4.990
0.0116	6.788
0.0146	8.499
0.0203	11.950
0.0210	10.789
0.0275	16.310

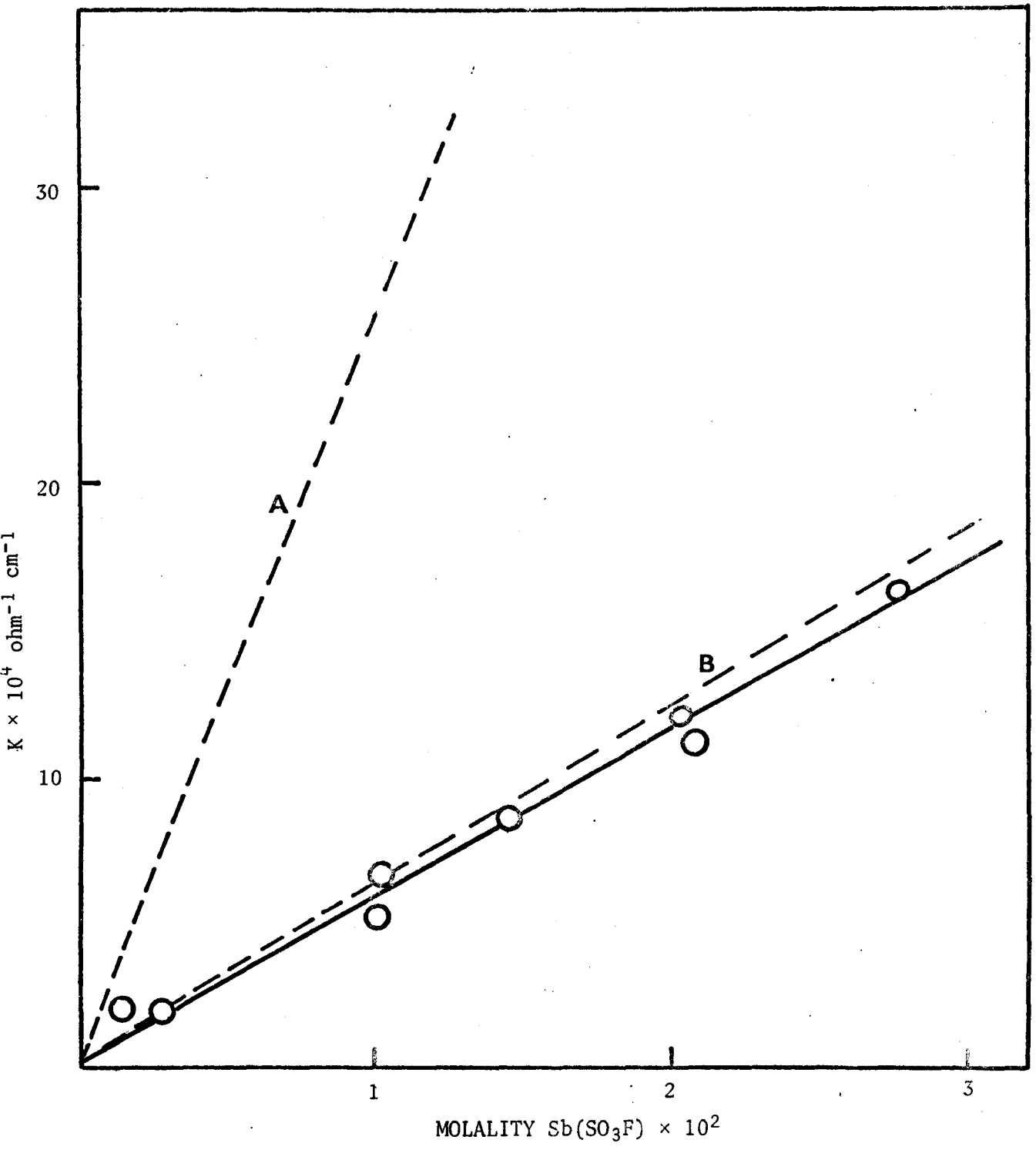

Fig. 16. Conductivities of $SbSO_3F$ solutions in HSO_3F at 25°C. Dotted lines (A) conductivities of KSO_3F solution; (B) sum of conductivities of SbF_3 and H_2SO_4 solutions in HSO_3F.

Both reactions require $\gamma = 0$.

Barr (36) observed that the solutions of SbF_3 and H_2SO_4 are slightly conducting in HSO_3F. If it is assumed that the conductivity of SbF_2SO_3F and $Sb(SO_3F)_3$ solutions is like that of SbF_3 solutions in HSO_3F then H_2SO_4 and SbF_2SO_3F will be contributing towards the conductivity of the solution of $SbSO_3F$ in HSO_3F. The specific conductivity curve for the solution of $SbSO_3F$ in HSO_3F compares well with the sum of the conductivities for SbF_3 and H_2SO_4 (dotted line, Fig. 16).

3b. Magnetic Susceptibility Measurements

The elemental analysis of the white solid filtered off from solution corresponds to the formula $SbSO_3F$. This simple formula suggests that the compound should be paramagnetic. A magnetic susceptibility measurement for this solid compound gave a molar susceptibility of -40×10^{-6} at 20°C. The diamagnetic contribution for this compound is -65×10^{-6} (74) suggesting that the compound is essentially diamagnetic at room temperature. This behaviour can be best explained on the basis of aggregation of the metal atoms to form polyatomic species.

3c. ^{19}F n.m.r. Spectrum

A fresh solution of $Sb_n(SO_3F)_n$ in HSO_3F shows only a single signal due to the solvent. When this solution is left for 48 hrs two signals appear in the spectrum on the high field side of the solvent signal with chemical shifts of +81.5 and +165 ppm with respect to $CFCl_3$. These signals are in the region of fluorine on Sb(III) and fluorine on silicon suggesting that Sb(I) is gradually oxidised to Sb(III) and HF formed during the process attacks glass to give SiF_4 and $Sb(SO_3F)_3$ to form the compound $SbF_n(SO_3F)_{3-n}$.

4. Coloured Solutions of $Sb_n(SO_3F)_n$

4a. UV and Visible Absorption Sepctra

Solutions of $Sb_n(SO_3F)_n$ in HSO_3F develop a greenish yellow colour in eight to ten hours. This coloured solution shows a strong band at 225-250 with a shoulder at 280 and another strong band at 310 nm and weak bands at 420, 580 and 710 nm (Fig. 17). The absorption band at 280 was found to be due to sulfur dioxide. The bands at 225-250, 420, 580 and 710 nm must be due to either an oxidised antimony species or additional products of reduction of the solvent.

4b. E.s.r. Spectrum

A greenish yellow solution of $Sb_n(SO_3F)_n$ in HSO_3F shows two e.s.r. signals at room temperature with $g = 2.014$ and $g = 2.027$. The signal with $g = 2.027$ has a greater intensity than the other signal indicating that the radical that gives rise to this signal has a higher concentration than that due to the signal at $g = 2.014$. The intensity of the signal decreases as the temperature of the solution is lowered (Fig. 18). A very weak signal is observed at -80°C suggesting dimerisation of the radical species giving these e.s.r. signals.

$Sb_n(SO_3F)_n$ decomposes to a black mass at 121°C. However, when it was heated under vacuum at 60°C a light yellow solid deposited on the cold finger in two to three days. The Raman spectrum of this solid showed it to be elemental sulfur (75).

Elemental sulfur was also deposited when a solution of $Sb_n(SO_3F)_n$ was left for about a month. Crystals of this material gave similar Raman spectrum to that obtained from the sublimate and single crystal X-ray diffraction data obtained by Dr. C. Davies showed conclusively that the material was sulfur.

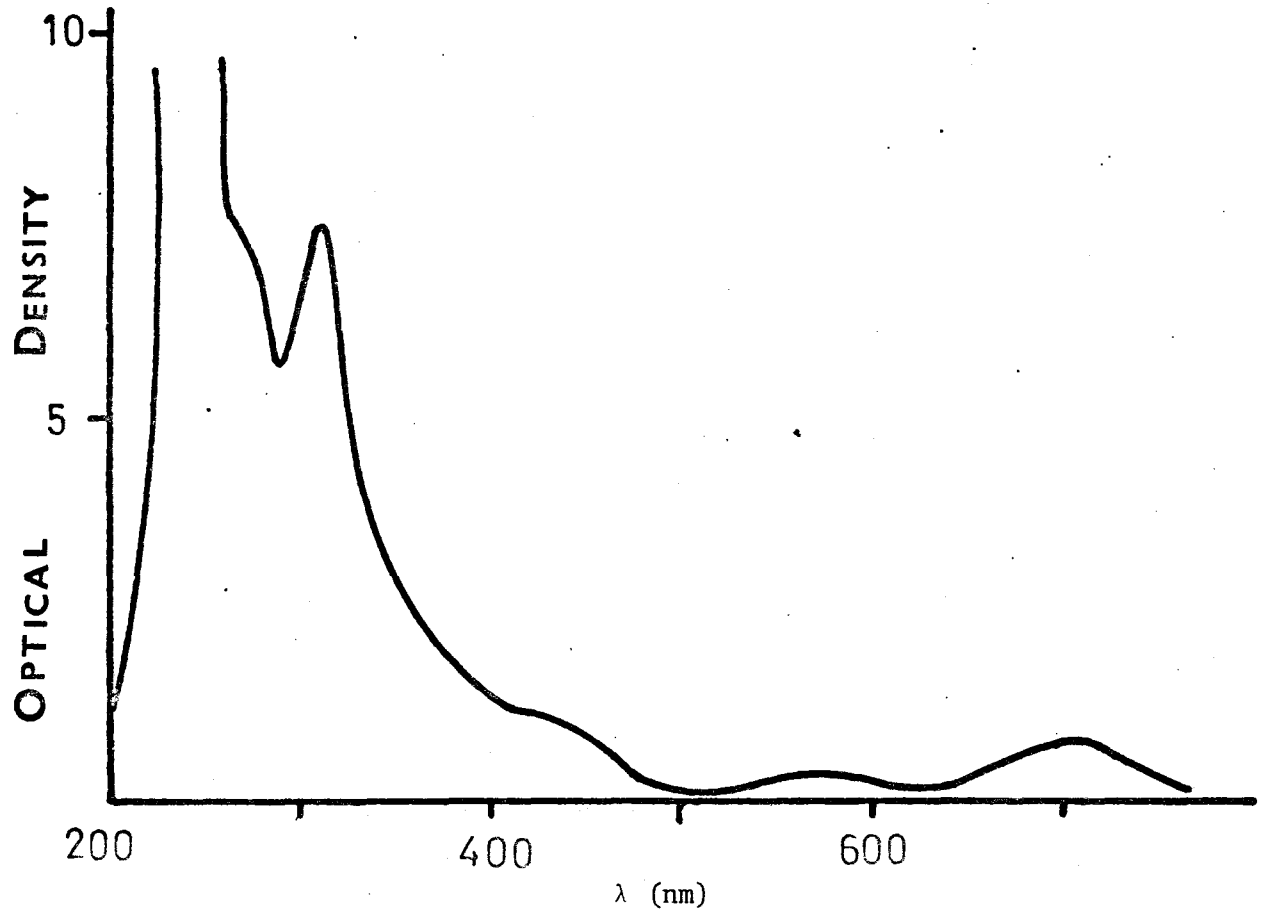

Fig. 17. UV and visible absorption spectrum of $Sb_n(SO_3F)_n$ solution in HSO_3F after 10 hrs.

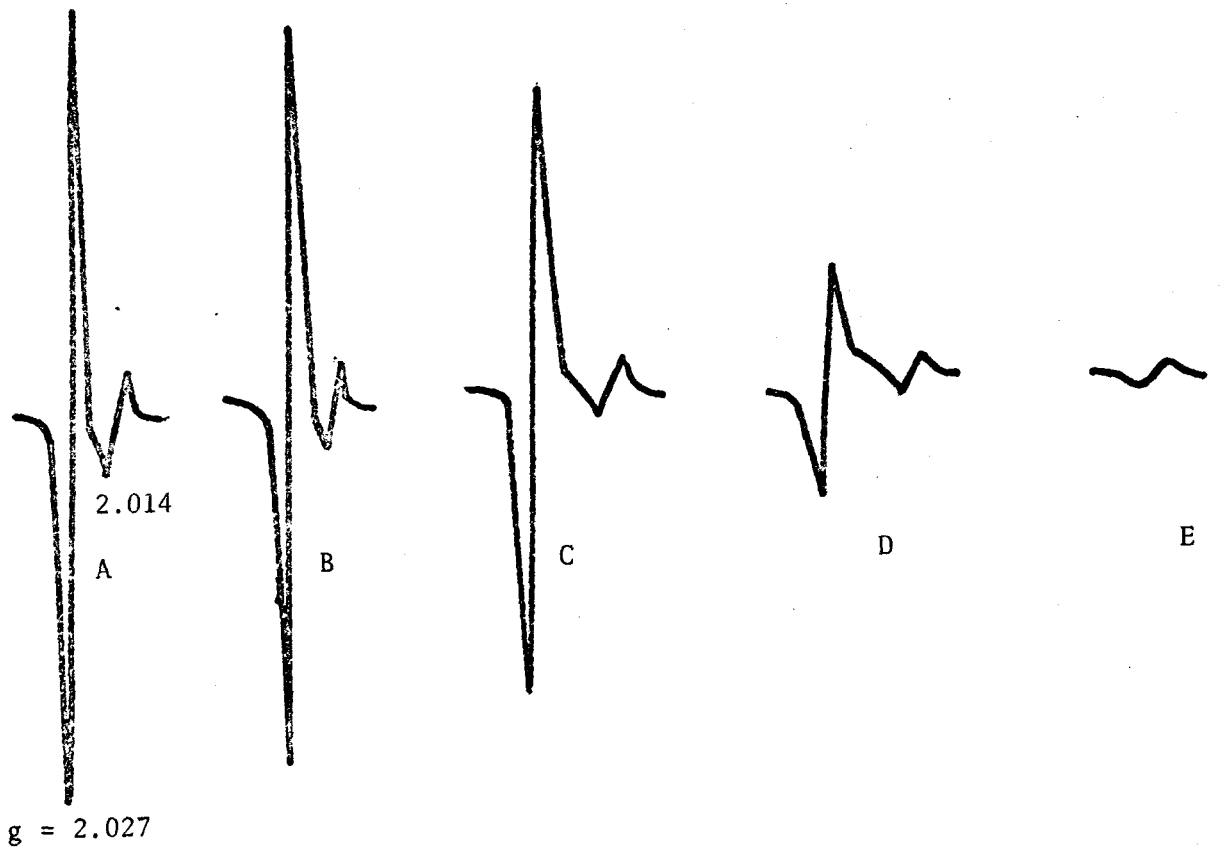

Fig. 18. E.s.r. spectrum of coloured solutions of $SbSO_3F$ in HSO_3F. (A) 20°C; (B) -20°C; (C) -40°C; (D) -60°C; (E) -80°C.

Hence we conclude that $Sb_n(SO_3F)_n$ reduces HSO_3F not only to SO_2 but also to sulfur cations and elemental sulfur

VII $3SbSO_3F + 10HSO_3F \xrightarrow[\gamma = 1]{} 3Sb(SO_3F)_3 + 3H_3O^+ + 3SO_3F^- + HF + S$

VIII $3SbSO_3F + 6HSO_3F \xrightarrow[\gamma = 0]{} 2SbF_2SO_3F + Sb(SO_3F)_3 + 3H_2SO_4 + S$

Formation of sulfur is very slow and not quantitative. The sulfur formed in the above reaction is oxidised by the solvent to give coloured solutions. These cations and radical cations of sulfur have been discussed in the preceeding chapter. It has been shown that solutions of S_{16}^{2+} which are in equilibrium with the low concentration of S_8^+ have absorption maxima at 235, 350, 430 and 715 nm; S_8^{2+} is in equilibrium with S_4^+ and has a band at 580 and S_4^{2+} at 330 nm respectively. The coloured solutions of antimony metal and $Sb_n(SO_3F)_n$ in HSO_3F show absorptions at 225-250, 280, 310, 430, 580 and 715 nm. Sulfur dissolves in HSO_3F to give first an equilibrium mixture of S_{16}^{2+} and S_8^+ which has absorption bands at 235, 350, 430 and 715 nm respectively. Bands at 430 and 715 nm are observed in the spectrum but since the solution shows a strong absorption in the 225-250 nm region the 235 nm band would be masked by this absorption. The S_8^+ radical shows an e.s.r. signal with $g = 2.027$. The coloured solutions of antimony and $Sb_n(SO_3F)_n$ also show an e.s.r. signal with $g = 2.027$ and which may be reasonably attributed to the S_8^+ radical. It has been shown that the equilibrium shifts to the right at low temperatures and the e.s.r. signal decreases in intensity according to the equation

$$S_8^+ \rightleftharpoons S_{16}^{2+}$$

It is clear that the colour of the solution of antimony and $Sb_n(SO_3F)_n$

in HSO_3F is due to sulfur cations and not to antimony cations.

5a. Reaction of Antimony metal with SbF_5 and AsF_5 in Liquid SO_2

Antimony metal can be oxidised to the (+1) state with arsenic or antimony pentafluorides in liquid sulfur dioxide.

$$2Sb + 3MF_5 \longrightarrow 2SbMF_6 + MF_3$$

In a typical reaction 2.1672 g of antimony reacted with 4.5526 g of arsenic pentafluoride in solution in SO_2 at 20°C to give 5.2797 g of the white product insoluble in sulfur dioxide (theoretical yield required for $SbAsF_6$ = 5.5248 g). The supernatant liquid became yellow coloured during the reaction and after the white solid $Sb(AsF_6)$ had been filtered off the solvent was removed under vacuum to yield a small amount of a yellow solid. In the oxidation of antimony with antimony pentafluoride the SbF_3 formed in the reaction could not be separated from the products so no pure compound could be obtained. However a similar yellow solid was obtained from the solution on evaporating the solvent.

Attempts to prepare the compound $SbSb_2F_{11}$ by the reaction

IX $$2Sb + 5SbF_5 \longrightarrow 2SbSb_2F_{11} + SbF_3$$

were not successful. The yield was poor and it was difficult to separate the SbF_3 from the products. The supertanant liquid was found to have a blue colour in this reaction. A blue solid was obtained from the solution after filtering off the solution and removing the sulfur dioxide under vacuum.

The amounts of the yellow and blue solids obtained from the above reactions were not sufficient for elemental analysis. On exposing each of these solid compounds to moisture a light yellow coloured product was

obtained. This was dissolved in carbon disulfide and recrystallised and identified as sulfur from its mp (113°C).

The coloured species in sulfur dioxide are thus not antimony compounds but sulfur cations. The formation of sulfur in solution indicates that antimony metal reduces S(IV) to S(0) in a solution of SO_2/AsF_5 or SbF_5. For the Sb/MF_5 mole ratio of 2:3 the amount of the oxidising agent left after reacting with antimony is not sufficient to oxidise the sulfur beyond S_{16}^{2+} and a yellow solution is obtained. For the Sb/SbF_5 mole ratio of 2:5 an excess of oxidising agent is present and sulfur is oxidised to S_8^{2+} which gives the blue solution.

No antimony metal was obtained on hydrolysis of the coloured compounds. This makes it unlikely that these compounds contain any polyatomic cations of antimony.

5b. ^{19}F n.m.r. Spectrum

The ^{19}F n.m.r. spectrum of the solution of $Sb_n(AsF_6)_n$ in fluorosulfuric acid shows a single signal with a chemical shift of +63 with respect to $CFCl_3$ in addition to the solvent signal (Fig. 19). This signal is in the region of fluorine on As(V). A solution of $NaAsF_6$ in fluorosulfuric acid gives a signal with a chemical shift of +60 ppm with respect to $CFCl_3$. A solution of $Sb_n(AsF_6)_n$ is not stable with time and another signal with a chemical shift of +79 ppm with respect to $CFCl_3$ gradually appears in the spectrum. This new signal is in the region of fluorine on Sb(III). However no signal due to AsF_3 was observed in the spectrum although this would be expected if the following reaction took place

$$Sb_n(AsF_6)_n \longrightarrow SbF_3 + AsF_3$$

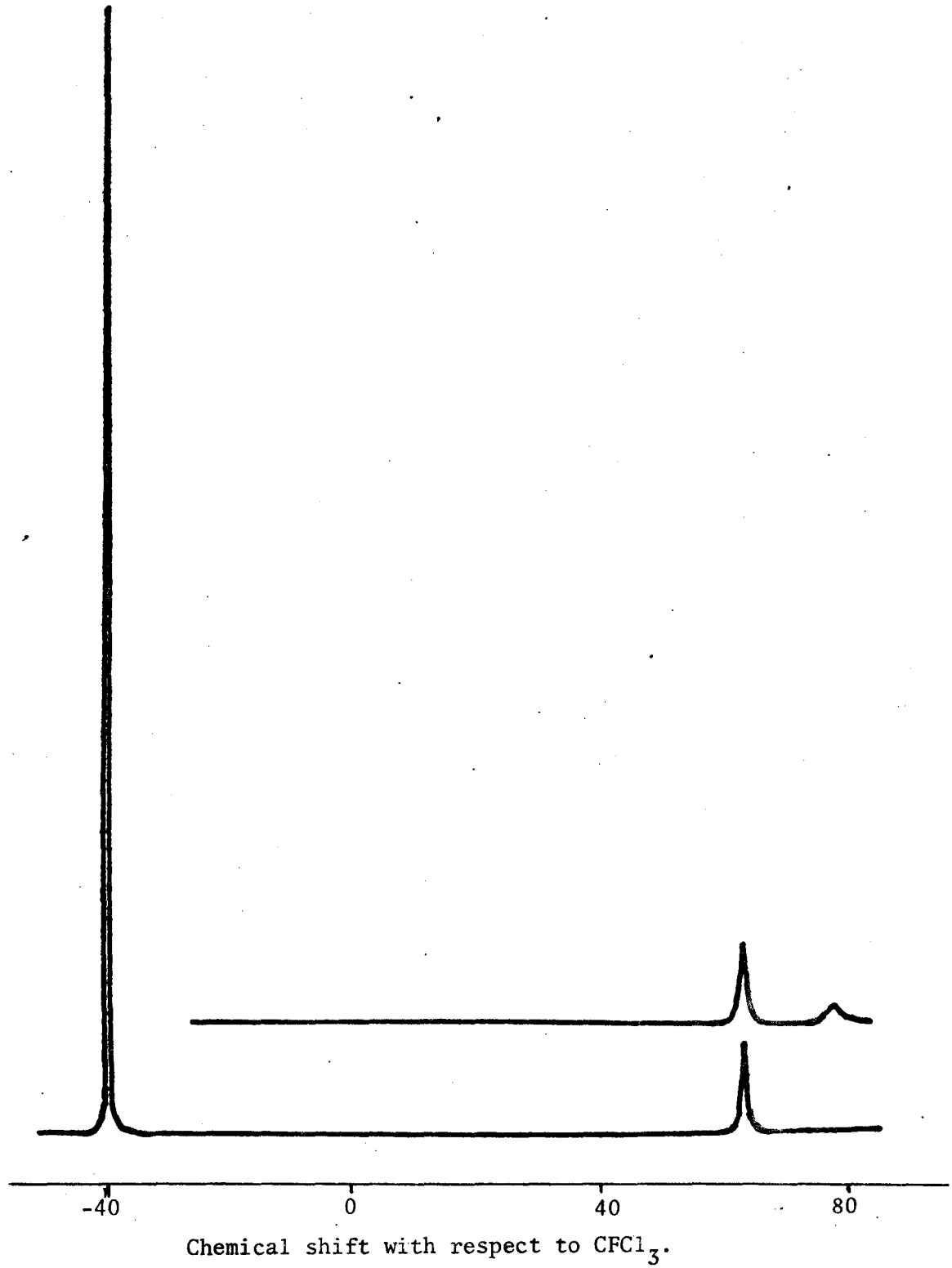

Fig. 19. ^{19}F n.m.r. spectrum of $SbAsF_6$ solution in HSO_3F at -80°C.

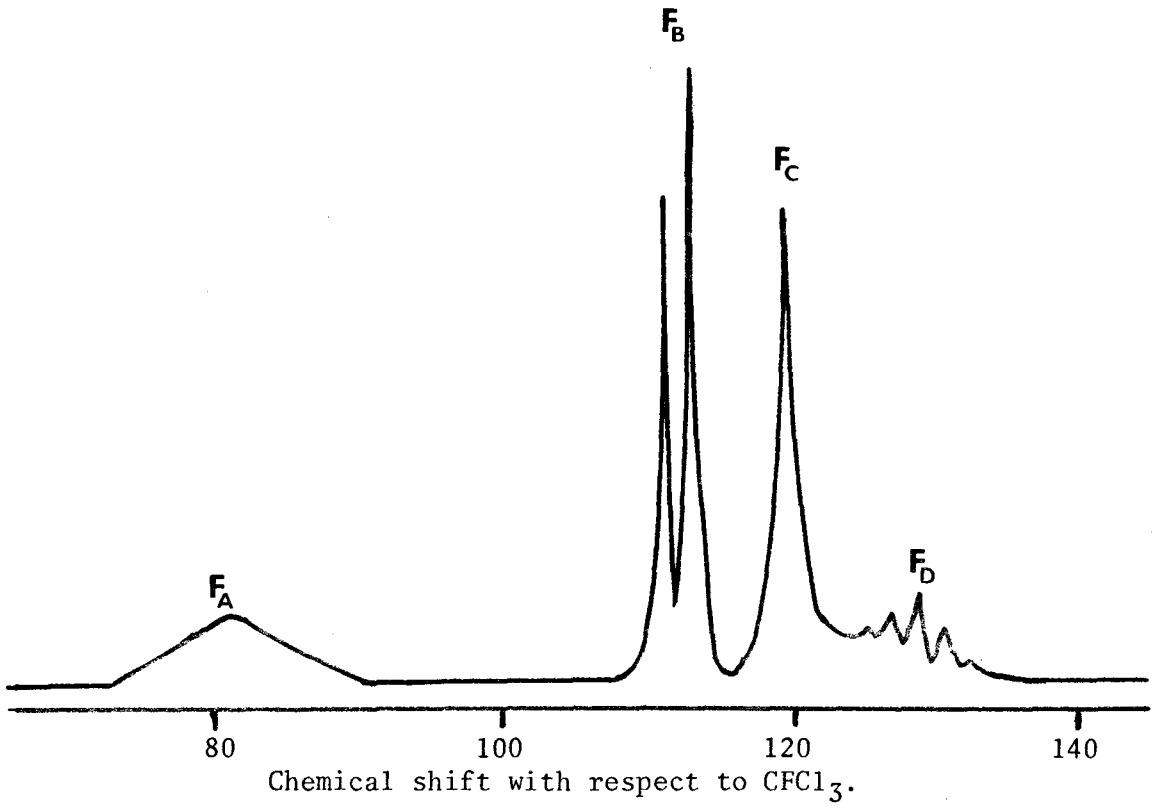

Fig. 20. ^{19}F n.m.r. spectrum of the solution of the white product obtained from the reaction Sb/SbF_5 (2:3) in HSO_3F at -80°C.

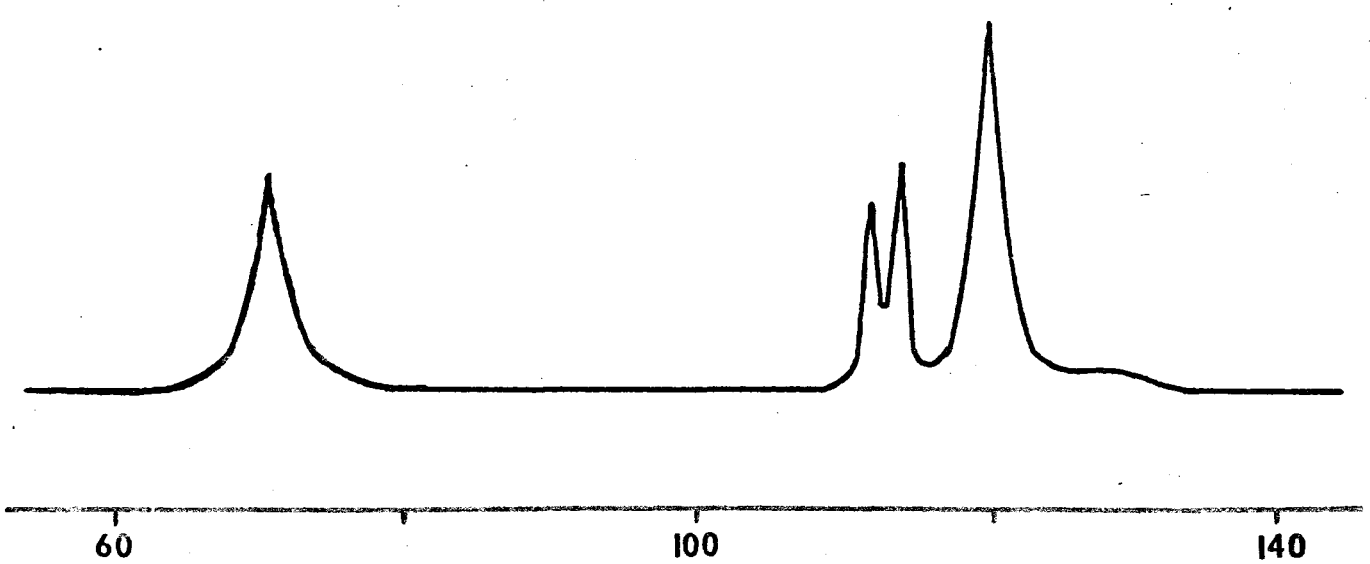

Fig. 21. ^{19}F n.m.r. spectrum of the solution of the white solid obtained from the reaction Sb/SbF_5 (2:5) in HSO_3F at -80°C.

Presumably the fluorine on Sb(III) must arise from the oxidation of Sb(I). The ^{19}F spectrum of the solution of the white solid obtained by the oxidation of antimony metal with SbF_5 (Sb/SbF_5 = 2:3) in fluorosulfuric acid is shown in Fig. 20. The broad signal F_a at +81 ppm (from $CFC\ell_3$) is assigned to SbF_3. A solution of SbF_3 in HSO_3F shows a signal with a chemical shift of +82 ppm (from $CFC\ell_3$). The signal F_c at +119 ppm is due to SbF_6^- (a solution of $(C_2H_5)_4NSbF_6$ shows a signal at +120 ppm in HSO_3F). A doublet at +111 and +113 and a quintet at +133 ppm arise from the anion $SbF_5(SO_3F)^-$ which is formed in the solution as a result of the following reaction

$$SbF_6^- + HSO_3F \longrightarrow SbF_5(SO_3F)^- + HF$$

The doublet arises from the four equivalent fluorines F_b and the quintet

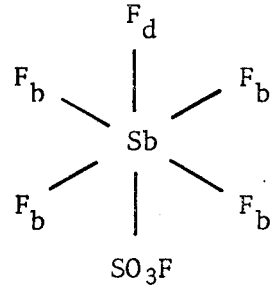

from F_d (76). The HF formed in the above reaction attacks glass and shows up at +160 ppm as fluorine on silicon.

The ^{19}F spectrum of the solution of white solid obtained from the reaction Sb/SbF_5 2:5 in HSO_3F is not very clear (Fig. 21). It shows fluorine on Sb(III) at +70 ppm and SbF_6^- at +119 ppm (from $CFC\ell_3$). The lowering of the chemical shift from +82 to +70 ppm may be due to the formation of the compound SbF_2SbF_6. The doublet at +111 and +113 ppm with respect to $CFC\ell_3$ may arise from $Sb_2F_{11}^-$ or $SbF_5(SO_3F)^-$. The weak signals of the spectrum

are not clear so definite conclusion about the anion can not be made.

5c. Raman Spectrum of $Sb_n(AsF_6)_n$

Attempts to obtain the Raman spectrum of $Sb_n(SO_3F)_n$ using the 6328 Å line of He/Ne or the 5145 line of Argon laser as exciting radiation were not successful at room temperature. At -140°C the 6328 Å He/Ne laser showed a band at 140 cm^{-1} and a strong fluoroscence above 200 cm^{-1}. A spectrum was obtained from $Sb_n(AsF_6)_n$ using the 5145 Å line of Argon ion laser beam and is given in Fig. 22. The bands observed in the spectrum, their relative intensities and the assignment of the bands are given in Table XII.

The anion AsF_6^- (point group O_h) has six fundamental modes ($A_{1g} + E_g + 2T_{1u} + T_{2g} + T_{2u}$). The A_{1g}, E_g and T_{2g} modes are Raman active, the T_{1u} modes are i.r. active and the T_{2u} is both Raman and i.r. inactive. If $SbAsF_6$ is a simple ionic compound $Sb^+AsF_6^-$ only three bands due to AsF_6^- should be present in the spectrum. But in fact more than three bands are observed. Fluorine bridging between the anion and cation may reduce the symmetry from O_h to D_{4h}, C_{4v} or C_{2v}. The changes expected in the spectrum are given in Table XIII. Splitting of all the bands except the ν_1 (A_{1g}) mode occurs and also some forbidden bands become Raman and i.r. active. The assignment of the bands in the Raman spectrum of AsF_6^- anion has been made by comparison of the spectrum of the hexafluoroarsenate of $MF_3^+(AsF_6)^-$ and $MF_2^+AsF_6$ reported by Gillespie and coworkers (77,78). The strong band at 687 cm^{-1} has been assigned to ν_1 (A_{1g}) mode. The ν_2 (E_g) mode has been observed to be split and occur at 530 and 569 cm^{-1} in the spectrum of SeF_3AsF_6 and at 544 and 602 cm^{-1} in the spectrum of ClF_2AsF_6. This mode may be assigned at 520 and 592 cm^{-1} in the spectrum $Sb_n^n(AsF_6)_n$.

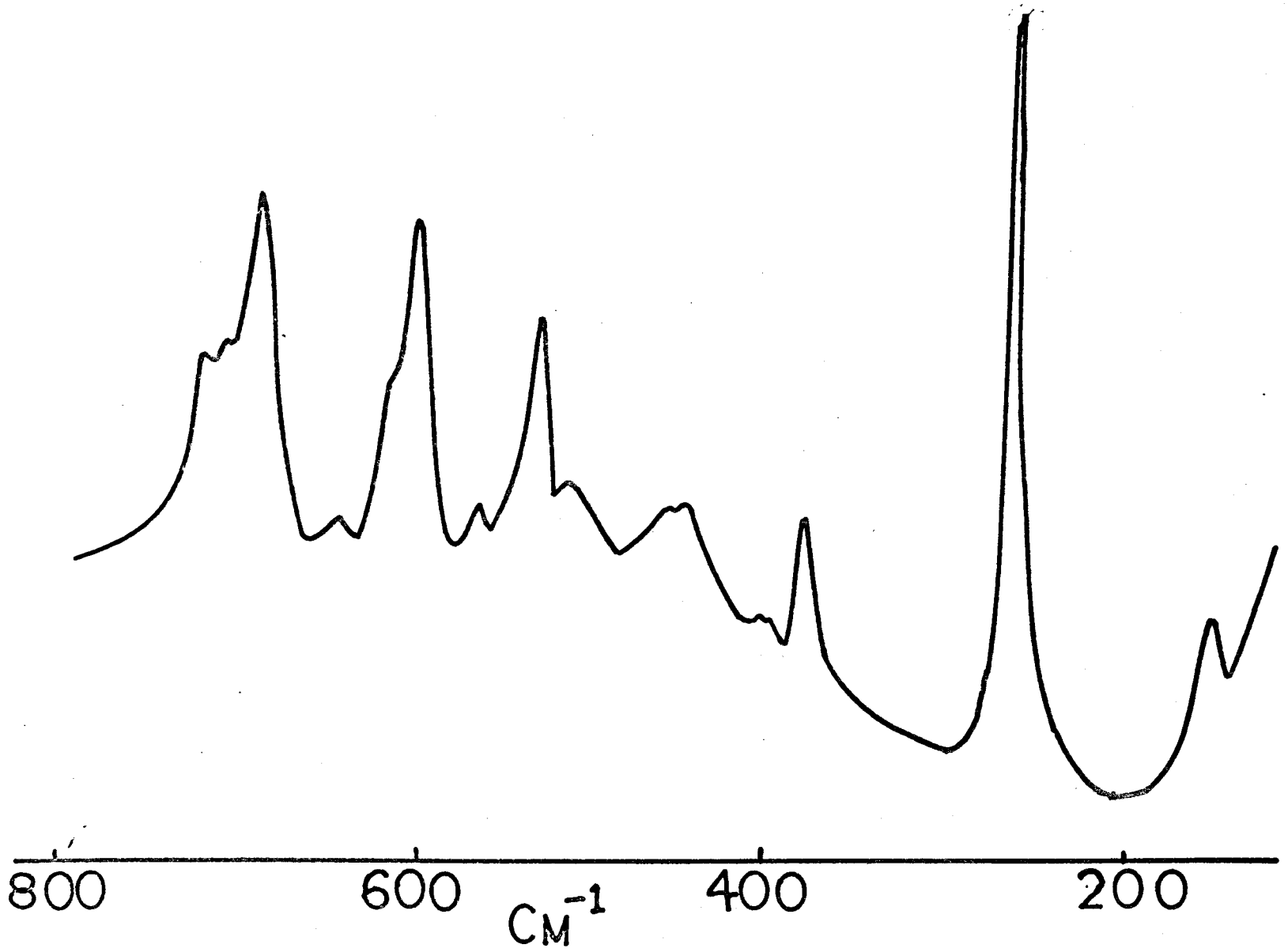

Fig. 22. Raman spectrum of $SbAsF_6$.

TABLE XII

BANDS IN THE RAMAN SPECTRUM OF $Sb_n(AsF_6)_n$

Raman Bands	Relative Intensity	Assignment of the Band	AsF_6^- Bands (77) SeF_3AsF_6
133	9		
259	100	Sb-Sb	
373	10	ν_5 AsF_6^-	372 ν_5
393	3	ν_4 AsF_6^-	
398	3		
442	6		
456	5	Bridging F	
510	3		
520	14	ν_2 AsF_6^-	530
556	3		ν_2
592	18	ν_2 AsF_6^-	569
609 sh			
645	3		
687	19	ν_1 AsF_6^-	675 ν_1
692	11	ν_3 AsF_6^-	691 ν_3
713	9		

I.R. Bands	Bands in the i.r. spectrum of SbF_3
134 w	
	227 w
227 w	
259 w	
	278 st
280 st	

st = strong w = weak

TABLE XIII

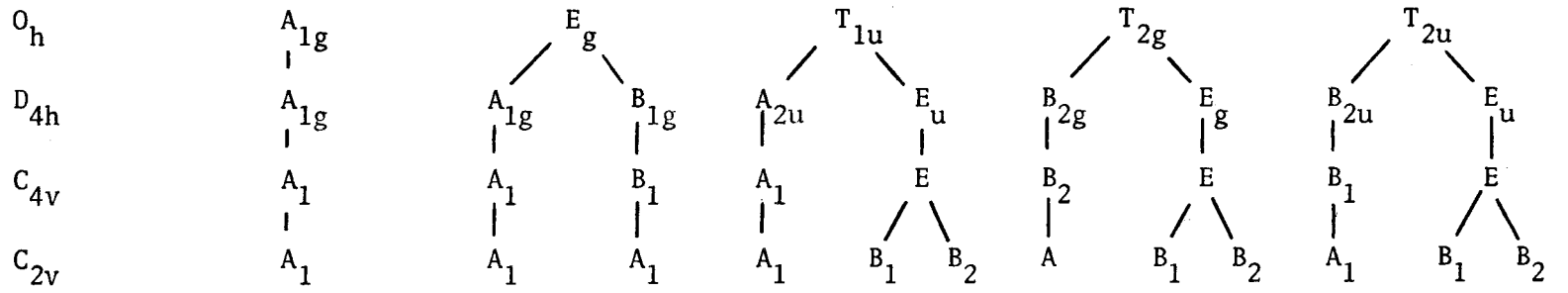

	Raman Active				I.R. Active			
O_h	A_{1g}	E_g	T_{2g}		T_{1u}			
D_{4h}	A_{1g}	B_{1g}	B_{2g}	E_g	A_{2u}	E_g	E_u	
C_{4v}	A_1	B_1	B_2	E	A_1	E		
C_{2v}	A_1	A_2	B_1	B_2	A_1	A_2	B_1	B_2

The ν_3 and ν_4 (T_{1u}) which become Raman active in the reduced symmetry appear as doublets at 695, 713 cm^{-1} and 393 and 398 cm^{-1} respectively. The ν_5 (T_{2g}) is also predicted to be split in the reduced symmetry but no splitting is observed in this band unless the difference is so small that the bands overlap to give a single peak at 373 cm^{-1}. A ν_6 (T_{2u}) mode forbidden in the O_h symmetry becomes Raman active in the C_{4v} symmetry but has not been observed in the spectrum of $MF_3^+AsF_6^-$ and $MF_2^+AsF_6^-$ compounds. Aubke and coworkers (79) have calculated this mode for AsF_6^- near 229 cm^{-1}. The Raman spectrum of $Sb_n(AsF_6)_n$ does not show any Raman band near this region. The intensity of the band at 259 cm^{-1} is much greater than would be expected for a formally forbidden vibration and is therefore not assigned as ν_6 (AsF_6^-). The weak bands at 442, 456, 510 and 556 cm^{-1} may arise from the vibrations of the bridging fluorines.

The lowest band observed for AsF_6^- anion at 373 cm^{-1} is assigned as ν_5 mode. There are also two very strong bands at 259 and at 133 cm^{-1}. Metal-metal stretching vibrations for dialkyl tin and phenyl ditin compounds have been reported in the region of 192-207 cm^{-1} (80). The symmetric stretch ν_1 for Te_4^{2} (D_{4h}) has been observed at 219 cm^{-1} (19). The symmetric stretch ν (A_1) for the tetrahedral P_4 and As_4 molecules have been observed at 606 and 340 cm^{-1} respectively (81,82). Comparison of this data suggests that the bands at 259 and 133 cm^{-1} can be assigned to the Sb-Sb vibrational region.

5d. I.r. Spectrum

The i.r. spectrum of $Sb_n(AsF_6)$ has been studied between 200 and 400 cm^{-1} (Fig. 23). The spectrum below 240 cm^{-1} obtained using a Fourier spectrophotometer which showed a single weak band at 134 cm^{-1}. The bands observed

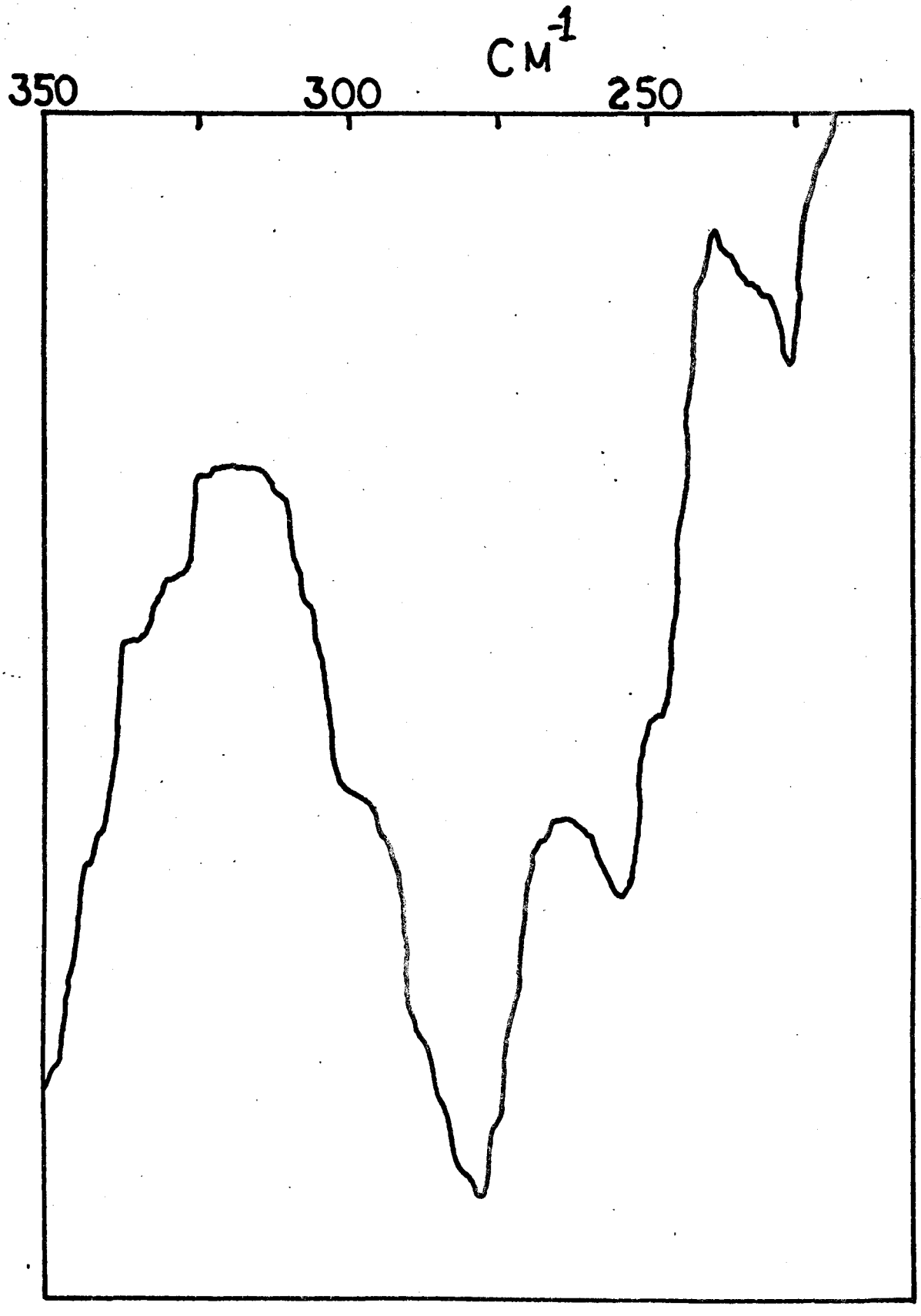

Fig. 23. I.r. spectrum of $SbAsF_6$ in 200-350 cm^{-1} region.

in the i.r. spectrum in this region are given in Table XII. The bands at 134 and 255 cm^{-1} are probably due to the vibrations which appear in the Raman spectrum at 133 and 259 cm^{-1}. The other two bands are a weak one at 227 and a strong band at 280 cm^{-1}. The i.r. spectrum of SbF_3 shows two bands at 227 and 278 cm^{-1}. Raman spectrum of $Sb_n(AsF_6)$ does not show any band characteristic of SbF_3. So it appears that $Sb_n(AsF_6)_n$ decomposes partially during the preparation of the polyethylene pellets used for obtaining the spectrum.

The observation of strong low frequency bands that can not be assigned to AsF_6^- makes it unlikely that the antimony cation is monoatomic.

6a. Reaction of Antimony Metal with $S_2O_6F_2$ in HSO_3F

Antimony metal does not react with fluorosulfuric acid at temperatures below -20°C over a period of 10-12 hrs. Attempts were made to oxidise the metal with $S_2O_6F_2$ in fluorosulfuric acid at -20°C. Reactions of antimony metal with fluorosulfuric acid have shown that it can be oxidised to a mixture of (+1) and (+3) oxidation states. The reaction of the metal with $S_2O_6F_2$ in the mole ratio $Sb/S_2O_6F_2$ = 1:1 gave a colourless solution.

The ^{19}F n.m.r. spectrum of this shows fluorine on Sb(III) at +71 ppm with respect to $CFC\ell_3$ and a number of signals in the region of Sb(V) (Fig. 24). The two AX_4 spectra are slightly downfield from the AX_4 spectrum reported by Gillespie and coworkers for the anion $SbF_5SO_3F^-$ (76). There are a number of other bands in the spectrum at +96, +104, +106 and +107 ppm. Some of the signals are broad and there may be more than one signal in the region. The spectrum is not well resolved; the exact assignment of the signals could not be made.

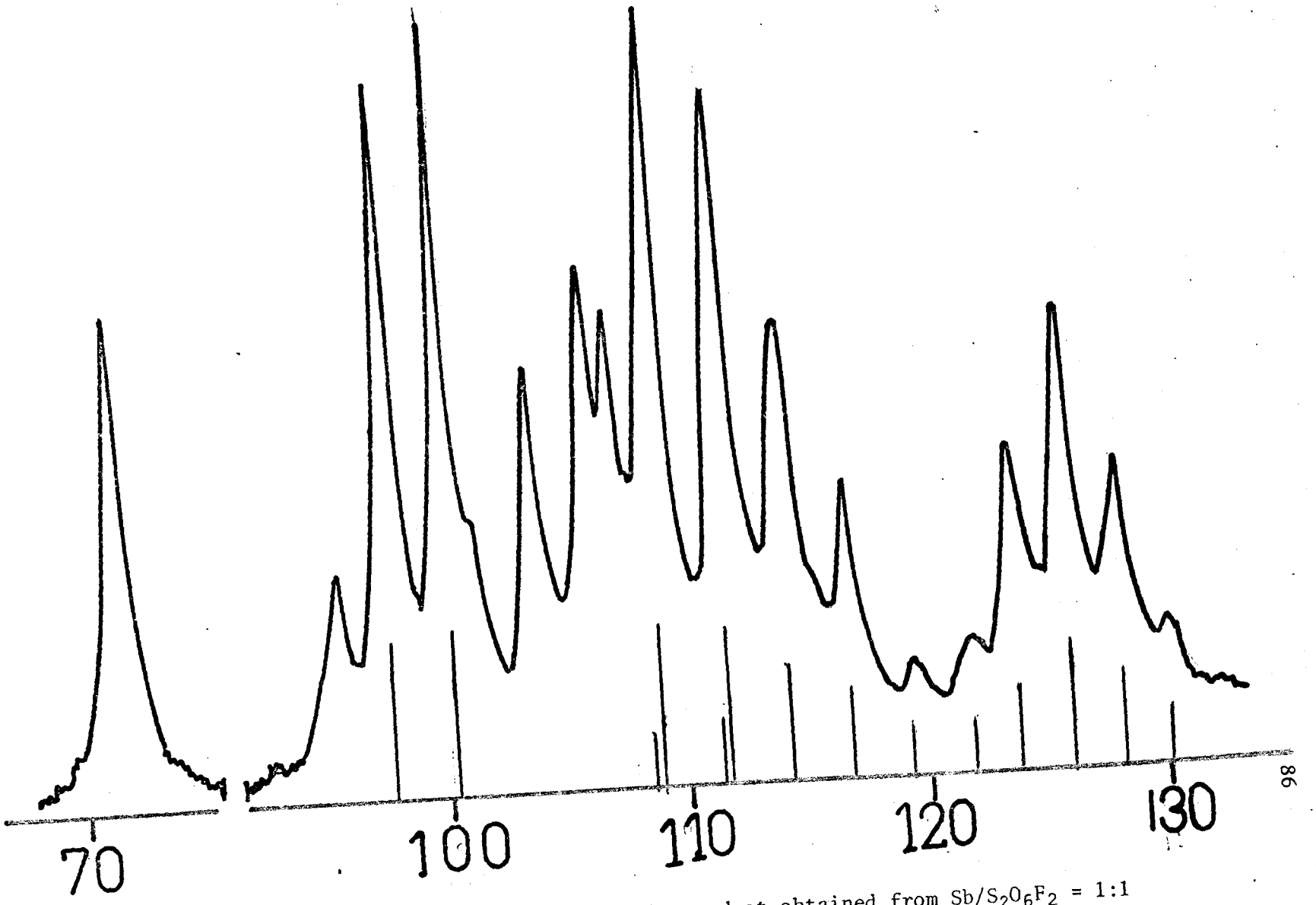

Fig. 24. ^{19}F n.m.r. spectrum of the solution of the product obtained from $Sb/S_2O_6F_2 = 1:1$

Attempts to prepare the compound $Sb_n(SO_3F)_n$ by the reaction of $Sb/S_2O_6F_2$ in HSO_3F in the mole ratio of 2:1 gave a white solid product. The elemental analysis of this compound corresponds to the formula $Sb(SO_3F)_3$ (found Sb = 30.05%, F = 14.80% and S = 22.75%; required Sb = 29.29%, F = 13.84% and S = 22.90%).

The reaction of the metal with $S_2O_6F_2$ in the $Sb/S_2O_6F_2$ mole ratios of 4:1 and 8:1 in HSO_3F in attempts to oxidise the metal to the $(+\frac{1}{2})$ and $(+\frac{1}{4})$ oxidation states respectively at -21°C, gave in both cases a grey coloured product. The mixture changed to white at room temperature. The grey solid was found to be a mixture of Sb(III) and antimony metal from its Mössbauer spectrum (83).

6b. Raman Spectrum of $Sb(SO_3F)_3$

The Raman spectrum of $Sb(SO_3F)_3$ is given in Fig. 25. The bands observed in the Raman spectrum and their relative intensities are given in Table XIV. Milne and coworkers (84) have studied the Raman and i.r. spectra of a number of metal fluorosulfates. They have shown that there are changes in the spectrum as the symmetry of the SO_3F^- ion changes from C_{3v} to C_s with increasing covalency of the metal-oxygen bond. For C_{3v} symmetry six fundamentals are expected but these increase to nine for C_s symmetry, all of them Raman and i.r. active. The $Sb(SO_3F)_3$ molecule may be expected to have a pyramidal ammonia type structure with C_{3v} symmetry, but no structural data is available at present. Antimony metal in SbF_3 is known to acquire six coordination through fluorine bridging (85). Recent X-ray crystallographic studies on $SnF_2(SO_3F)_2$ has shown that the tin atom has two Sn-O long bonds to have the six coordination round the central metal atom (86). If a similar type of oxygen bridging is present in $Sb(SO_3F)_3$ the antimony atom could have three Sb-O normal bonds and three Sb-O long bonds and the seventh

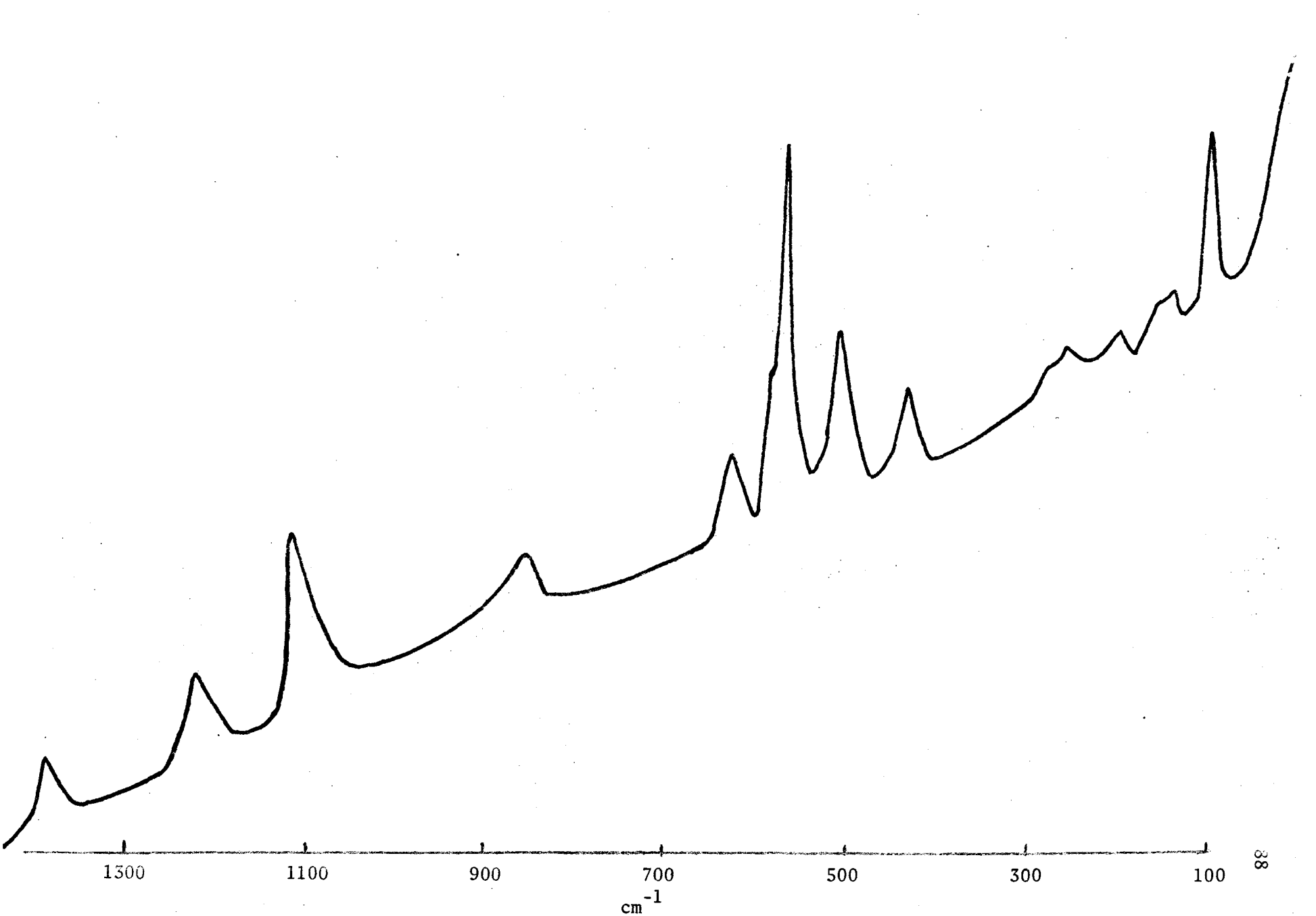

Fig. 25. Raman spectrum of $Sb(SO_3F)_3$.

TABLE XIV

Raman	Assignment of the Band	Relative Intensity	KSO_3F (84) (Raman)	$Fe(SO_3F)_3$ (i.r.)
92		48		
128		16		
197		13		
253		9		
286		7		
422		23	405 ν_6(e) S-F defn	442
502	Sb-0 anti sym str	48		
561	Sb-0 sym str	100		
571			571 ν_3(a) SO_3 asy defn	551 579
616		32	587 ν_2(a) SO_2 asy defn	630
817		16	741 ν_1(a) S-F str	850
1066		43	1084 ν_1(a) SO_3 sym str	1090
1163		18		1137
1347		25	1285 ν_4(e) SO_3 asy str	1360

coordination place occupied by the lone pair. The Raman spectrum under such conditions would not be simple due to the low symmetry of the molecule.

In its simplest form the molecule $Sb(SO_3F)_3$ will have C_{3v} symmetry and twenty-eight fundamentals are predicted.

$$3N - 6 = 9A_1 + 5A_2 + 14E_u.$$

As A_1 and E_u modes are both Raman and I.R. active and A_2 Raman and i.r. inactive the spectrum should show twenty-three bands. Only thirteen bands were observed in the 80-1500 cm^{-1} region. Some of the bands are very broad and may consist of two or more overlapping bands. An approximate assignment of the spectrum can be made by treating the SO_3F^- group as a separate unit and assuming that in addition to the vibrations of the SO_3F^- group there will be the vibrations due to the three Sb-O bonds.

The assignment of the vibrational bands due to OSO_2F can be made by comparing the bands in the spectrum of $Fe(SO_3F)_3$ and KSO_3F reported by Milne and coworkers. These workers have observed that as the covalent character in the bonding increases ν_6 (S-F defn.), ν_5 (SO asy. defn.) and ν_2 (S-F st.) shift to higher frequency regions. Similar shifts are observed in the spectrum of $Sb(SO_3F)_3$, Table XIV.

After assigning the bands for the SO_3F^- group there remain strong bands at 561, 502, and 92 cm^{-1}, medium intensity bands at 197 and 128, and weak bands at 286 and 253 cm^{-1}.

The Sb-O stretching vibration has been reported in the region of 500-530 cm^{-1} by Kawasaki and Noltes and coworkers (87,88). Fluck and coworkers have reported this vibration at 720 cm^{-1} in tetrachloro antimony dimethoxy phosphate which has a cyclic structure (89). It seems probable that the band at 562 cm^{-1} can be assigned to Sb-O symmstric stretch and at 502 cm^{-1}

to Sb-O antisymmetric stretching vibration. The bands of medium intensity at 197 and 128 cm^{-1} may be due to symmetric and antisymmetric bending modes respectively. The weak bands at 286 and 253 may be due to torsional modes or vibrations due to oxygen bridging. The strong band at 92 cm^{-1} is too low to be assigned to a symmetric bending mode and the exact assignment of this mode can not be made in the absence of the structural data for this compound.

7. Conclusion

Antimony metal dissolves in HSO_3F to give a colourless solution and formation of sulfur dioxide shows that the metal is oxidised. Cryoscopic and conductivity measurements on the solutions of antimony in HSO_3F suggests that the metal is oxidised to a mixture of the (+1) and (+3) oxidation states and when excess of antimony metal is used the compound $SbSO_3F$ separates out of the solution. Solutions of $SbSO_3F$ in HSO_3F are not stable and the n.m.r. spectrum and conductivity measurements show that Sb(I) is gradually oxidised to Sb(III). During this oxidation reaction the solvent is reduced to SO_2 and S. The formation of sulfur cations and sulfur in the solution of antimony metal and $SbSO_3F$ in HSO_3F has been confirmed by U V and visible absorption, e.s.r. and Raman spectroscopy and X-ray diffraction studies.

Compounds of antimony in the (+1) oxidation states can also be obtained by oxidising antimony metal with AsF_5 or SbF_5. The magnetic measurements on $SbSO_3F$ and Raman and i.r. spectra of $SbAsF_6$ suggests that the compounds are not monoatomic.

No evidence for oxidation states lower than (+1) was obtained. The oxidation of antimony metal with $S_2O_6F_2$ shows that it oxidises the metal to a mixture of the (+3) and (+5) oxidation states of antimony.

CHAPTER VI

SOLUTIONS OF ANTIMONY METAL IN SUPERACID

1a. Introduction

Recent studies of the solvent properties of the acidic media have shown that a mixture of SbF_5 and HSO_3F provides a much stronger acidic medium than HSO_3F alone (90,91). Carbonium ions and polyatomic cations of bromine, Br_2^+ and Br_3^+, which are not stable in HSO_3F have been studied successfully in Sb/HSO_3F and $SbF_5/SO_3/HSO_3F$ mixtures (9). In the preceeding chapter it has been shown that fluorosulfuric acid oxidises antimony metal to the (+1) and (+3) oxidation states. Solutions of antimony in the (+1) oxidation state are not stable in fluorosulfuric acid. So an attempt was made to study the behaviour of antimony metal in super acid (SbF_5/HSO_3F mixture). In the present investigations a mixture of SbF_5 and HSO_3F in ratio 1:9 by weight has been used and will be referred to as super acid.

Antimony metal dissolves in super acid in 8 to 10 hrs to give light yellow, blue and greenish solutions depending upon the concentration of the metal. Up to the concentration of 0.5 g per 100 g of the solvent antimony dissolves to give a light yellow solution. This solution shows strong absorptions at 225-250 and 310 nm (Fig. 26A). At higher concentration of the metal the colour of the solution is blue and up to 2 g of the metal can be dissolved in 100 g of the solvent. The U V visible absorption spectrum of this solution shows strong peaks at 225-250, 330 and 580 nm (Fig. 26B). Further addition of the metal while stirring results in further colour change of the solution to greenish yellow while some of the metal remains undissolved. The absorption spectrum of the supertanant

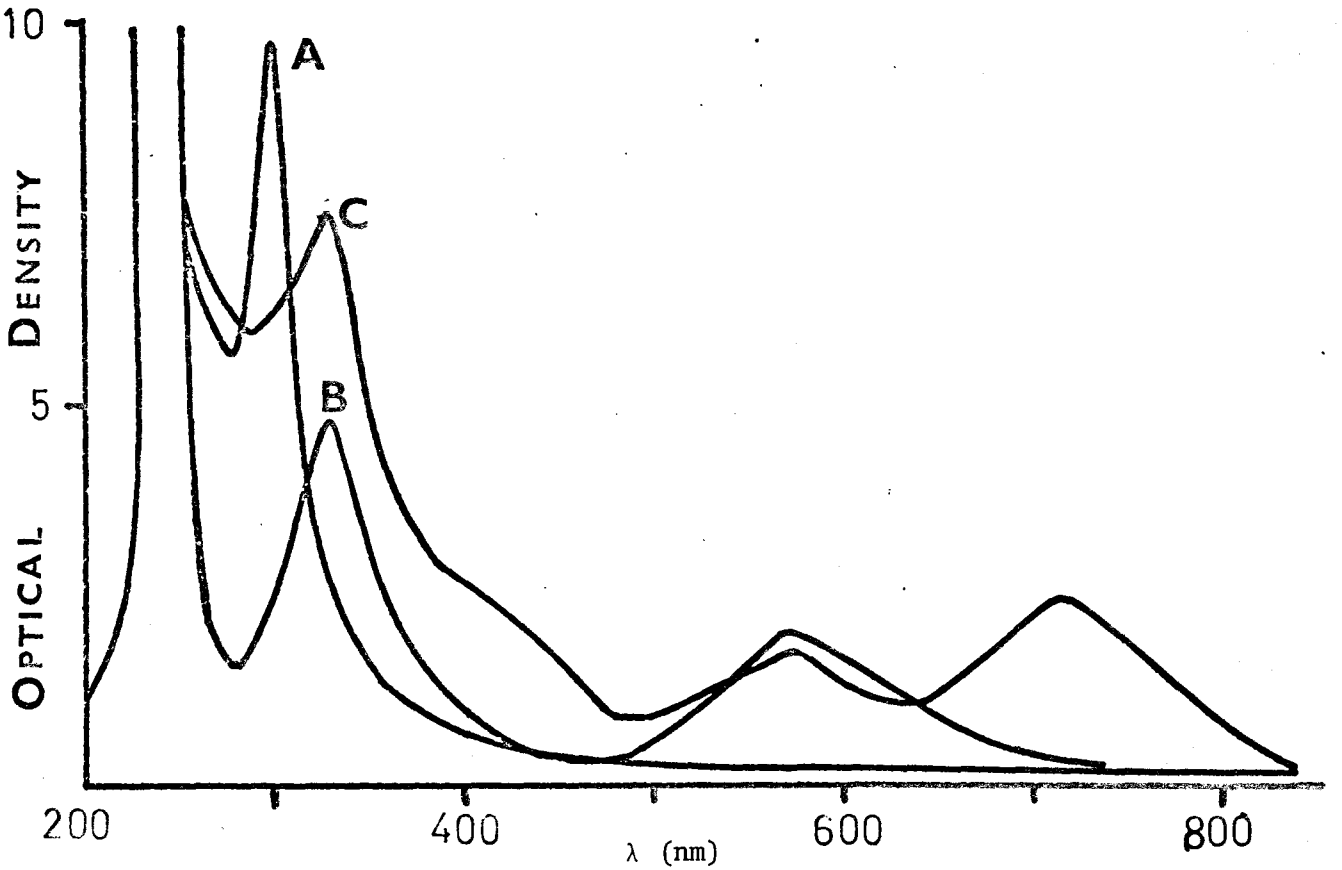

Fig. 26. UV and visible absorption spectra of antimony solutions in HSO_3F/SbF = 9:1 mixtures. (A) 0.0321mol(Sb) solution; (B) 0.0938mol(Sb) solution; (C) supertanant liquid when excess of antimony is added to the solution.

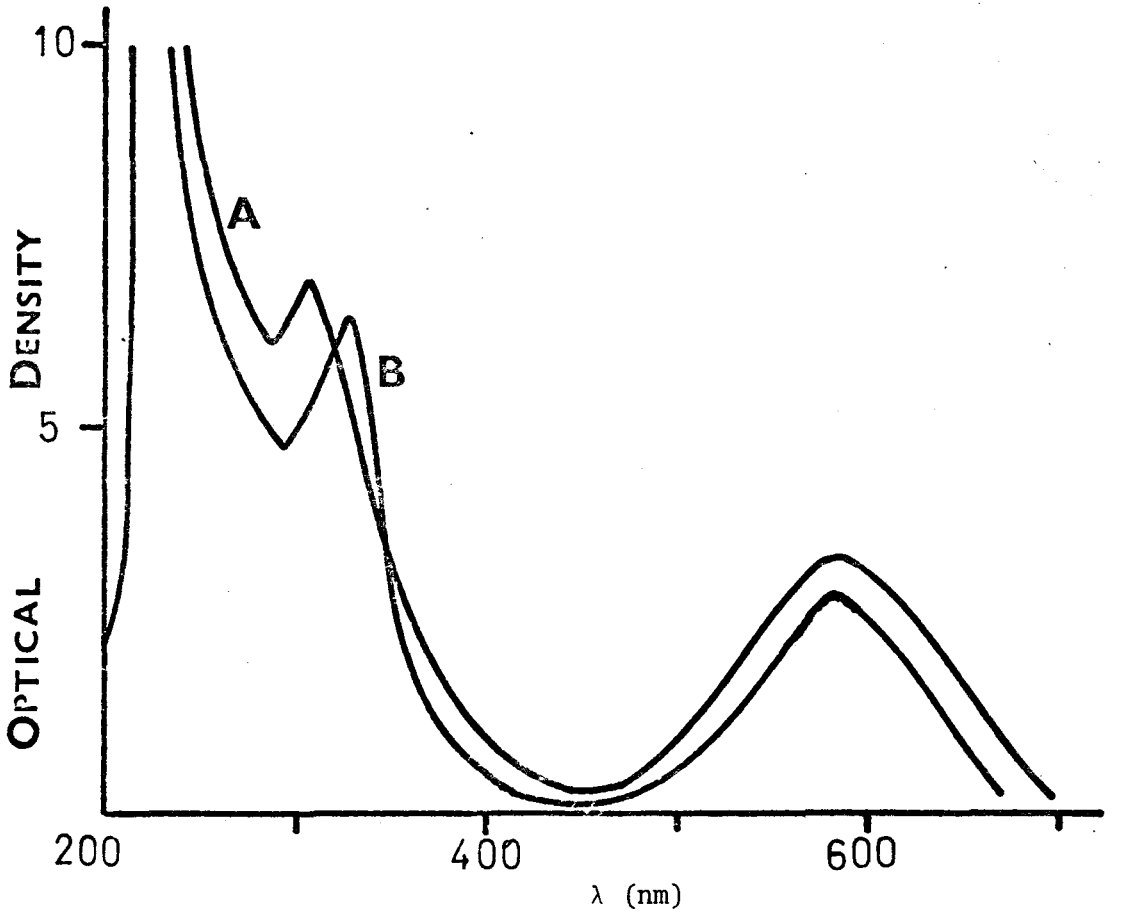

Fig. 27. UV and visible absorption spectra of sulfur solutions in HSO_3F/SbF_5 = 9:1 mixture. (A) 2×10^{-3} mol(S) solution; (B) solution A after 10 hrs.

liquid is shown in Fig. 26, Curve C. This spectrum shows bands at 420 and 710 nm in addition to the bands in the spectrum 26B. On storing this solution for half an hour after removing excess undissolved metal the colour of the solution changes to blue which has the same absorption spectrum as Fig. 26B, and a white solid separates out of the solution.

For comparison the absorption spectra of a solution of sulfur in super acid was studied. The fresh solution of sulfur (2×10^{-3} M) shows strong absorption bands at 225-250, 310 and 580 nm (Fig. 27). The 580 nm band is due to S_8^{2+}. When this solution is left for 8-10 hrs the band at 310 nm disappears and another band at 330 nm appears in the spectrum. The 330 nm band has been attributed to the S_4^{2+} cation. The comparison of the two spectra strongly suggests that the colour of the solutions of antimony metal in super acid are due to the formation of sulfur cations.

The bands at 430 and 710 nm which appear in the spectrum when excess of antimony metal is added to the solution slowly diminish in intensity. It appears that antimony metal reduces the HSO_3F to an equilibrium mixture of S_{16}^{2+} and S_8^{2+} which shows absorption bands at 235, 430, 580 and 710 nm. The S_{16}^{2+} is oxidised in solution to S_8^{2+} and S_4^{2+} which is shown by the disappearance of the 430 and 710 absorptions with time.

The formation of sulfur cations suggests that in super acid antimony metal is oxidised by HSO_3F which is reduced to sulfur cations.

1b. ^{19}F n.m.r.

The ^{19}F n.m.r. spectrum of the super acid medium SbF_5/HSO_3F was quite similar to that reported by Gillespie and coworkers (76). The spectrum shows two overlapping doublets and quintets in the fluorine on Sb(V) region due to the species $SbF_5(SO_3F)^-$ and $Sb_2F_{10}(SO_3F)^-$.

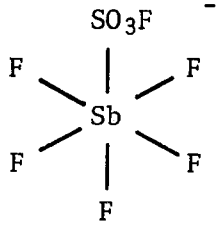

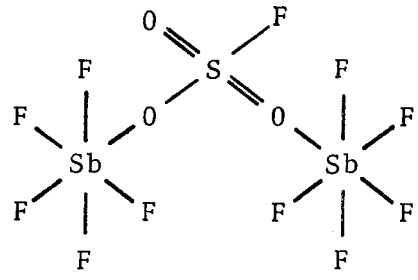

A solution of antimony metal in super acid showed two signals in addition to the solvent signals (Fig. 28) with a chemical shift of +60 and +120 ppm with respect to $CFC\ell_3$. The signal with a chemical shift of +60 ppm may be attributed to fluorine on Sb(III) and that at +120 ppm to SbF_6^-, since solutions of SbF_3 and $NaSbF_6$ in super acid show signals with chemical shifts +60 and +120 ppm with respect to $CFC\ell_3$ respectively. A solution of SbF_3 in HSO_3F has a chemical shift of fluorine on Sb(III) at +82 ppm with respect to $CFC\ell_3$. The lowering of the chemical shift from +82 to +60 ppm is too large to be attributed to a solvent effect and it may reasonably be attributed to the formation of the SbF_2^+ cation in super acid. The X-ray crystallographic study of SbF_3AsF_5 has shown that it may be formulated as $SbF_2^+AsF_6^-$ (92).

The area ratio of the signals of fluorine on Sb(III) and Sb(V) showed that the two types of fluorine were present in the ratio of 1:3.5. The formation of SbF_2SbF_6 required the area ratio 1:3. The solution has a blue colour but the compounds SbF_2SbF_6 and $SbSbF_6$ are white solids and give colourless solutions. The blue colour of the solution is due to the presence of sulfur cation S_8^{2+}. The excess concentration of SbF_6^- may be due to the compound $SbSbF_6$ or the anion associated with the sulfur cations.

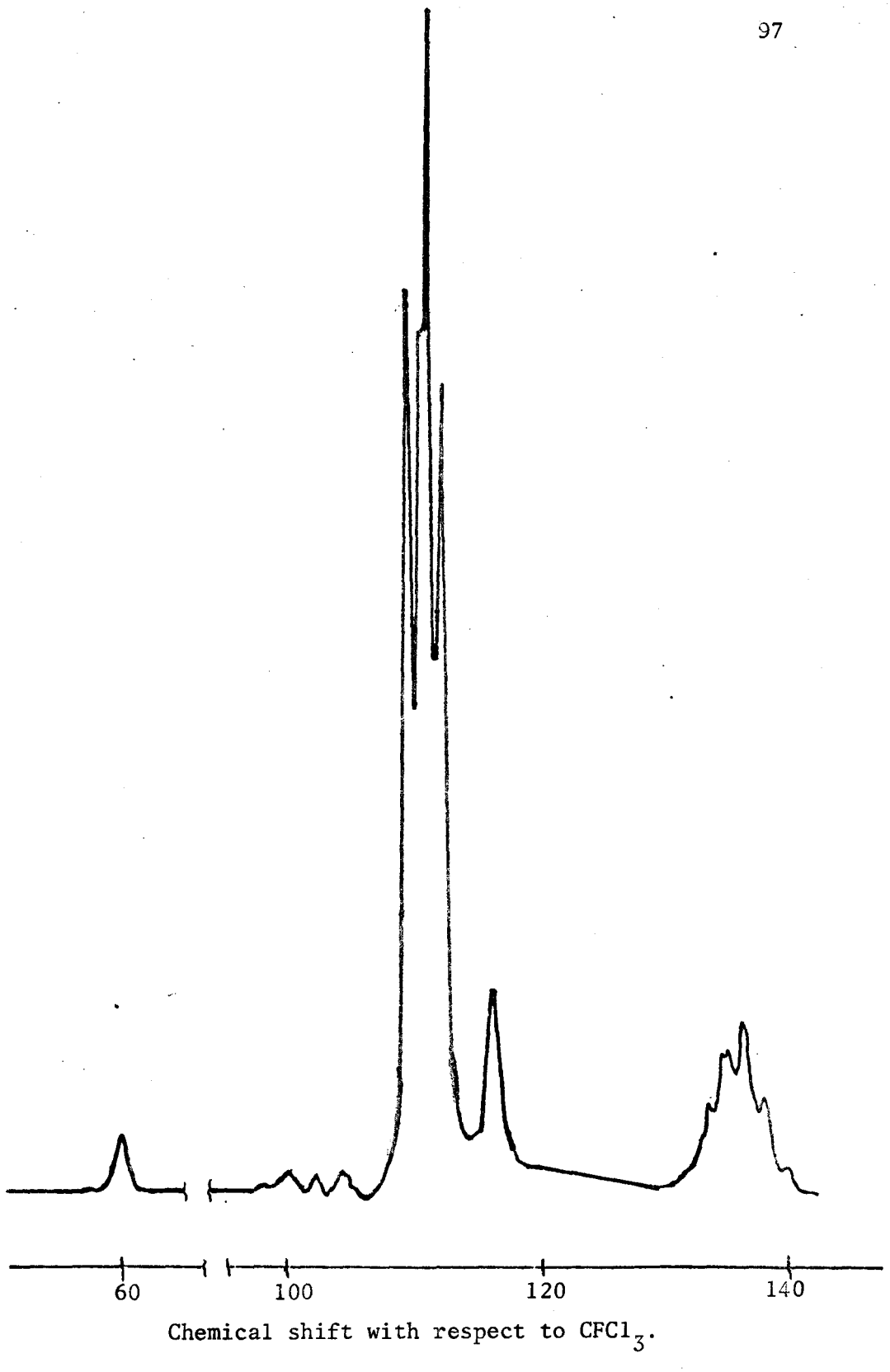

Fig. 28. ^{19}F n.m.r. spectrum of antimony solution in HSO_3F/SbF_5 9:1 mixture at -80°C.

1c. E.s.r. Spectrum

The solution of antimony metal in super acid that shows the absorption bands at 225-250 and 310 nm (Fig. 26A), does not show any e.s.r. spectrum. The solution that shows absorption at 225-250, 330 and 580 nm show two sharp e.s.r. signals. The strong signal in the high field side g = 2.014 and a weak signal g = 2.027 in the low field side. The intensity of the signals decreases as the temperature of the solution is lowered. The relative intensity of the e.s.r. signals at temperatures between 20 and -80°C are given in Fig. 29. The lowering of the intensity of the signals with temperature suggests that the paramagnetic species dimerises at low temperatures.

Antimony metal has two magnetic nuclei with spin 5/2 and 7/2 with natural abundances of 57.25 and 47.75% respectively. Coupling of the electron spin with the nuclear magnetic moment should give a six and an eight line spectrum. The signals that are observed showed no hyperfine coupling so it appears that the e.s.r. signals are not due to antimony radicals.

The formation of the sulfur cations in the solution of antimony metal in super acid has already been shown by the absorption spectra of the solutions. Sulfur in the +1/8 and +1/4 oxidation states is associated with the radicals S_8^+ and S_4^+ which have g = 2.027 and 2.014 respectively. As these are the same as the g values of the e.s.r. signals observed in the solution of the antimony metal in the super acid it is reasonable to conclude that these signals are also due to the sulfur radicals S_8^+ and S_4^+. In dilute solutions of antimony the solvent is reduced only to S_4^{2+} and in more concentrated solutions S_8^{2+} is obtained and then finally S_{16}^{2+}. The temperature dependence of the e.s.r. signals was similar to that observed in solutions of sulfur in oleum.

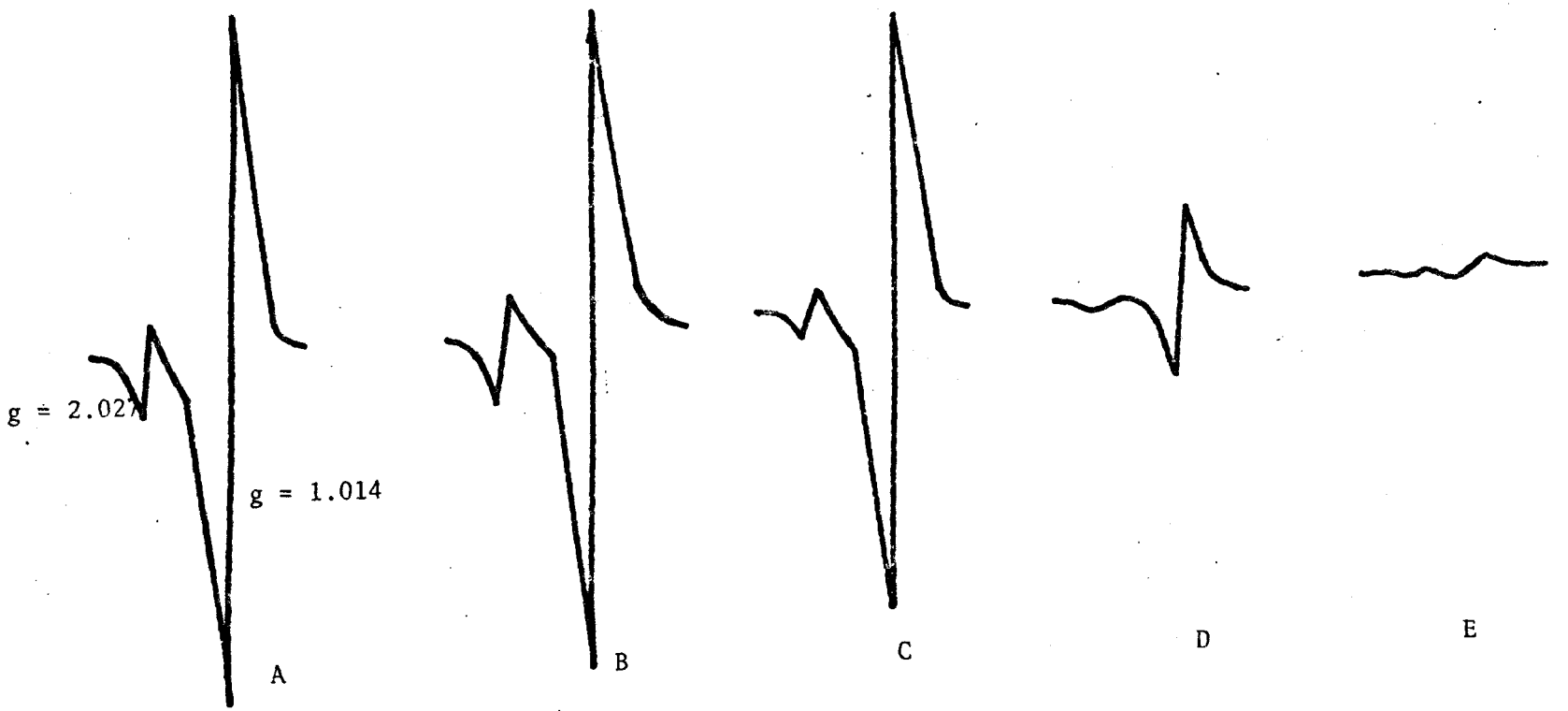

Fig. 29. E.s.r. spectra of Sb solutions in superacid. (A) 22°C; (B) -20°C; (C) -40°C; (D) -60°C; (E) -80°C.

2. Reaction of Antimony Metal with AsF_5 in HF

Antimony metal does not react with HF at room temperature. Attempts were made to prepare the Sb(I) compound by oxidising antimony metal with AsF_5 in HF according to the reaction represented by the equation

$$2Sb + 3AsF_5 \xrightarrow{HF} 2SbAsF_6 + AsF_3$$

In a typical reaction 0.4782 g of antimony reacted with 1.0021 g of AsF_5 in HF. A white solid formed in a rapid reaction. No colour was observed in the supertanant liquid. On evacuating the solvent 1.4563 g of the white product was obtained. The yield of the product required for SbF_3 and Raman spectrum showed it to be SbF_3. It is reasonable to conclude that the following reaction takes place in HF

$$2Sb + 3AsF_5 \longrightarrow 2SbF_3 + 3AsF_3$$

3. Reaction of Antimony Metal with SbF_5

Antimony metal was mixed with excess of SbF_5. A very slow reaction is observed. A white solid and some unreacted antimony was formed even after two months. No colour was observed in the SbF_5. The mixture does not show any e.s.r. spectrum.

4. Conclusion

Antimony metal dissolves in super acid to give coloured solutions. U V visible absorption and e.s.r. spectra show that the colour and e.s.r. signals are due to sulfur cations and radicals. The formation of sulfur cations in HSO_3F suggests that the metal is oxidised by HSO_3F and not by SbF_5

No evidence for lower oxidation states of antimony other than the (+1) oxidation state has been obtained.

CHAPTER VII

CONCLUSIONS

The electronegative elements of group VI and VII elements are commonly known in the anionic form. Very recently it has been shown that these elements can be obtained in the form of polyatomic cations in a medium of very low basicity. The discovery of these hitherto unsuspected cationic forms of these elements has opened a new field of chemistry. During the past few years polyatomic cations of iodine, bromine, chlorine, selenium and tellurium have been characterised in this laboratory.

In the case of tellurium, it has been observed that tellurium metal can be oxidised to the (+1/2) and (+1) oxidation states which give red and yellow solutions respectively. The red solution has been shown to contain the Te_4^{2+} cation. The yellow solution was found to be diamagnetic and formulated as Te_n^{n+} (n = 2,4,6). Some evidences for the lower positive oxidation states of sulfur were obtained in the previous studies. The red and blue compounds of sulfur which were formulated as $S_{8n}(AsF_6)_n$ and $S_{4n}(AsF_6)_n$ respectively on the basis of elemental analysis and diamagnetic properties, but the exact nature of the cation present in these compounds were not known.

In the present investigations further studies have been carried out, particularly cryoscopic measurements in order to obtain information on the nature of the Te(+1) species present in solution in HSO_3F and $H_2S_2O_7$. In order to obtain added information on the nature of the various sulfur cations that can be obtained in solution and those sulfur species previously obtained by the reaction of sulfur with AsF_5 which lead to the formation of

the sulfur cations S_{8n}^{n+} and S_{4n}^{n+}, these species have been investigated by cryoscopic, conductivity and e.s.r. measurements.

Tellurium metal can be oxidised with $S_2O_6F_2$ in HSO_3F to the (+1) oxidation state at -23°C. The cryoscopic measurements of $Te/S_2O_6F_2$ = 2:1 solutions are not consistent with the dimer Te_2^{2+} but suggest that either Te_4^{4+}, Te_6^{6+} or Te_8^{8+} may be present in the solution. The cryoscopic results were not accurate enough to distinguish between these possible alternatives.

Elemental sulfur is not soluble in HSO_3F but it can be oxidised with $S_2O_6F_2$ in HSO_3F to give coloured solutions. The UV and visible spectra show that three compounds are formed in the solution at $S/S_2O_6F_2$ mole ratios of 16:1, 8:1 and 4:1. These solutions are respectively orange, blue and yellow. The $S/S_2O_6F_2$ = 16:1 solution is stable in HSO_3F and has a strong absorption band at 235 nm. The results of cryoscopic and conductivity measurements on this solution are consistent with the formation of the S_{16}^{2+} cation. The blue $S/S_2O_6F_2$ = 8:1 solution in HSO_3F which has an absorption maxima at 590 nm, is not very stable. A solution of sulfur in 44.9% oleum also has an absorption maxima at 590 nm indicating that the same sulfur species is present in the two solutions. This solution is also not very stable. Cryoscopic measurements on fresh solutions of sulfur in disulfuric acid suggest that the S_8^{2+} cation is formed in the solution. The solution of $S_8(AsF_6)_2$ also shows an absorption band at 590 nm and is blue; the X-ray crystal structure of this compound has shown that it contains the cation S_8^{2+}. This supports our conclusion that the cation S_8^{2+} is also present in $S/S_2O_6F_2$ = 8:1 in HSO_3F and in solutions of sulfur in disulfuric acid. The $S/S_2O_6F_2$ = 4:1 solution absorbs at 330 nm. Solutions of sulfur in 60% oleum

also show an absorption band at 330 nm which may be attributed to the S_4^{2+} cation.

With the confirmation of the sulfur cations in solution it is now known that all the group six elements except polonium which has not been studied because of its radioactive properties, form polyatomic cationic species. The polyatomic cations of the group VIB elements are summarised in Table XV.

TABLE XV

Cations of Group VIB Elements

O		O_2^+ (93)			
S		S_4^{2+}		S_8^{2+}	S_{16}^{2+}
Se		Se_4^{2+}		Se_8^{2+}	
Te	Te_n^{n+}	Te_4^{2+}	Te_6^{2+}		

Of the group V elements only bismuth is known from previous studies to form polyatomic cations. Evidence for several such cations such as Bi_9^{5+}, Bi_8^{2+} and Bi_5^{3+} has been obtained from the studies of solutions of bismuth and $BiC\ell_3$ in $NaA\ell C\ell_4$ and $A\ell C\ell_3$ mixtures. The object of the present work was to obtain evidences for corresponding cations of antimony in acid solvents.

Antimony metal dissolves in HSO_3F to give colourless solution. UV and visible absorption spectral, cryoscopic and conductivity measurements show that the metal is oxidised to the (+1) and (+3) oxidation states in this solution. The compound $SbSO_3F$ containing antimony in the (+1) oxidation state separates out of the solution when excess metal is added. In the simple formula $SbSO_3F$ the metal atom would have two 5p unpaired electrons and would be expected to be paramagnetic. Magnetic susceptibility measure-

ments show that the compound is essentially diamagnetic at room temperature. This behaviour can be best explained by formulating the compound as $Sb_n(SO_3F)_n$. Solutions of $Sb_n(SO_3F)_n$ in HSO_3F are not stable and the Sb(I) is oxidised to Sb(III) and the solvent is reduced to sulfur cations and elemental sulfur. The formation of sulfur cations and sulfur have been confirmed by UV and visible absorption, e.s.r., Raman spectroscopy and X-ray diffraction studies.

Antimony metal can be oxidised to the (+1) oxidation state with AsF_5 and SbF_5 to form the compounds $SbAsF_6$ and $SbSbF_6$. The anions AsF_6^- and SbF_6^- in these compounds have been characterised by ^{19}F n.m.r. spectroscopy. The diamagnetic behaviour and Raman spectrum of $SbAsF_6$ suggests that the compound is $Sb_n(AsF_6)_n$.

Oxidation of antimony metal with $S_2O_6F_2$ shows that the metal is oxidised to the (+3) and the (+5) oxidation states. No evidence for any lower oxidation state was obtained during these reactions.

In super acid antimony metal is oxidised to give coloured solutions. These have been shown by UV-visible absorption and e.s.r. spectroscopy to be due to sulfur cations. No evidence for oxidation states of antimony lower than (+1) was obtained in this study.

We conclude that the only lower oxidation state of antimony for which there is definite evidence is the (+1) oxidation state. No evidence has been obtained for the (+1/2) and (+1/4) oxidation states reported by Paul et al, or for any cations analogous to those reported for bismuth.

There still remains many questions to be answered regarding the stability and structure of these cations. The cations of tellurium and antimony in the (+1) oxidation state have been obtained and have been formulated as Te_n^{n+} and

Sb_n^{n+} respectively. The value of 'n' for both these cations could not be obtained with certainty during these studies. It appears that X-ray crystallographic studies of single crystals will be necessary to find the structure and molecular weight of these compounds.

REFERENCES

1. I. Masson, J. Chem. Soc., 1708 (1938).

2. J. Arotsky, H. C. Mishra and M. C. R. Symons, J. Chem. Soc., 2582 (1962).

3. R. A. Garrett, R. J. Gillespie and J. B. Senior, Inorg. Chem., 4, 563 (1965).

4. R. J. Gillespie and J. B. Milne, Inorg. Chem., 5, 1577 (1966).

5. R. J. Gillespie, J. B. Milne and M. J. Morton, Inorg. Chem., 7, 2221 (1968).

6. M. C. R. Symons, Q. Rev. Chem. Soc., 16, 282 (1962).

7. V. M. McRae, Ph.D. Thesis, University of Melbourne (1966).

8. R. J. Gillespie and M. J. Morton, Chem. Comm., 1565 (1968).

9. R. J. Gillespie and M. J. Morton, Inorg. Chem. (In Press).

10. A. J. Edward and G. R. Jones, J. Chem. Soc. (A) 2318 (1971).

11. G. A. Olah and M. B. Commisarow, J. Am. Chem. Soc., 90, 5033 (1968).

12. M. J. Morton, Ph.D. Thesis, McMaster University (1969).

13. R. S. Eachus, T. P. Sleight and M. C. R. Symons, Nature, 222, 769 (1969).

14. K. O. Christe and J. S. Muirhead, J. Am. Chem. Soc., 91, 7777 (1969).

15. M. H. Klaproth, Phil. Mag., 1, 78 (1798).

16. J. Barr, R. J. Gillespie, R. Kapoor and G. P. Pez, J. Am. Chem. Soc., 90, 6855 (1968).

17. N. J. Bjerrum and G. P. Smith, J. Am. Chem. Soc., 4472 (1968).

18. John D. Corbett, private communication.

19. J. Barr, R. J. Gillespie, G. P. Pez, P. K. Ummat and O. C. Vaidya, Inorg. Chem., 10, 362 (1971).

20. J. W. Mellor, "Comprehensive treatise on inorganic and theoretical chemistry", Longmans, Green and Co., London, 1930; Vol. 10, pp. 184-186, 922; Vol. 11, pp. 116-117.

21. G. Magnus, Ann. Physik [2] 10, 491 (1827); [2] 14, 328 (1828).

22. J. Barr, R. J. Gillespie, R. Kapoor and K. C. Malhotra, Can. J. Chem., 46, 149 (1968).

23. R. J. Gillespie and G. Pez, Inorg. Chem., 8, 1229 (1969).

24. I. D. Brown, D. B. Crump, R. J. Gillespie and D. P. Santry, Chem. Comm., 853 (1968).

25. R. K. McMullan, D. J. Prince and J. D. Corbett, Chem. Comm., 1438 (1969).

26. R. K. McMullan, D. J. Prince and J. D. Corbett, Inorg. Chem., 10, 1749 (1971).

27. R. D. Burbank, Acta Cryst., 4, 140 (1951).

28. R. E. Marsh, L. Pauling and J. D. McCullough, Acta Cryst., 6, 71 (1953).

29. D. B. Sharma and J. Donohue, Acta Cryst., 16, 891 (1963).

30. A. G. Turner and F. S. Mortimer, Inorg. Chem., 5, 775 (1952).

31. A. A. Woolf, J. Chem. Soc., 433 (1955).

32. R. J. Gillespie, J. B. Milne and R. C. Thompson, Inorg. Chem., 5, 468 (1966).

33. J. Barr, R. J. Gillespie and R. C. Thompson, Inorg. Chem., 3, 1149 (1964).

34. R. C. Thompson, J. Barr, R. J. Gillespie, J. B. Milne and R. A. Rothenbury, Inorg. Chem., 4, 1641 (1965).

35. R. J. Gillespie, Accounts of Chemical Research, July (1968).

36. J. Barr, Ph.D. Thesis, McMaster University (1959).

37. F. B. Dudley and G. H. Cady, J. Am. Chem. Soc., 79, 513 (1957).

38. R. J. Gillespie and K. C. Malhotra, J. Chem. Soc. (A) 1994 (1967).

39. J. B. Milne, Ph.D. Thesis, McMaster University (1962).

40. G. Jones and D. M. Bollinger, J. Am. Chem. Soc., 57, 280 (1935).

41. G. Jones and B. C. Bradshaw, J. Am. Chem. Soc., 55, 1780 (1933).

42. G. W. Haubt, J. Opt. Soc. Am., 42, 441 (1952).

43. B. N. Figgis and J. Lewis in J. Lewis and R. J. Wilkins (Editors), "Modern Co-ordination Chemistry", Interscience Publishers, New York (1960).

44. J. Barr, R. J. Gillespie, G. P. Pez, P. K. Ummat and O. C. Vaidya, J. Am. Chem. Soc., 92, 1081 (1970).

45. R. J. Gillespie and K. C. Malhotra, J. Chem. Soc. (A) 1933 (1968).

46. R. Weber, Ann. Phys. (Leipzig), [2] 156, 531 (1875).

47. I. Vogel and J. R. Partington, J. Chem. Soc., 127, 1514 (1925).

48. R. Auerbach, Z. Phys. Chem., (Leipzig) 121, 337 (1926).

49. J. R. Brayford and P. A. H. Wyatt, Trans. Faraday Soc., 52, 642 (1956).

50. M. C. R. Symons, J. Chem. Soc., 2440 (1957).

51. D. J. E. Ingrams and M. C. R. Symons, J. Chem. Soc., 2437 (1957).

52. D. A. C. McNeil, M. Murry and M. C. R. Symons, J. Chem. Soc. (A) 1019 (1967).

53. H. Lux and E. Bohm, Chem. Ber., 98, 3210 (1965).

54. J. M. Schreeve and G. H. Cady, J. Am. Chem. Soc., 83, 4521 (1961).

55. R. J. Gillespie and J. Passmore, Chem. Comm., 1333 (1969).

56. P. K. Ummat, Ph.D. Thesis, McMaster University (1970).

57. W. F. Giggenbach, Chem. Comm., 852 (1970).

58. M. Stillings, M. C. R. Symons and J. G. Wikinson, Chem. Comm., 372 (1971).

59. R. A. Beaudet and P. J. Stephens, Chem. Comm., 1083 (1971).

60. R. J. Gillespie and P. K. Ummat, Inorg. Chem. (In Press).

61. P. J. Stephens, Chem. Comm., 1496 (1969).

62. R. J. Gillespie, J. Passmore, P. K. Ummat and O. C. Vaidya, Inorg. Chem., 10, 1327 (1971).

63. C. G. Davies, R. J. Gillespie, J. J. Park and J. Passmore, Inorg. Chem. (In Press). December 1971.

64. J. D. Corbett, Inorg. Chem., 7, 198 (1968).

65. N. J. Bjerrum, C. R. Boston and G. P. Smith, Inorg. Chem., 6, 1162 (1967).

66. N. J. Bjerrum and G. P. Smith, Inorg. Chem., 6, 1968 (1967).

67. R. M. Friedman and J. D. Corbett, Chem. Comm., 422 (1971).

68. J. N. Brazier and A. A. Woolf, J. Chem. Soc. (A) 99 (1967).

69. R. C. Paul, K. K. Paul and K. C. Malhotra, Chem. Comm., 453 (1970).

70. P. A. W. Dean and R. J. Gillespie, Chem. Comm., 853 (1970).

71. R. J. Gillespie, J. B. Milne and J. B. Senior, Inorg. Chem., 5, 1233 (1966).

72. F. A. Cotton and T. E. Haas, Inorg. Chem., 3, 10 (1964).

73. R. D. Burbank, Inorg. Chem., 5, 1491 (1966).

74. P. W. Selwood, "Magnetochemistry", Interscience Publishers, New York (1956).

75. G. A. Ozin, J. Chem. Soc. (A) 116 (1969).

76. R. C. Thompson, J. Barr, R. J. Gillespie, J. B. Milne and R. A. Rothenbury, Inorg. Chem., 4, 1641 (1965).

77. R. J. Gillespie and A. Whitla, Can. J. Chem., 48, 657 (1970).

78. R. J. Gillespie and M. J. Morton, Inorg. Chem., 9, 811 (1970).

79. A. M. Qureshi, A. H. Hardin and F. Aubke, Can. J. Chem., 49, 816 (1971).

80. N. A. D. Carey and H. C. Clark, Chem. Comm., 292 (1967).

81. C. S. Venkateswaren, Proc. Indian Acad. Sci., A4, 345 (1946).

82. I. R. Beattie, G. A. Ozin and R. O. Perry, J. Chem. Soc., (A) 2071 (1970).

83. Basil P. Della Valle, M.Sc. Thesis, McMaster University (1971).

84. J. Gaubeau and J. B. Milne, Can. J. Chem., 45, 2321 (1967).

85. A. J. Edward, J. Chem. Soc., (A) 2751 (1970).

86. F. A. Allen, J. Lerbschev and J. Trotter (In Press).

87. Y. Kawasaki, Inorg. Nucl. Chem. Letters, 5, 805 (1969).

88. H. A. Meinema, E. Rivarla and J. G. Noltes, J. Organometallic Chem., 17, 71 (1969).

89. R. Schmitt, K. Dehnicke and E. Fluck, Z. Anorg. Chem., 366, 316 (1969).

90. G. A. Olah, G. Klopman and R. H. Shlosberg, J. Am. Chem. Soc., 91, 3261 (1969).

91. A. Commeyras and G. A. Olah, J. Am. Chem. Soc., 91, 2929 (1969).

92. A. J. Edward and R. J. C. Sills, J. Chem. Soc. (A) 942 (1971).

93. J. B. Beal, Jr., C. Dupp and W. E. White, J. Inorg. Chem., 8, 828 (1969).